

Selection of the Appropriate Infrared Detector Based on Customer Requirements

By

Donna Maestas

A MASTER OF ENGINEERING REPORT

Submitted to the College of Engineering at Texas Tech University in partial
Fulfillment of the Requirements for the Degree of

MASTER OF ENGINEERING

Approved

Dr. J. Borrelli

Dr. A. Ertas

Dr. T.T. Maxwell

Dr. M.M. Tanik

October 12, 2002

ACKNOWLEDGEMENTS

I would like to express my sincerest thanks to Dr. A. Ertas for working so diligently at putting this program into place and ensuring its success. His guidance throughout the last year has been invaluable. Further thanks go to the remaining members of my committee, Dr. T. Maxwell, Dr. M. Tanik, and Dr. J. Borrelli.

I would also like to express my thanks to Raytheon management in North Texas for sponsoring this program and believing that continuous training is paramount to success.

I extend a very special thanks to my program management and colleagues. Thank you!

Finally, I would like to thank my husband Aaron, for his unconditional love, support, and continuous encouragement throughout this entire process. He endured untold late nights, missed weekends, and more. For that and much more, this is dedicated to him.

ABSTRACT

The intent of this paper is to show the application of basic systems engineering practices/processes in the selection of an infrared detector system. Specifically, I will select the most appropriate infrared detector based on the customer's requirements within the technical, cost and schedule restraints imposed.

Customer X desires an infrared night vision system for border surveillance. This system can be mounted either on a land vehicle or on an unmanned aerial vehicle. Its main purpose is to detect unauthorized border incursions by smugglers, terrorists or opposing military forces. The detailed customer requirements will be used to determine the most cost-effective solution that meets or exceeds those requirements.

The four detector types examined will consist of a mid-wave staring detector, a mid-wave scanning detector, a long-wave staring detector, and a long-wave scanning detector. The technology behind each type will be explained along with the pros and cons. The detailed customer requirements will be compared against these options. Basic systems engineering practices, such as system modeling, requirements flow-down and prototyping will be used to rank the four options. Risk reduction planning, as well as costing constraints, will be applied to the decision process. The final ranking will be fully justified and presented in a manner appropriate for the customer's decision.

The overall scope of this effort is to demonstrate the application of basic systems engineering practices. I will attempt to distill customer requirements, and differentiate from customer "desirements", into a workable cost-effective solution by choosing one of the complex system designs while insuring everything from the technical to the financial aspects are taken into consideration for the final decision.

4.4	Results Summary	83
CHAPTER V	Selection Criteria	85
5.1	Cost/Schedule Risk	85
5.1.1	Supportability of LWIR Scanning Detector	90
	5.1.1.1 LWIR Scanning Detector Components	91
5.1.2	Supportability of MWIR Staring Detector	92
5.1.3	Supportability of LWIR Staring Detector	92
CHAPTER VI	Summary and Conclusions	93
6.1	Summary	93
6.2	Conclusion	93
REFERENCES		95
APPENDIX A	List of Acronyms	99
APPENDIX B	Model input information	100
APPENDIX C	Model output information	105

LIST OF FIGURES

<i>Number</i>		<i>Page</i>
Figure 1	1-1 Representation of IR worldwide business in US dollars by platform	11
Figure 2	3-1 Generic Electro-Optical functional block diagram	20
Figure 3	3-2 Various contributors that affect perceived image quality	21
Figure 4	3-3 Location of scanning mechanism, outside the detector	23
Figure 5	3-4a Multiple detectors operating in serial mode in horizontal direction, producing raster scan patterns from vertical interlace	23
Figure 6	3-4b TDI delay elements	24
Figure 7	3-5 Generic representation of a square staring detector array	25
Figure 8	3-6 Relative scattering coefficients for different sized spherical particles	28
Figure 9	3-7 Atmospheric transmittance and 300 K blackbody curve	29
Figure 10	3-8 Incremental signal available from $\Delta T=5K$ target on a 300 K Background	29
Figure 11	3-9 Incremental detector output created by a $\Delta T= 5 K$ target on a 300 K background for MWIR and LWIR systems	30
Figure 12	3-10 Spectrally averaged atmospheric transmittance for representative MWIR and LWIR systems	31
Figure 13	3-11 Spectrally averaged atmospheric transmittance for representative MWIR and LWIR systems, tropical environment	32
Figure 14	3-12 Spectrally averaged atmospheric transmittance for representative MWIR and LWIR systems, mid-latitude winter environment	33
Figure 15	3-13 Wave fronts and rays at various distances from a source	35
Figure 16	3-14 Optical system represented as a single optical element	36
Figure 17	3-15 Representation of spherical planes	36
Figure 18	4-1 Model interactions and how they contribute to one another	41
Figure 20	4-2 MRTs for Scanning MWIR detector system: two VFOVs	48
Figure 21	4-3 MRTs for Scanning LWIR detector system: two VFOVs	49
Figure 22	4-4 MRTs for Staring MWIR detector system: two VFOVs	50
Figure 23	4-5 MRTs for Staring LWIR detector system: two VFOVs	51
Figure 24	4-6 Probability of Detection Ranges in Tropical Atmosphere Utilizing Scanning LWIR Detector for the Two FOVs of Interest	54
Figure 25	4-7 Probability of Detection Ranges in Tropical Atmosphere Utilizing Scanning MWIR Detector for the Two FOVs of Interest	55
Figure 26	4-8 Probability of Recognition Ranges in Tropical Atmosphere Utilizing Scanning LWIR Detector for the Two FOVs of Interest	56
Figure 27	4-9 Probability of Recognition Ranges in Tropical Atmosphere Utilizing Scanning MWIR Detector for the Two FOVs of Interest	57
Figure 28	4-10 Probability of Detection Ranges in Mid-Latitude Summer Atmosphere Utilizing Scanning LWIR Detector for the Two FOVs of Interest	59
Figure 29	4-11 Probability of Detection Ranges in Mid-Latitude Summer Atmosphere Utilizing Scanning MWIR Detector for the Two FOVs of Interest	60
Figure 30	4-12 Probability of Recognition Ranges in Mid-Latitude Summer Atmosphere Utilizing Scanning LWIR Detector for the Two FOVs of Interest	61
Figure 31	4-13 Probability of Recognition Ranges in Mid-Latitude Summer Atmosphere Utilizing Scanning MWIR Detector for the Two FOVs of Interest	62
Figure 32	4-14 Probability of Detection Ranges in Mid-Latitude Winter Atmosphere Utilizing Scanning LWIR Detector for the Two FOVs of Interest	64
Figure 33	4-15 Probability of Detection Ranges in Mid-Latitude Winter Atmosphere Utilizing Scanning MWIR Detector for the Two FOVs of Interest	65
Figure 34	4-16 Probability of Recognition Ranges in Mid-Latitude Winter Atmosphere Utilizing Scanning LWIR Detector for the Two FOVs of Interest	66

Figure 35	4-17	Probability of Recognition Ranges in Mid-Latitude Winter Atmosphere Utilizing Scanning MWIR Detector for the Two FOVs of Interest	67
Figure 36	4-18	Probability of Detection Ranges in Tropical Atmosphere Utilizing Staring LWIR Detector for the Two FOVs of Interest	69
Figure 37	4-19	Probability of Detection Ranges in Tropical Atmosphere Utilizing Staring MWIR Detector for the Two FOVs of Interest	70
Figure 38	4-20	Probability of Recognition Ranges in Tropical Atmosphere Utilizing Staring LWIR Detector for the Two FOVs of Interest	71
Figure 39	4-21	Probability of Recognition Ranges in Tropical Atmosphere Utilizing Staring MWIR Detector for the Two FOVs of Interest	72
Figure 40	4-22	Probability of Detection Ranges in Mid-latitude Summer Atmosphere Utilizing Staring LWIR Detector for the Two FOVs of Interest	74
Figure 41	4-23	Probability of Detection Ranges in Mid-latitude Summer Atmosphere Utilizing Staring MWIR Detector for the Two FOVs of Interest	75
Figure 42	4-24	Probability of Recognition Ranges in Mid-latitude Summer Atmosphere Utilizing Staring LWIR Detector for the Two FOVs of Interest	76
Figure 43	4-25	Probability of Recognition Ranges in Mid-latitude Summer Atmosphere Utilizing Staring MWIR Detector for the Two FOVs of Interest	77
Figure 44	4-26	Probability of Detection Ranges in Mid-latitude Winter Atmosphere Utilizing Staring LWIR Detector for the Two FOVs of Interest	79
Figure 45	4-27	Probability of Detection Ranges in Mid-latitude Winter Atmosphere Utilizing Staring MWIR Detector for the Two FOVs of Interest	80
Figure 46	4-28	Probability of Recognition Ranges in Mid-latitude Winter Atmosphere Utilizing Staring LWIR Detector for the Two FOVs of Interest	81
Figure 47	4-29	Probability of Recognition Ranges in Mid-latitude Winter Atmosphere Utilizing Staring MWIR Detector for the Two FOVs of Interest	82
Figure 48	5-1	Cost/Schedule Containment Analysis Network Flow	85
Figure 49	5-2	Distribution for High Risk Task (LWIR scanning detector)	87
Figure 50	5-3	Distribution for Moderate Risk Task (LWIR staring detector)	87
Figure 51	5-4	Distribution for Low Risk Task (MWIR staring detector)	88
Figure 52	5-5	Cost/Schedule Containment Curve	89
Figure 53	5-6	Cost/Schedule Containment Analysis Calculations-Representation of Data	90

LIST OF TABLES

<i>Number</i>		<i>Page</i>
Table 1	3-1 Elements of a scanning imaging system	23
Table 2	3-2 Elements of a staring imaging system	25
Table 3	3-3 System wavelength response	30
Table 4	4-1 LOWTRAN/MODTRAN choices	43
Table 5	4-2 MODTRAN Transmittance Data for both Midwave and Longwave Cases	45
Table 6	4-3 Model configurations for the eight detector systems decided upon	47
Table 7	4-4 Ranging results summary	84
Table 8	5-1 Values for Cost/Schedule Containment analysis network flow	85

CHAPTER I

INTRODUCTION

Analysis on the performance of an infrared imaging or FLIR (Forward Looking Infrared) system (a detector) is, in part, the subject of this paper. The infrared imaging industry has expanded rapidly since its practical beginnings in the mid 1960's with the history of IR research dating even farther back, i.e., Sir William Herschel's experiments in the early 1800's [1]. Upon discovery, Herschel referred to the new portion of the spectrum in its entirety by such names as "the invisible rays," "the thermometric spectrum," "the rays that occasion heat," and "dark heat" [1]. We recognize today that infrared (or heat radiation) and visible light are both forms of electromagnetic radiation and that they differ from one another in wavelength and frequency.

The infrared spectrum is part of the electromagnetic spectrum, with wavelengths ranging from about 0.75 μm to 1000 μm (1 mm) [2]. The infrared spectrum lies just above the visible spectrum, which spans the region from 0.3 μm to 0.8 μm , and below the millimeter region. There are various names for the various parts of the infrared spectrum, and they are used differently by different people. Most people consider the far infrared as ranging from about 25 μm to 1000 μm . This portion of the infrared spectrum is used primarily by astronomers and solid state physicists and will not be addressed in this paper. The remaining portion of the infrared spectrum, ranging from 0.75 μm to 25 μm , is divided into the short-wave infrared (SWIR), from 0.75 μm to 3 μm , the midwave infrared (MWIR), from 3 μm to 5 μm , and the long-wave infrared (LWIR), from 8 μm to 12 μm . The range from 12 μm to 25 μm is not used a great deal, but is referred to as the very long-wave infrared (VLWIR) and also will not be addressed in this paper. Thus, a FLIR system is a 'thermal imaging' system that allows one to

“see” electromagnetic radiation naturally emitted by warm objects in the region of $0.75\mu\text{m}$ to $25\mu\text{m}$, i.e., night vision.

As IR matured into a recognized technology, the annual sales of IR devices assumed significant proportions. The exact dollar figure in the United States today is up for considerable speculation, but it is possible to indicate some general limits on the figure. Most estimates assume that the sales to the military constitute about two-thirds of the total IR market. The remaining one third of the market consists of equipment for such applications as analytical infrared spectroscopy, process control, intrusion detection, fire monitoring or warning, law enforcement applications, astronomical applications, forensics, and medical diagnosis. One report given in 1968 estimated the total value of the IR industry at \$350 million [1]. Estimations today have the IR industry’s total worldwide worth reaching upwards of five billion U.S. dollars by the year 2010, Figure 1-1 [3]. It is obvious that Herschel’s discovery led to an important and lucrative industry.

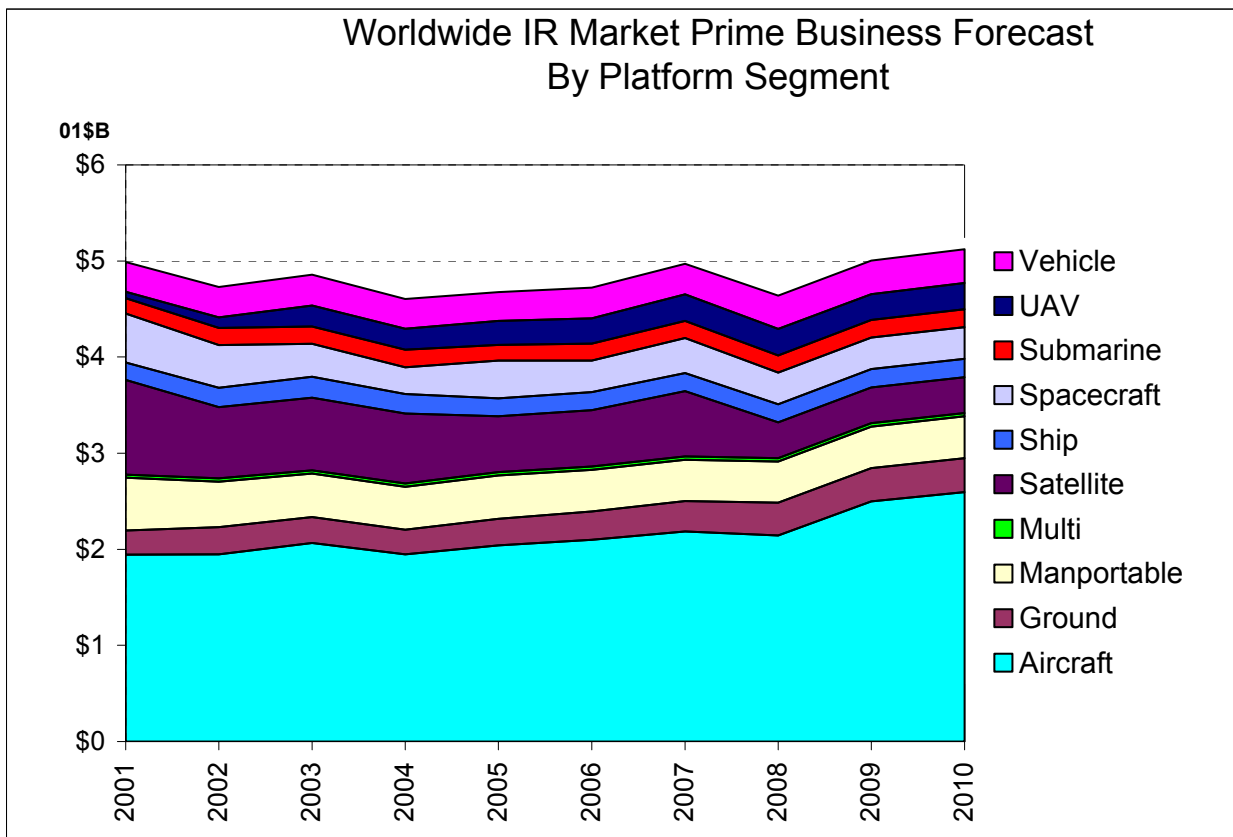


Figure 1-1 Representation of IR Worldwide Business in US Dollars by Platform [3]

Not only has IR technology spawned a very large industrial community dedicated to the manufacture of thermal imaging systems, it has spawned a need for their integration into many platforms, i.e., weapons systems, aircraft, vehicles, ships, spacecraft, submarines, and portable hand held devices. As a result, the characteristics of the people required to design and analyze these systems have changed dramatically from the lone inventor to a diverse team organized to follow a general discipline termed “organized creative technology” [4]. Organized creative technology covers the entire range of techniques and accepted methodologies that can be applied to transform a basic discovery into a manufacturable, usable item. *Systems engineering* offers a methodology specifically designed to discern the most efficient and most cost effective path through the entire process of developing and manufacturing a new product.

A general IR analysis on the performance of an infrared imaging detector is presented, in part, to familiarize the reader with the topic. The subject of the remaining portion of this paper is the methodology of practices and procedures Systems Engineers use to analyze, model, perform trade studies, and perform cost/risk assessment on these systems.

CHAPTER II

BACKGROUND INFORMATION

2.1 Literature Review

Recent advances have been reported on in nearly all of the major IR technologies and their incorporation into sensors for both military and civilian applications [5-10]. It is becoming more and more obvious that the technology and application issues are inseparable. In these days of decreased budgets or increased budget restraints (wanting more for less), technologists carry out research and development work with the specific requirements of the systems engineers foremost in their minds. The systems engineers, on the other hand, attempt to make efficient use of available and emerging technologies to satisfy the requirements of the customers and end users of the products. These problems are shared for all aspects of a thermal imaging sensor, i.e., IR optics, cooled and uncooled FPAs, signal processing, dual band sensing, and the design of systems in general. Considerations for systems, in general, range everywhere from the two main facets of the evolving requirements of the FPA (the detector and the read out integrated circuit) [5], to the manufacture of detectors and materials used for these systems [5, 11-13], to the operating size and applications of these systems [14-16].

IR optics and optical materials pose unique challenges for designers and engineers. From the materials typically used for the IR systems to the cold stops and thermal behavior of a system, relative to the visible region, many differences exist for the designer, manufacturer, and user of the IR optics [9, 17-20]. Both the designers and the engineers must consider these issues prior to implementing a system design. One large problem that has risen to the top has been

introduced by a requirement for simultaneous operation in the MWIR and the LWIR regions, while using a common optical system.

Progress toward third-generation thermal imagers is making leaps and bounds into the technological forefront, and a question continually asked is, “Do we need higher performance sensors, or should we concentrate on reducing sensor cost and increasing reliability?” In the case of military sensors, protecting high value platforms such as tanks, UAVs, and aircraft, the answer is always a resounding “YES!” Both aspects of this question need to be addressed and continually improved upon. This is true for all three services, although performance needs, and therefore requirements, are different for the Army, Navy, and Air Force. The translation of performance requirements into specific technological need will also be different. For example, one application may require a higher frame rate, while another no cryogenic cooling, and yet another a longer ranging capability for future thermal imagers. The one issue all three services seem to agree on is the need for simultaneously employing operation in two (or three) spectral bands. It is becoming more and more clear that multiband operation contributes to increasing target contrast, reducing background clutter and false alarms, decreasing vulnerability to countermeasures, and improving target designation accuracy in many scenarios under an expanded set of atmospheric conditions. [21-25]

There has been and continues to be significant studies and varying opinions about the “correct” wavelength for imaging system applications. There are two very distinct camps: one has deep roots in the midwave IR region of the electromagnetic spectrum and the other has deep roots in the longwave IR region of the electromagnetic spectrum, although, as mentioned above, these arguments may subside if acceptable dual band sensors are developed. It is not my intention to describe radiometric or atmospheric theory. There are many texts available for in

depth study of these two fields. I present an example in Chapter 3, which attempts to point out why the design of a system and its applications are important. The design parameters, and the modeling of these parameters, will be discussed in much more detail in Chapter 4.

Another question is one of technological capability, i.e., a scanning detector or a staring detector. This question is certainly much easier to answer and will be addressed in more detail in the reliability, risk analysis, and cost effectiveness portions of this paper (Chapter 5).

2.2 Background

In the design and development of a detector, an important step is to determine the operational requirements of the intended applications. This involves customer requirements and an analysis of the IR radiance levels of the expected imagery and generic descriptions of anticipated optics and cold shielding. Choice of spectral band is important in achieving good contrast between objects of interest and background clutter. Background levels may have large variations in terms of the standard deviation of the radiance within a given scene [26]. As the scene changes over time due to motion or slewing of the system, the apparent mean background radiance may change dramatically. The system FPA must be capable of supplying continuous imagery of high dynamic range without saturating the detector. Many applications require detection of point source edges while others involve target with various levels of detail and scene contrast. These specifics will dictate resolution and sensitivity requirements for the sensor, which in turn specify detector size and noise levels.

2.2.1 Customer Requirements

Customer X desires an infrared system for surveillance. The requirements given by the customer are that the system be one of the following:

- midwave IR or
- longwave IR.

Part of the selection criteria will be based on the least expensive system for the performance achieved. A second requirement from Customer X is that the IR detection system be either a detector of

- staring technology or
- scanning technology.

The selection criteria here is based on both the total cost of the system (with maintainability and reliability taken into consideration) and size as a whole of the system. The IR detection system will also be capable of being mounted on either

- a land vehicle or
- an unmanned aerial vehicle.

The selection criteria here is that the system with the least desirable performance will have to be more heavily weighted.

The customer has stated that the main purpose of this IR system is to detect unauthorized border incursions. The customer, as detection and recognition requirements, has also levied the following requirements:

- system shall not have a larger operating effective focal length than 18 cm due restrictions within the gimbal

- system shall be capable of detecting a man-sized target at minimum of 2 km (1 cycle based on the Johnson criteria)
- image shall be of high enough quality to enable the operator the ability to differentiate between a man-sized target and a smaller target (a rabbit, for example) at the detection range (2 km) to prevent false alarms (recognition at 4 cycles based on the Johnson criteria)
- image shall be of high enough quality to enable the operator the ability to detect and differentiate between stationary and moving targets
- image shall be of high enough quality to enable the operator the ability to distinguish between an organic (human) target and a mechanical (robot or engine) target.

It is known that the customer is located in southwestern Asia, which implies that the system will be used in mountainous regions as well as in coastal regions.

Because of the desired design of the detector system, some detector parameters of interest include the active size of the detector, the field of view (FOV), the speed of the optics (f/number), the operational wavelength, responsivity, integration time, and spectral detectivity (D^*). Other factors of interest include atmospheric conditions, system vibration, monitor characteristics, and scene content. Following is a discussion on each of these parameters in terms of both scanning detectors and staring detectors.

Performance parameters and the other factors of interest will be exploited through various iterations of “performance modeling”. Models to be discussed include MODTRAN, ACQUIRE, and NVTherm.

CHAPTER III

GENERIC DETECTOR PHYSICS

3.1 Infrared Imaging System Operation

Photon imaging systems are superior in performance to other passive sensing Electro-optical imaging devices. This is especially true when operability at any time of the day or night and under all weather conditions is of primary concern. The largest factors contributing to the superior performance of these sensors are the high contrast images produced and the availability of good atmospheric window materials [2]. Photon imaging systems tend to suppress the average value of the scene radiance so that only scene variations around that particular average are displayed, thus producing the high contrast image desired. Image intensifiers and low light level television systems rely largely on reflectance differences between the target and the background for detection and recognition, and in the visible region of the spectrum broadband reflectance difference between a target and its background tends to be small [27].

It is worth noting that ‘photon detectors’ are mentioned as a class of detectors. There are several types of photon detectors, namely Silicide Schottky-barrier devices, indium antimonide (InSb) detectors, mercury cadmium telluride (HgCdTe or MCT) detectors, SPRITE (signal processing in the element) detectors, and QWIP (quantum well infrared photodetector) detectors. For the purposes of this paper, only the InSb and the MCT photon detectors will be discussed.

InSb detectors are very well suited for MWIR operation and are very cost effective for fabrication at production level quantities. InSb detectors have an operating temperature range of 10 to 50 K. Although InSb detectors are only operable in the MWIR region, they can

accommodate very large size arrays. A recent example of which is 2048 by 2048 μm produced by Raytheon Infrared Operations in Goleta, CA. [5]

In contrast, HgCdTe detectors can span the entire IR portion of the electromagnetic spectrum. This means that the cutoff wavelength can be very well tuned to any desired value between 2 and 13 μm . HgCdTe detectors have an operating temperature range of approximately 30 to 300 K. Even with these seeming advantages, HgCdTe detectors still present some deficiencies. There are technological hurdles that must be overcome to increase the limited size of the array formats. Currently, the largest readily producible MCT array is 1000 by 1000 μm due to the limitations that lie with the current substrate configuration of cadmium zinc telluride (CdZnTe). [27]

As a standard convention, targets are labeled as either hot or cold with respect to the immediate background. For IR systems of interest, i.e., MWIR and LWIR, the term *thermal* is a bit misleading. Infrared imaging systems do not sense warmth or cold. They sense radiation emitted by an object, with respect to an ambient background. *Hot* refers to targets that appear warmer than the immediate background and *cold* means that a target appears cooler than its immediate background. The choice of hot objects appearing white and cold objects appearing black, in any given Electro-optical imaging system, is arbitrary and can be reversed with electronic polarity reversal, i.e., white hot or black hot. [27]

An Electro-optical (EO) imaging system consists of many subsystems. Each of these subsystems processes information differently. This can sometimes lead to certain EO systems displaying artificial artifacts or variations in an image that may not have been present in the original scene. The interplay of these subsystems, although slightly different within each system, is a factor in an EO system's performance. For the purposes of discussion, Figure 3-1 shows an

example of a general EO imaging system with five major subsystems: optics and scanner, detector and detector electronics, digitization, image processing, and post reconstruction.

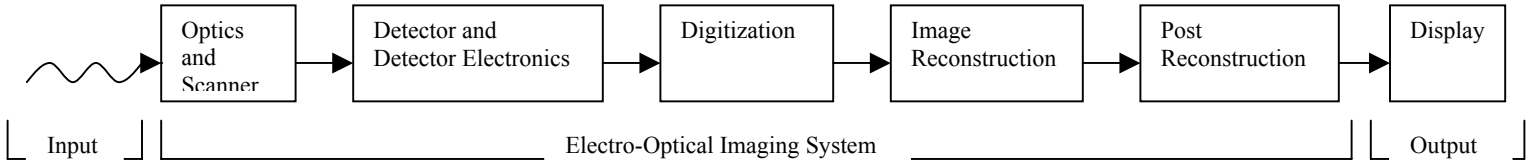


Figure 3-1 Generic Electro-Optical IR System functional block diagram

The specific design depends on the number of detector elements and the required detector output. The optical system images the radiation onto the detector(s). Scanners optically move the detector's instantaneous field of view across the FOV to produce an output voltage proportional to the 'local' scene intensity. In a scanning system, the output of a single detector represents the scene intensity across a single line. Staring arrays do not have scanning mechanisms and the adjacent detector(s) outputs provide scene variations. (Both types of array detectors will be discussed in more detail in subsequent sections.) The specific electronics design depends on the detector configuration and the desired output. The electronics design is beyond the scope of this paper and will not be discussed.

The detector is the heart of every EO system because it converts scene radiation into measurable electrical signal. Amplification and signal processing create an electronic *image* in which voltage differences represent scene intensity differences due to the various objects emitting radiation at different levels within the FOV. Each detector should have its own amplifier. The amplifier outputs are multiplexed together and then digitized. Signals are digitized because of the relative ease of manipulating digital data. Some systems rely heavily

upon software for gain/level normalization, image enhancement, and line-to-line interpolation. To produce a linear input-to-output system, a gamma correction algorithm removes the cathode ray tube (CRT)-based nonlinear response. The monitor, or display line pair quantity, may or may not be an integral part of the EO imaging system's perceived performance. The number of channels multiplexed together depends upon the specific design. Some systems currently in operation have several multiplexers and several A/D converters operating in parallel. [27]

System characteristics, observer experience, scene content, atmospheric transmittance, monitor settings, and a variety of other factors affect the perceived image quality. Figure 3-2 shows the connection between various image quality contributors that affect the perceived image quality of a detector.

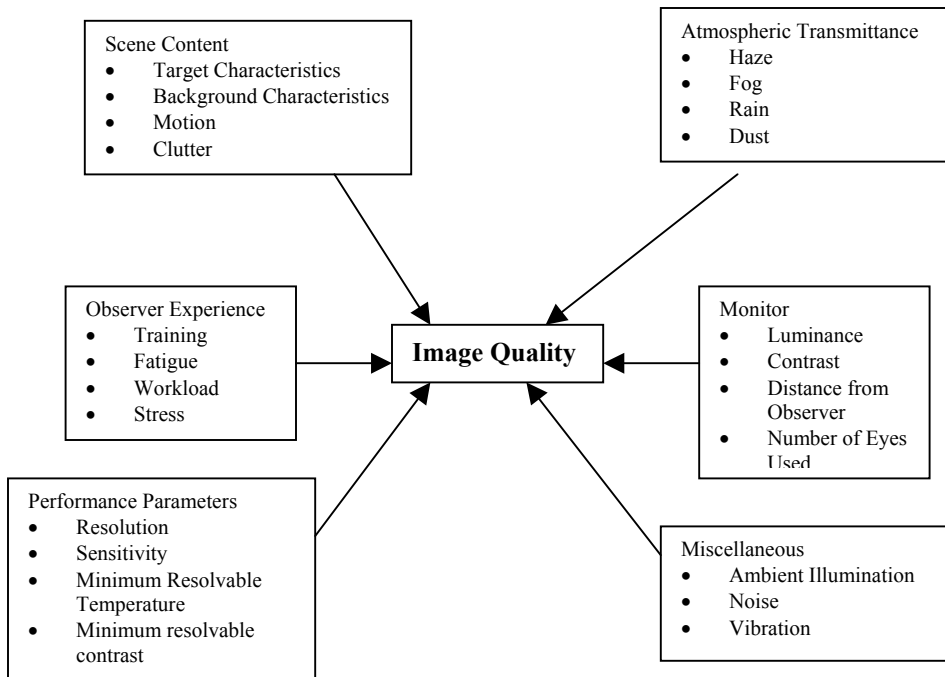


Figure 3-2 Various contributors that affect perceived image quality

The cause of a less than desirable image cannot be determined simply by looking at the image. To determine whether or not optimum quality has been achieved, it is necessary to verify focus, adjust level and/or gain, tune the monitor, measure the response to different sized targets, and measure the response to different target intensities. What does this all mean? Performance parameters for EO systems need to be quantified and understood to determine true detector performance, not just better image quality through electronic enhancement.

3.2 Scanning System Particulars

Scanning systems, which contain anywhere from 140 by 1 detector element assemblies to 480 by 4 detector element assemblies, have been widely used. Components of a conventional scanning thermal imaging system are listed in Table 3-1. This is the basic functionality that is incorporated into scanning detectors as a class. Particular systems may combine some functions and eliminate others. One possible implementation of a scanning FLIR is that the optical system collects, spectrally filters, spatially filters, and focuses the radiation pattern from the scene onto a focal plane containing a single detector element. An opto-mechanical scanner consists of a set of two mirrors, one sweeping vertically and the other sweeping horizontally. This scanner is generally placed outside the optical system and the detector, Figure 3-3. The amount of radiation reaching the detector(s) from the object moves as the mirrors move, tracing out a raster (unidirectional) pattern in object space, Figure 3-4a. Figure 3-4b illustrates how this series of detectors are summed together to provide time-delay and integration (TDI). The TDI data obtained is continually displayed in a waterfall manner, i.e., the imagery constantly moves down the monitor screen as the platform moves forward [28].

Table 3-1 Elements of a scanning imaging system

Scan synchronizer	Detector bias and preamplification circuits
Scan encoders	Video processor
Collecting optics and filters	Video monitor
Stabilization and pointing gimbals	System controls
Opto-mechanical scanner	Visual Optics
Detector assembly	Man in the loop
Detector cooler	

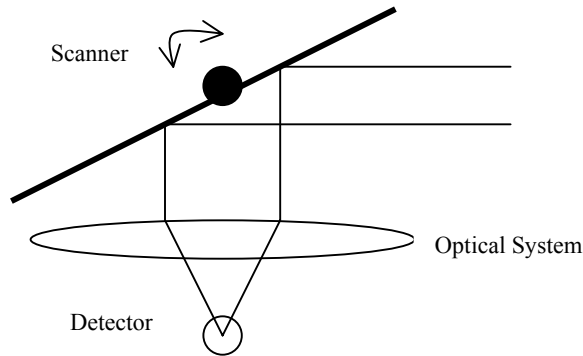


Figure 3-3 Location of scanning mechanism, outside the detector

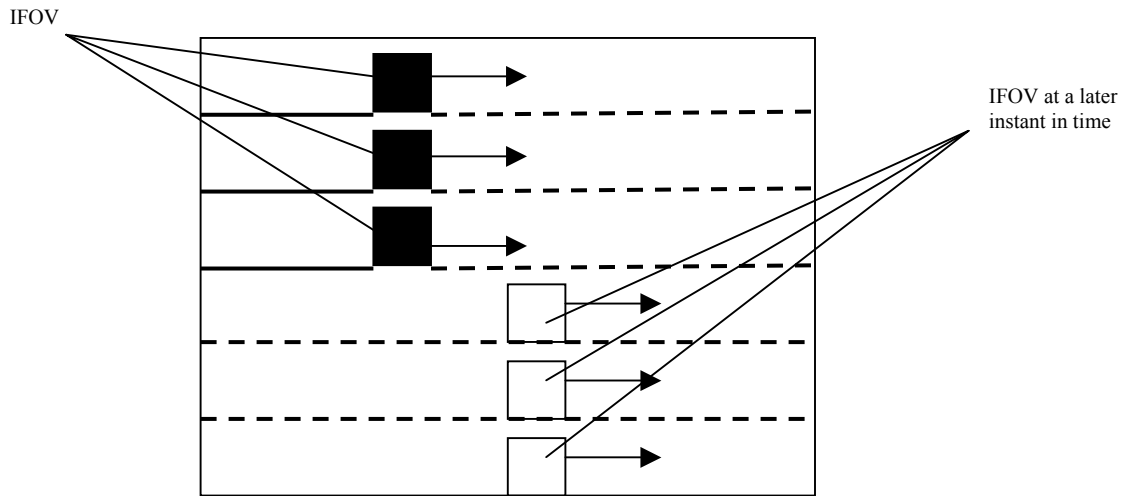


Figure 3-4a Multiple detectors operating in serial scan mode in horizontal direction, producing raster scan patterns from vertical interlace

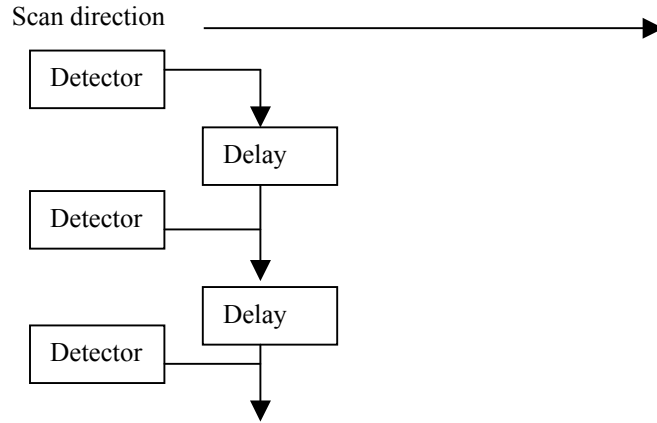


Figure 3-4b TDI delay elements

The noise of a scanning system is reduced by the square root of the number of TDI elements. A TDI arrangement has the additional advantage of multiple detectors, i.e., if a single detector element fails the remaining detectors will still produce an output.

Although scanning systems have been in production for years, they face a short lived and uncertain future on many platforms. These systems are generally larger and contain many more moving parts, which inevitably leads to more sources of possible failure. Likewise, because many new platforms are switching technologies, many parts are no longer manufactured, leading to a parts obsolescence issue. This issue will be discussed further in a later section of this paper.

3.3 Staring System Particulars

Staring detector systems are becoming more readily available, stable, and are sized anywhere from $40\mu\text{m}$ by $16\mu\text{m}$ to $2052\ \mu\text{m}$ by $2052\ \mu\text{m}$. [29] Figure 3-5 illustrates a generic, square staring detector array geometry. Components of a conventional staring thermal imaging system are listed in Table 3-2. It does not have a scanner. Each detector output is digitized by

the detector mux. While the amplifiers and filters exist in the mux, they do not process the signal in the same manner as the scanning system.

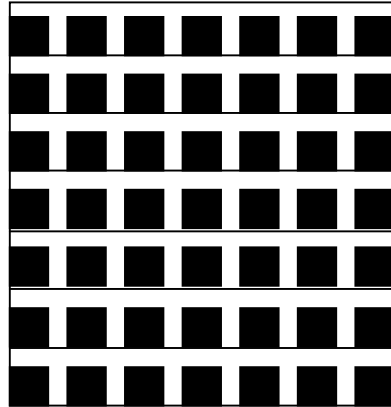


Figure 3-5 Generic representation of a square staring detector array

Table 3-2 Elements of a staring imaging system

Collecting optics and filters	Mux
Stabilization and pointing gimbals	Signal processing electronics
Reimager	System controls
Detector Assembly	Video monitor
Detector cooler	Man in the loop

Every detector/amplifier combination will have a different gain (responsivity) offset point. These variations result in a fixed pattern, or spatial, noise. If large deviations in responsivity exist, the image quality may be poor and result in an unrecognizable image. As a result, systems utilizing more than one detector may require a gain/level normalization or nonuniformity correction (NUC) algorithm to produce an acceptable image.

It is worth mentioning that LWIR staring detectors are currently in the research and development phase of their lifecycle and, therefore, are not currently in large scale production. This is due, in part, to the fact that industry focus has been shifted to dual band sensors and

image fusion. It is still going to be considered as a customer option for the purposes of this paper.

3.4 MWIR vs. LWIR

Since the advent of thermal imaging systems, many studies [1, 2, 26-28] and arguments have resulted over whether MWIR is a better imaging band than LWIR. There are volumes of material that cover the study and effects of the atmosphere. I only intend to give a general overview on why these two portions of the electromagnetic spectrum are of interest in thermal imaging applications with regard to certain platforms and customer requirements. Note that MWIR and LWIR are used in a generic sense. To call a system “MWIR” or “LWIR” says nothing about the precise response, which is a function of the detector material.

When electromagnetic radiation is propagated through the atmosphere from a source to a receiver, three major phenomena are observed:

- 1) Absorption and scattering of scene radiation out of the FOV reduce target signature, and the intensity of the radiation reaching the sensor is reduced,
- 2) Non-scene path radiance scattered into the FOV reduces target contrast,
- 3) Turbulence and aerosol forward scattering distort the image [2].

In addition, for background limited systems, path radiance and radiation scattered into the FOV affect the noise level. The nature and magnitude of these effects depend on the sensor type, sensor characteristics (spectral response, sensitivity, spatial resolution), the atmospheric components, and environmental conditions. [27]

Unfortunately, the merits of systems with different designs, i.e., scanning detector systems versus staring detector systems, are mingled with the relative merits of the atmospheric

transmittance values. Consequently, a comparison is made between a MWIR system and a LWIR system with the only difference being the detector spectral response and detectivity. This section identifies atmospheric effects.

The first argument for the merits of different system design is that the Rayleigh criterion. This suggests the MWIR region has a better resolution over an equivalent sized LWIR system [27]. The Rayleigh criterion is the ability to distinguish two point sources and is a good means of estimating the resolution capability of any diffraction-limited optical system. Thus the minimum separation at which two point sources can just be resolved is:

$$\theta = 1.22 (\lambda/D)$$

where θ is the angle (mrad) subtended by the two sources at the first principal point, λ is the wavelength in microns, and D is the effective aperture diameter in centimeters [1].

The second is that there is more differential signal available in the LWIR region when viewing terrestrial objects. Figure 3-6 illustrates an example of spectral transmittance over a 2 km path length for a tropical environment with a rural aerosol and a 12 km meteorological range. A 300 K normalized blackbody curve and its effects on received radiation are shown. It appears that more radiance is available in the LWIR region than in the MWIR region.

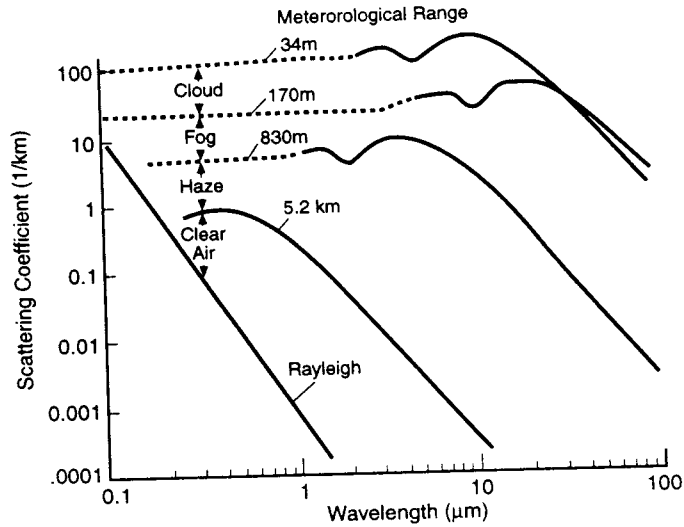


Figure 3-6 Relative scattering coefficients for different sized spherical particles. As particles grow in size, the scattering increases and they begin to affect the IR region. For small particles compared to the wavelength, scattering is proportional to Rayleigh scattering. For large particles, scattering is independent of wavelength. [27]

The approach shown in Figure 3-7 is appropriate for a DC coupled radiometer. The display is the difference between the target and its background. The small differences are amplified and displayed. Figure 3-8 shows the radiation difference between a 330 K background and a 305 K target. The LWIR still appears to provide more signal.

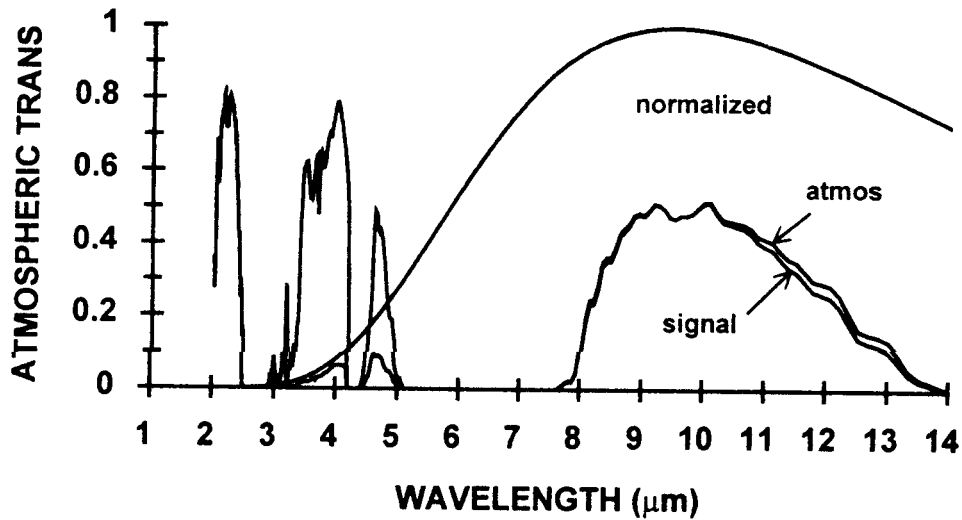


Figure 3-7 Atmospheric transmittance and 300 K blackbody curve. LWIR region appears to have more signal than the MWIR region. [27]

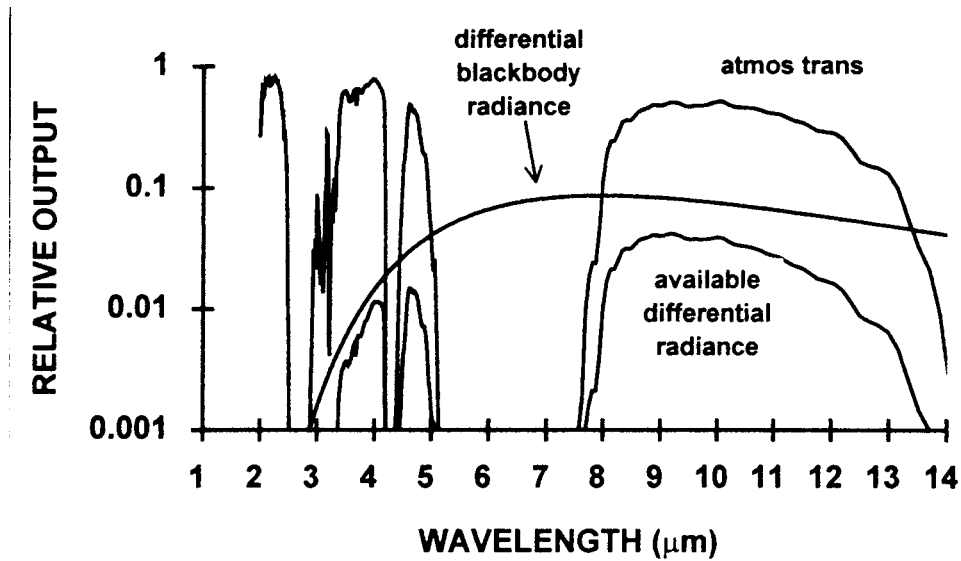


Figure 3-8 Incremental signal available from $\Delta T=5K$ target on a 300 K background. The detector output is proportional to the area under the differential radiance curve. [27]

Finally the detector spectral noise is added. Two systems are considered: a LWIR detector system and an identical system in which only the detector has been replaced with a MWIR detector. Table 3-3 provides the spectral response for each. Theoretically the detector peak response in the MWIR is about 3.8 times higher than the LWIR system [27]. The resulting output for the two spectral bands with the MWIR peak responsivity 3.8 times higher than the LWIR values is shown in Figure 3-9.

Table 3-3 System Wavelength Responses

SYSTEM	Normalized peak response	Minimum wavelength	Detector peak wavelength, λ_p	Detector cutoff wavelength, λ_c
MWIR	1	3.8 μm	4.8 μm	5.4 μm
LWIR	1/1.38	7.75 μm	10.8 μm	11.5 μm

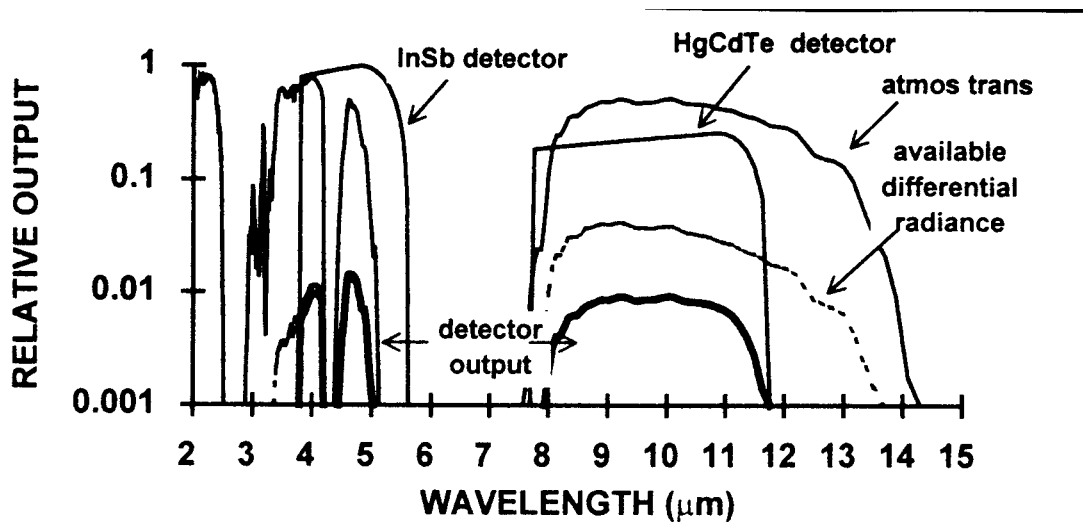


Figure 3-9 Incremental detector output created by a $\Delta T= 5$ K target on a 300 K background for MWIR and LWIR systems. [27]

The area under the curve is proportional to the detector output change in voltage and the outputs appear similar with no clear cut winner. The progression from Figure 3-7 to Figure 3-9 illustrates the system spectral response and system applications affect the spectrally averaged transmittance. (These results are unique to the values selected.)

The spectrally averaged transmittance has been calculated for the two detectors listed in Table 3-3. Three different environments were considered with three different meteorological ranges (7 km, 12 km, and 25 km) for each environment. An air to ground scenario was assumed in that the thermal imaging system is at a 500 ft altitude and the target is on the ground. The distance given in Figures 3-10 to 3-12 is the slant path.

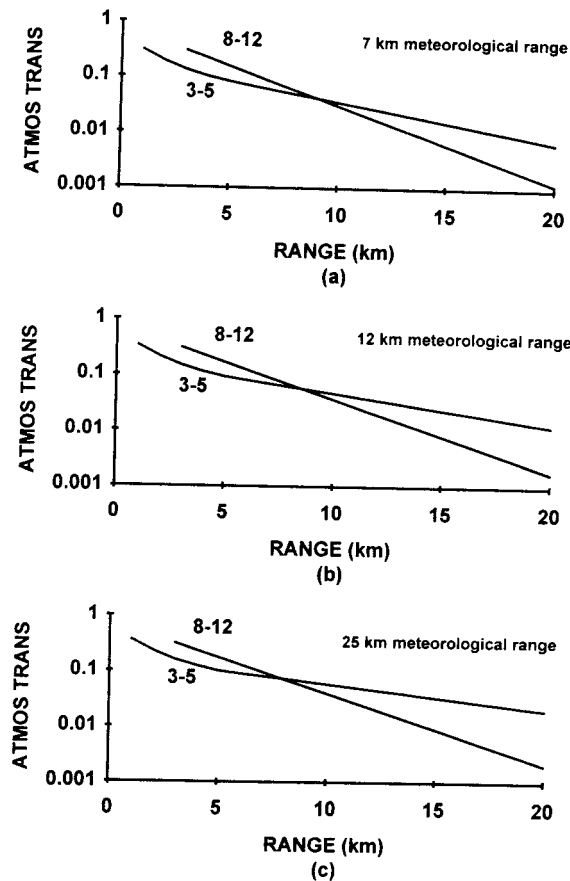


Figure 3-10 Spectrally averaged atmospheric transmittance for representative MWIR and LWIR systems. A tropical and urban aerosol were assumed. [27]

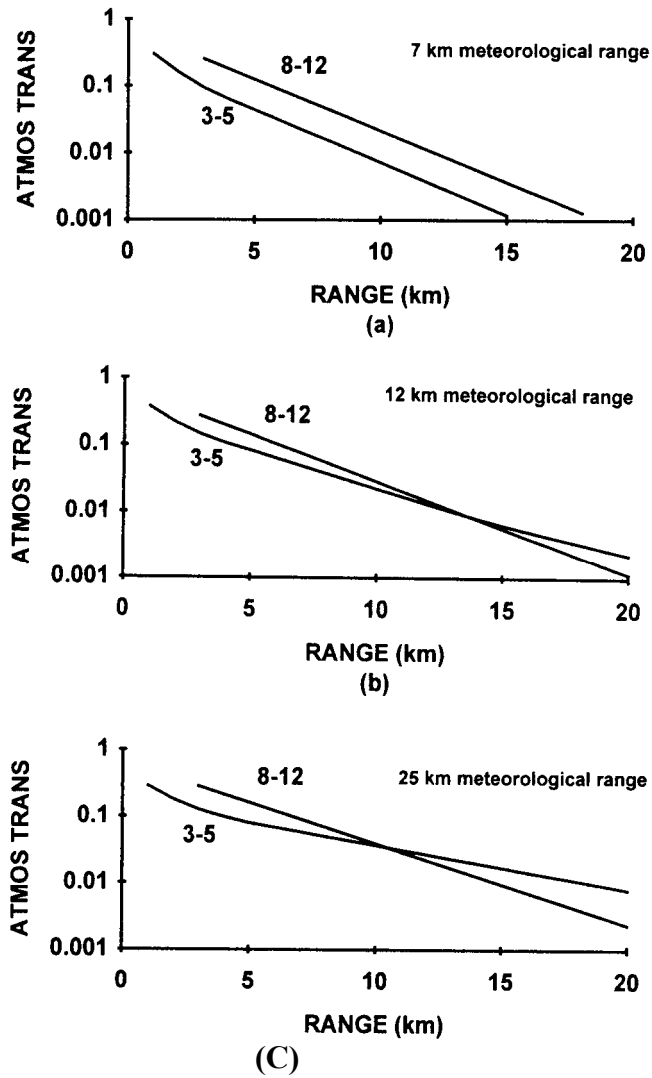


Figure 3-11 Spectrally averaged atmospheric transmittance for representative MWIR and LWIR systems. A tropical and a maritime aerosol were used. Different environmental conditions will produce different curves. [27]

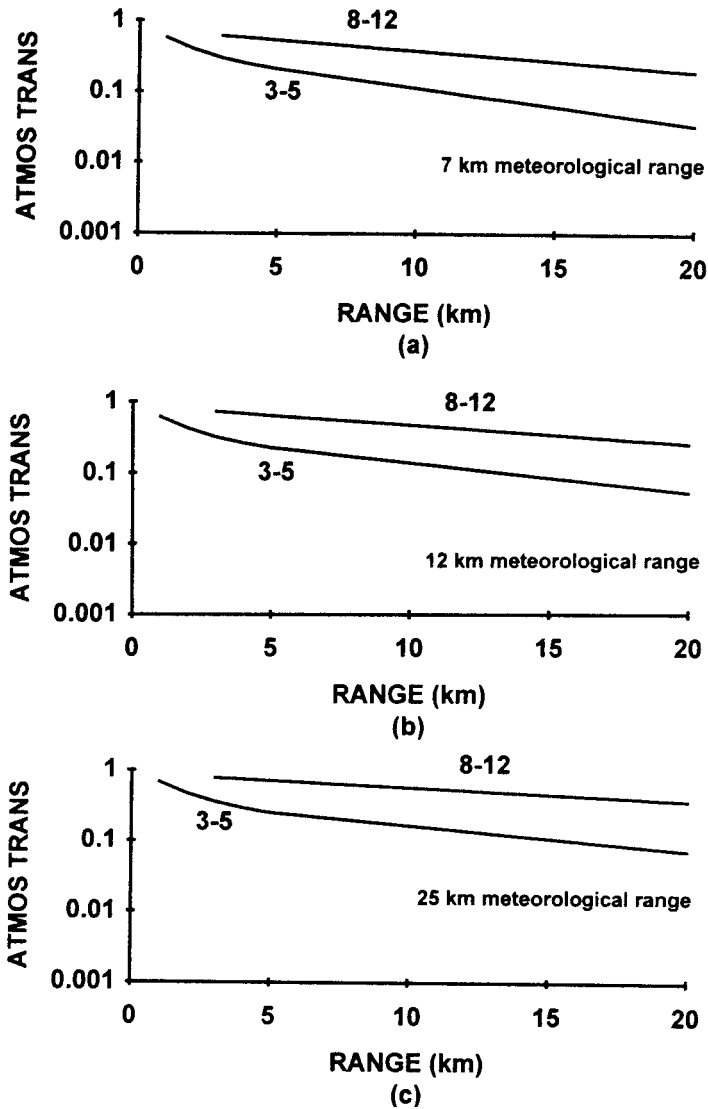


Figure 3-12 Spectrally averaged atmospheric transmittance for representative LWIR and MWIR systems. A mid-latitude winter environment and rural aerosol were assumed. [27]

The atmospheric transmittance depends on the amount of water vapor, aerosols, and other particulate species present. As the aerosol concentration increases, the particle sizes grow and the MWIR region is affected more than the LWIR region. The reverse is true in high humidity, low pressure situations where water vapor affects the LWIR region more than the MWIR region. Whether the MWIR transmittance is higher than the LWIR transmittance depends on the relationship between the visibility and the water vapor concentration. MWIR transmittance is

better only when the water vapor concentration and the aerosol concentration is low (long meteorological ranges). Even when this is true, the MWIR transmittance is better for the path lengths greater than 10 km for the particular sensors selected. The MWIR system must be designed to exploit the increased transmittance; if the task were to detect a target at a shorter range, then a LWIR detector should be selected.

Solar reflections are bothersome in the MWIR region. Some detectors have passive reflective filters which block radiation below about 3.4 μm . The function of this filter is to reduce the sensitivity of the detector and increase the noise equivalent temperature difference (NEDT). This needs to be taken into consideration if a detector system is required to have a very low NEDT. This is not an issue if the measurements are to be taken indoors or at night.

The selection of MWIR or LWIR depends on many factors. It is not possible to merely state that the MWIR region is better than the LWIR region, or vice versa. It is necessary to completely specify the system spectral response before making any conclusions. These include background temperature, atmospheric transmittance, system spectral response, and noise sources within the system. The magnitude of the noise depends on the integration time, amount of nonuniformity, optical transmittance, and operating temperature of the detector. Which band is better? As many sources say, "*It depends...*"

3.5 Optics

It is not my intention to describe theoretical optics or optical engineering in its entirety. I only try to give a general feeling for what function optical systems serve within the EO detector system as a whole. An assumption in describing the performance of an optical system is the use of a "distant source" or a "source at infinity" [1]. This means that the wave front (rays) entering

the optics can be considered as a plane rather than as a portion of a sphere due to the curvature of the lens as a function of the distance between the lens and the source of the emitted radiation.

This also means that the rays entering the optics appear parallel to one another, Figure 3-13.

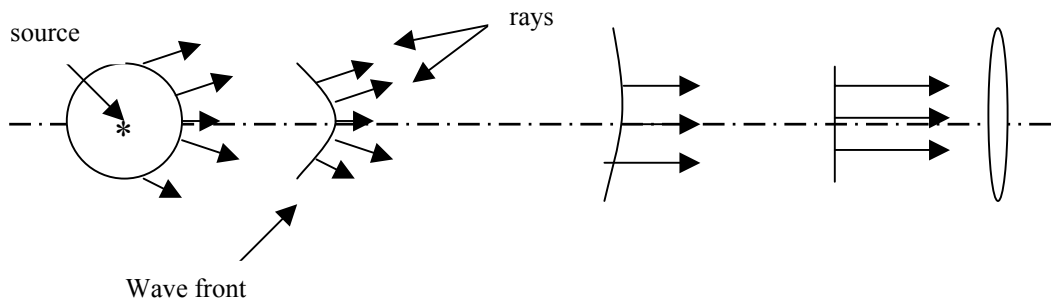


Figure 3-13 Wave fronts and rays at various distances from a source

The purpose of the optics in an IR system is to collect radiant flux, focus it, and deliver it to the detector. Optical systems operate analogously to a radar antenna used to receive echoes from a target. From the systems requirement document, the systems engineer knows what FOV the optics must cover, the speed of the optics ($f/\#$), the spectral region over which the system will operate, and into what space this system must fit.

Reduced to its basic elements, optical systems consist of one or more reflecting or refracting elements, i.e., individual lenses or mirrors. All elements are considered to be centered with respect to themselves; this means that the centers of curvature for each of the surfaces all lie on the same straight line (optical axis). Performance of the optics will be decreased if the optical axis is not held to due to poor manufacturing or careless mounting practices. Each element may have a different refractive index and shape to minimize aberrations. Optical subsystems are treated as a single element with one effective focal length (EFL), Figure3-14. The aperture is not

necessarily the diameter of an optical element, but it is determined by the optical design and limits the amount of scene radiation reaching the detector. P_1 and P_2 are principal surfaces and are assumed to be planes. The EFL is measured from the second principal plane. (The end lenses are assumed to be spherical and therefore every point on the surface is exactly a focal length distance away, Figure 3-15). [30]

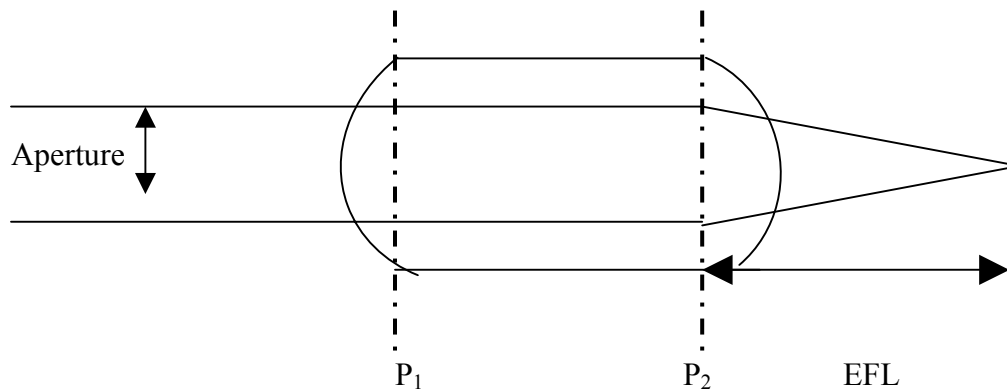


Figure 3-14 Optical system represented as a single optical element [30]

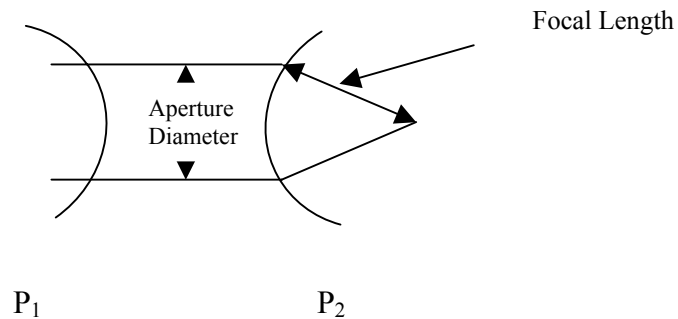


Figure 3-15 Representation of spherical planes [30]

CHAPTER IV

SYSTEM PARAMETERS AND MODEL DESCRIPTIONS

4.1 System Parameters

The factors involved in range performance analysis include

- the atmospheric spectral transmittance,
- background temperature,
- system spectral response (as a function of the detector material),
- system NETD,
- system MTF,
- target size,
- sensitivity,
- resolution,
- dwell time/integration time,
- target delta T,
- minimum resolvable temperature difference (MRT),
- range calculations (detection, recognition and identification).

These very important system parameters and the models used to obtain these parameters will be discussed in this chapter.

4.1.1 Minimum Resolvable Temperature (MRT)

For systems operating in the MWIR and the LWIR, a threshold value for radiance is needed to just perceive a target. This minimum value is the MRT. The MRT depends on the

systems sensitivity measurement as well as its resolution. (Resolution refers to the spatial frequency where the MRT asymptotically approaches infinity when MRT is plotted against delta temperature, ΔT .) In practice, MRT is measured by the ability of an observer to visually resolve a standard 4-bar target; in other words, MRT deals with an observer's ability to perceive low contrast targets embedded in noise. MRT measurements are used to predict the range at which a target can be detected, recognized, and identified. The Johnson criteria (methodology known as the equivalent bar pattern approach [27]) link the MRT to range performance for theoretical measurements and is used as an input in the ACQUIRE model for prediction of ranges. Different systems may have different MRTs, and those systems with lower MRT at low spatial frequencies, have a better thermal sensitivity.

4.1.2 Normalized Detectivity (D^*)

The normalized detectivity is a measure of detector performance. It includes the detector active area, the electronic bandwidth, and the noise equivalent power. Photon detectors usually desire a high D^* value and therefore are usually low noise devices. D^* can be calculated as follows:

$$D^* = R_D (\sqrt{A_D \Delta f}) / V_{rms}$$

where A_D is the active area of a detector, R_D is the responsivity (defined below), and V_{rms} is the root mean square of the input voltage. For photon detectors, it is often convenient to characterize D^* by its peak D^* and cutoff wavelength:

$$D^*(\lambda) = (\lambda / \lambda_p) D_p^*$$

4.1.3 Responsivity (R_D)

The responsivity of a detector is just the output voltage per unit input of radiant power.

The functional form of R_D is as follows:

$$R_D(\lambda) = [(q\lambda)\eta/(hc)] R_{\text{ext}}$$

where q is the electronic charge (1.6×10^{-19} coulombs), h is Planck's constant, c is the speed of light, and η is the quantum efficiency. The bracketed term is the detector's current responsivity with units of amps/watt. The external resistor, R_{ext} , converts the amps into a measurable voltage. It is noted that quantum efficiencies of both InSb and HgCdTe detectors can reach 90%. [27]

4.1.4 Noise Equivalent Temperature Difference (NETD) or Sensitivity

Sensitivity deals with the smallest signal that can be detected. It is usually taken as that signal that produces a signal to noise ratio of one (unity) at the system output. Sensitivity is dependent on the light gathering properties of the optical system (discussed earlier), the responsivity of the detector, and the noise of the system. For IR systems, the target-background intensity difference is specified by a differential in temperature, ΔT . The system noise is taken as the noise equivalent temperature difference, NETD.

4.1.5 MTF (Modulation Transfer Function)

The relationship between good image quality and best focus depends on MTF, the noise spectral density, the spatial frequency presented to the eye, and the scene content [27]. Generally, for a 'well-behaved' system, image sharpness is synonymous with the highest MTF. MTF is dependent on the wavelength of the incident radiation. For broad spectral response

systems, the MTF is a function of the spectral response of the system as well as the spectral characteristics of the source.

4.1.6 Dwell Time/Integration Time

Dwell time is an important parameter in scanning detectors. Dwell time is the time it takes for a target edge to be swept across a single detector element, and it is inversely proportional to the NETD. With many detectors scanning either in serial or parallel, the scan speed can be reduced. This increases the dwell time and lowers the NETD. Because each detector has a slightly different responsivity, multiple element systems suffer from fixed pattern noise that requires electronic correction [27]. The inability to fully compensate produces streaks in scanning arrays.

In staring systems, as the frame rate increases, the integration time decreases. The signal produced by the camera is proportional to the integration time in staring arrays. Therefore, the voltage produced drops as the integration time decreases. Increasing the system's internal gain can compensate for the voltage drop, but in staring arrays, NETD is inversely proportional to the square root of the integration time. As the integration time decreases, the NETD increases, which can in turn reduce the signal-to-noise ratio significantly when high frame rates are used. The reduction in signal-to-noise ratio (SNR) can be overcome by frame integration. The SNR improves by the square root of the number of frames averaged. Staring arrays, in principle, have the lowest NETD since the dwell time may be equal to the frame time, but because each detector has a slightly different responsivity, multiple element systems suffer from fixed pattern noise that requires electronic correction [28], which in staring arrays means NUC. Again, NUC is an

algorithm that electronically normalizes level and gain to remove most fixed pattern noise, thus aiding in image processing.

4.2 System Performance Models

The relationship between the three models to be described and detector system performance can be explained as follows. Atmosphere transmittance can be predicted from MODTRAN. These transmittances can then be used by ACQUIRE, along with minimum resolvable temperature differences obtained from NVTherm, to predict laboratory and field sensor performance, Figure 4-1.

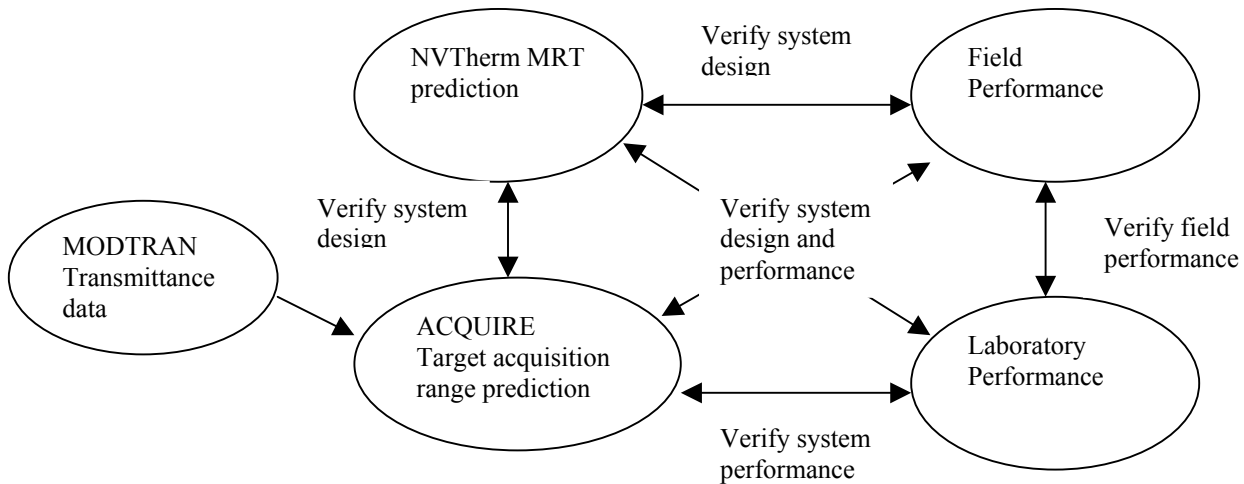


Figure 4-1 Model interactions and how they contribute to one another. NVTherm models the MRT achievable in the lab, and ACQUIRE models the target acquisition performance achievable in the field using transmittance data from MODTRAN and MRT data from NVTherm

4.2.1 Atmospheric Transmittance and LOWTRAN/MODTRAN

In principal determining the exact composition of the atmosphere over the path of interest can be done, but due to wide variations in weather conditions, it is desirable to have an

engineering approach to atmospheric modeling. This model should have several weather conditions and should be validated with available laboratory and field data.

To deal with these complex phenomena, the Philips Laboratory of Geophysics Directorate at Hanscom Air Force Base, Massachusetts developed codes to predict transmittance/radiance effects for varying conditions. LOWTRAN (low spectral resolution transmission), FASCODE (fast atmospheric signature code), MODTRAN (moderate spectral resolution transmission), and HITRAN (high-resolution transmission). [28]

MODTRAN's resolution is 200 μm , which should be sufficient for most wide band imaging systems. It provides spectral information from 0.25 to 28.5 μm . The code was developed in 1971 and has been continuously refined [28]. The code provides 32 plane-parallel layers with the boundaries extending from mean sea level to 100 km. 99.99997% of the molecular and particulate atmospheric constituents are found below 100 km [27]. The atmosphere is considered stable with no inversions, and each layer is homogeneous [26]. Layer thicknesses are 1 km from ground level to 25 km, 5 km from 25 km to 50 km (top of the stratosphere, and the last two layers are 20km and 30 km thick respectively [31].

The MODTRAN code contains representative (geographical and seasonal) atmospheric models, Table 4-1. The aerosol concentration is specified by meteorological range input. For any given slant geometry, it runs in two modes: 1) compute only transmittance and 2) compute both transmittance and radiance, which can be provided with and without solar or lunar scattering.

Table 4-1 LOWTRAN/MODTRAN Choices

ENVIRONMENT MODELS	AEROSOL MODELS
Tropical	Rural
Mid-Latitude Summer	Maritime
Mid-Latitude Winter	Urban
Sub-Arctic Summer	Desert
Sub-Arctic Winter	Troposphere
1976 Standard	Navy Aerosol Model

The rural, urban, and maritime models are boundary layer models that apply to the first two kilometers of the atmosphere. The troposphere model applies in the troposphere above the boundary layer but can also be used in the boundary layer under extremely good visibility conditions. It is worth stating that LOWTRAN/MODTRAN predict the atmospheric conditions of homogeneous environments only.

4.2.2 NVTHERM

NVTherm is a WindowsNT based computer program which models both scanning and staring thermal detectors that operate in the MWIR and LWIR portions of the electromagnetic spectrum. The model can only be used for thermal imagers which sense emitted radiation. NVTherm predicts the MRT difference that can be discriminated by a human when using a thermal imager. [33]

NVTherm uses specific detector parameters to calculate the MRT. This MRT is then used as an input for ACQUIRE for range calculation.

4.2.3 ACQUIRE

ACQUIRE is an analytical model that predicts acquisition performance for systems that image in the visible and IR spectral bands. Ranges and probabilities predicted by the model represent the expected performance of a trained observer with respect to an average target having a specified signature and size [32]. ACQUIRE can be operated in two modes: 1) target spot detection and 2) target discrimination. Calculations for target spot detection performance are based on signal to noise ratio theory and require that either minimum detectable contrast or minimum detectable temperature difference characterize the system. Calculations for target discrimination performance are based on a two-dimensional Johnson cycle criteria methodology and require that the system be characterized by either minimum resolvable contrast (MRC) or MRT difference. Application of the model is restricted to man in the loop systems [33]. Operation of this model is currently performed on a DOS platform.

The transmittance data is taken from the atmospheric transmission models and input into ACQUIRE along with the MRT data from NVTherm for the calculation and prediction of the target acquisition performance likely to be achieved by the sensor for detection, recognition, and identification range.

4.3 Modeling Results

4.3.1 MODTRAN results

For the purposes of Customer X and his requirements, three environmental models in combination with one aerosol model were used. These models were 1) *Tropical*, 2) *Mid-Latitude Summer*, and 3) *Mid-Latitude Winter*, with an aerosol model of *no aerosol attenuation*. Each of the three combinations was run with three slant path distances (2 km, 5 km, and 10 km) at three different altitudes (200 ft, 800 ft, and 3000 ft). These twenty-seven conditional

combinations were chosen because it was known that Customer X is located in southwestern Asia. (The mid-latitude winter environment was run with additional path lengths, accounting for a total of forty-three total runs. This is explained in the ACQUIRE results section.) Table 4-2 lists the resulting transmittance data for each of the conditional combinations for both the midwave and the longwave cases.

Table 4-2 MODTRAN Transmittance Data for both Midwave and Longwave Cases

Conditional Combination (Atmosphere, Altitude, Path Length)	Midwave Case (3.7 μ m- 5.05 μ m)	Longwave Case (8.2 μ m- 12.0 μ m)
Tropical, 200 ft, 2.0 km	.4606	.4755
Tropical, 200 ft, 5.0 km	.3191	.1843
Tropical, 200 ft, 10.0 km	.2062	.0434
Tropical, 800 ft, 2.0 km	.4662	.4950
Tropical, 800 ft, 5.0 km	.3254	.2023
Tropical, 800 ft, 10.0 km	.2121	.0514
Tropical, 3000 ft, 2.0 km	.4856	.5596
Tropical, 3000 ft, 5.0 km	.3471	.2683
Tropical, 3000 ft, 10.0 km	.2337	.0867
Mid-latitude Summer, 200 ft, 2.0 km	.4955	.6189
Mid-latitude Summer, 200 ft, 5.0 km	.3565	.3380
Mid-latitude Summer, 200 ft, 10.0 km	.2421	.1336
Mid-latitude Summer, 800 ft, 2.0 km	.5008	.6336
Mid-latitude Summer, 800 ft, 5.0 km	.3626	.3568
Mid-latitude Summer, 800 ft, 10.0 km	.2481	.1475
Mid-latitude Summer, 3000 ft, 2.0 km	.5193	.6807
Mid-latitude Summer, 3000 ft, 5.0 km	.3838	.4211
Mid-latitude Summer, 3000 ft, 10.0 km	.2698	.2008
Mid-latitude Winter, 200 ft, 2.0 km	.6088	.9091
Mid-latitude Winter, 200 ft, 5.0 km	.4876	.8121
Mid-latitude Winter, 200 ft, 10.0 km	.3752	.6862
Mid-latitude Winter, 200 ft, 15.0 km	.3036	.5864
Mid-latitude Winter, 200 ft, 20.0 km	.2529	.5039
Mid-latitude Winter, 200 ft, 25.0 km	.2148	.4354
Mid-latitude Winter, 200 ft, 30.0 km	.1849	.3774
Mid-latitude Winter, 800 ft, 2.0 km	.6121	.9122
Mid-latitude Winter, 800 ft, 5.0 km	.4921	.8183
Mid-latitude Winter, 800 ft, 10.0 km	.3803	.6957
Mid-latitude Winter, 800 ft, 15.0 km	.3087	.5981
Mid-latitude Winter, 800 ft, 20.0 km	.2580	.5172
Mid-latitude Winter, 800 ft, 25.0 km	.2196	.4492
Mid-latitude Winter, 800 ft, 30.0 km	.1896	.3917
Mid-latitude Winter, 800 ft, 35.0 km	.1654	.3421
Mid-latitude Winter, 800 ft, 50.0 km	.1149	.2301
Mid-latitude Winter, 3000 ft, 2.0 km	.6234	.9221
Mid-latitude Winter, 3000 ft, 5.0 km	.5078	.8382
Mid-latitude Winter, 3000 ft, 10.0 km	.3979	.7268
Mid-latitude Winter, 3000 ft, 15.0 km	.3271	.6372
Mid-latitude Winter, 3000 ft, 20.0 km	.2759	.5611
Mid-latitude Winter, 3000 ft, 25.0 km	.2370	.4963
Mid-latitude Winter, 3000 ft, 30.0 km	.2064	.4407
Mid-latitude Winter, 3000 ft, 35.0 km	.1815	.3919
Mid-latitude Winter, 3000 ft, 50.0 km	.1288	.2780

Regardless of the atmospheric condition, as slant path distances increased, transmittance values decreased for both midwave and longwave cases. In general, the transmittance values are marginally higher in the longwave case, which follows reason given that there is more energy available in the longwave region of the electromagnetic spectrum. This is not meant to imply that the LWIR is the better operational region. Transmittance data is only one aspect of the modeling and decision making criteria.

4.3.2 NVTHERM results

Based on the requirements stated by Customer X, the four primary parameters of concern for actual model of the detector are:

- 1) the type of technology (scanning or staring),
- 2) the objective lens configuration for operating wavelength (MWIR or LWIR) and effective focal length (EFL),
- 3) the operating FOV,
- 4) the actual dimensions of the detector along with its D^*_p .

Table 4-3 lists the model configurations for each of the eight detector systems decided upon.

Table 4-3 Model configurations for the eight detector systems decided upon

Technology	Objective lens configuration: Operating wavelength	EFL	Operating FOV (Horizontal by vertical)	Actual Detector specifics: Size and number	Peak D* (cm-sqr(Hz)/Watt)
Scanning	LWIR	18 cm	2.0° x 1.5°	(12 x 20)μm 1 (h) x 140 (v)	6e11
Scanning	LWIR	18 cm	2.66° x 2.0°	(12 x 20)μm 1 (h) x 140 (v)	6e11
Scanning	MWIR	18 cm	2.0° x 1.5°	(12 x 20)μm 1 (h) x 140 (v)	6e11
Scanning	MWIR	18 cm	2.66° x 2.0°	(12 x 20)μm 1 (h) x 140 (v)	6e11
Staring	LWIR	18 cm	2.0° x 1.5°	(20 x 20)μm 320 (h) x 240 (v)	6e11
Staring	LWIR	18 cm	2.66° x 2.0°	(20 x 20)μm 320 (h) x 240 (v)	6e11
Staring	MWIR	18 cm	2.0° x 1.5°	(20 x 20)μm 320 (h) x 240 (v)	6e11
Staring	MWIR	18 cm	2.66° x 2.0°	(20 x 20)μm 320 (h) x 240 (v)	6e11

The EFL, 18 cm, was a fixed variable from the customer and could not be changed. The vertical field of view is a function of the actual detector specifics, primarily size, number of detectors, and the EFL. The D*, as previously mentioned, is a performance measurement of the detector. The physical size of the detectors is a function of what is technologically available and manageable within the customer constraints.

Each of these eight detector configurations was input into NVTherm along with other information, such as display information and operator’s viewing distance from the monitor, for the calculation of system specific MRT data. (An example of a LWIR and a MWIR configuration input file can be found in Appendix B.)

Operating MRTs are shown for each of the eight detector configurations on four different graphs. The data is grouped by technology and wavelength, i.e., LWIR staring, LWIR scanning, MWIR scanning, and MWIR staring, with each of the two FOV configurations represented, Figures 4-2 through 4-5. In each of the following graphs, MRT is represented as a function of

cycles per milliradian as the temperature changes. The 2D MRT data is plotted because it takes both horizontal and vertical operating dimensions into account simultaneously and most closely represents an actual operating system.

Two FOV representation of Scanning Detector MRT data for MWIR

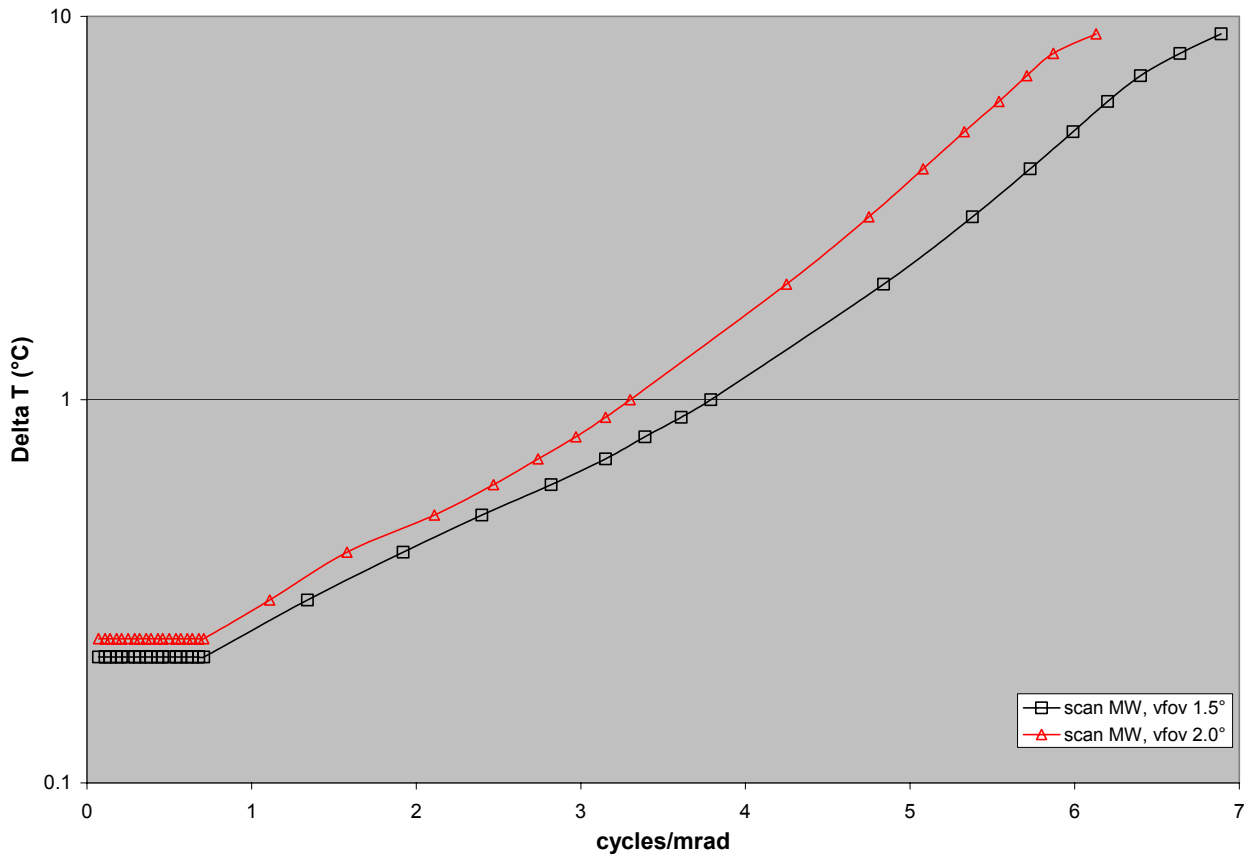


Figure 4-2 MRTs for Scanning MWIR detector system: two VFOVs

Two FOV representation of Scanning Detector MRT data for LWIR

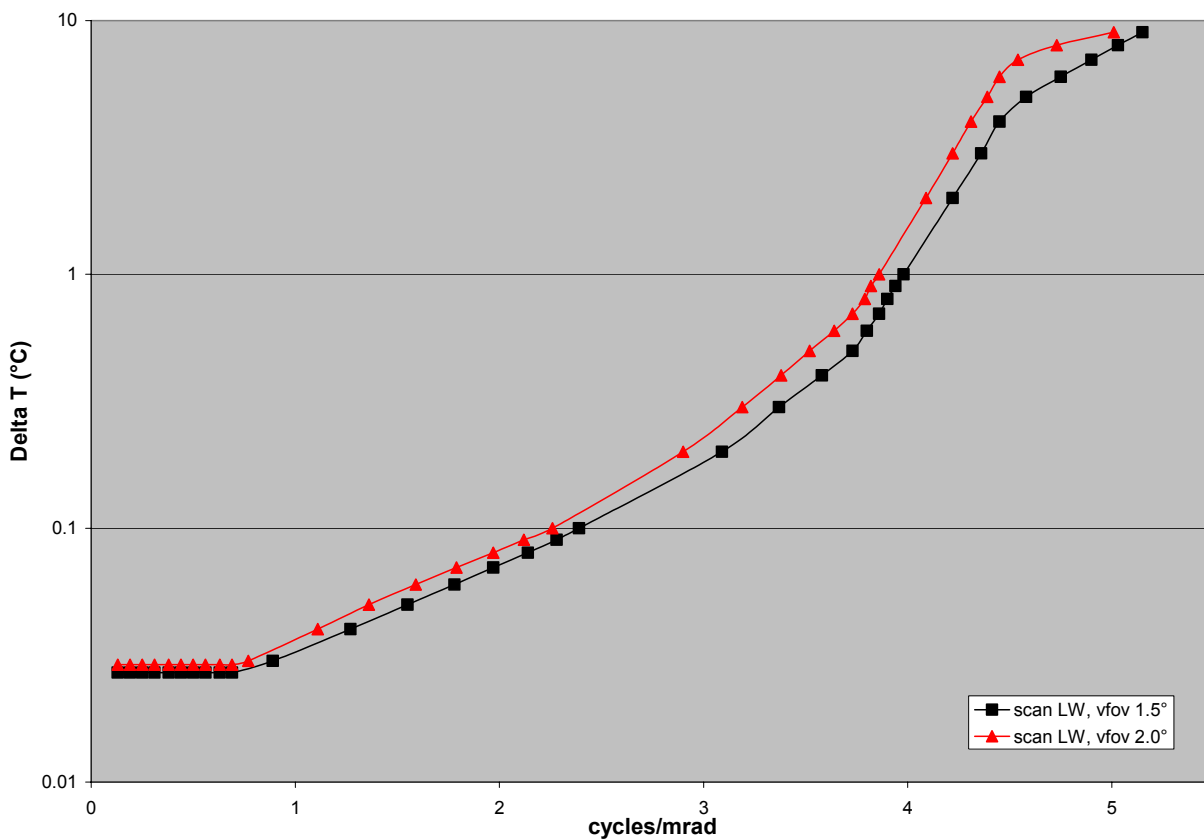


Figure 4-3 MRTs for Scanning LWIR detector system: two VFOVs

Two FOV representation of Staring Detector MRT data for MWIR

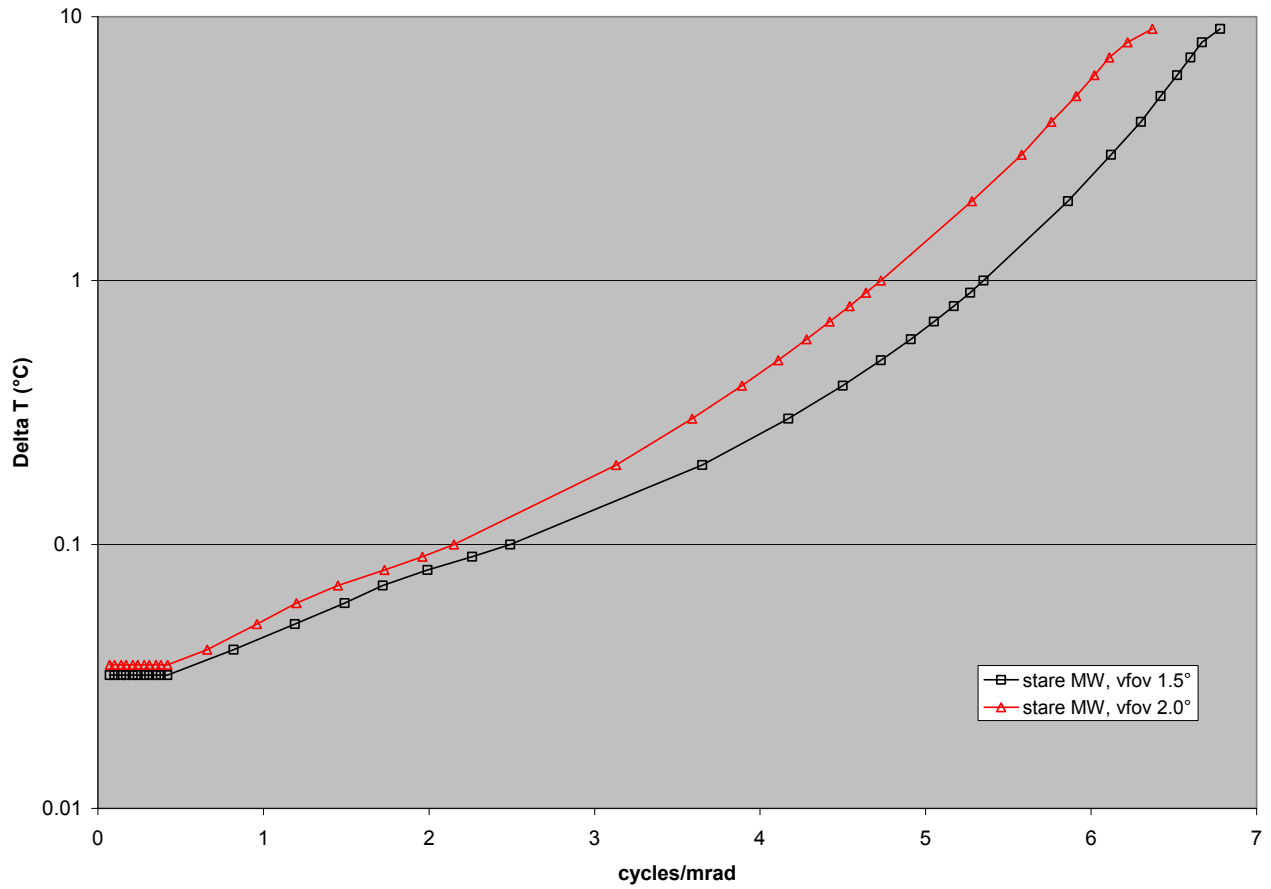


Figure 4-4 MRTs for Staring MWIR detector system: two VFOVs

Two FOV representation of Staring Detector MRT data for LWIR

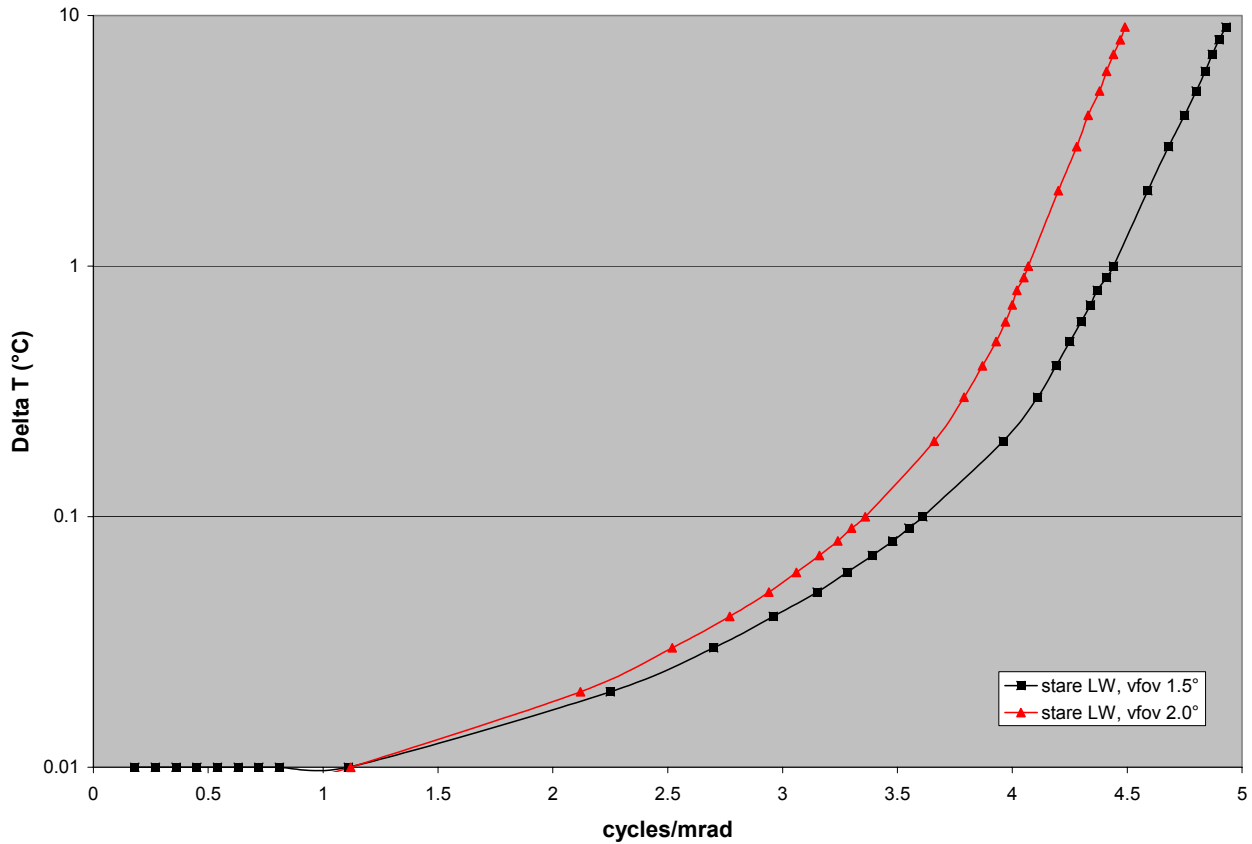


Figure 4-5 MRTs for Staring LWIR detector system: two VFOVs

The MRT depends on the systems' sensitivity measurement as well as their resolution. Resolution in these graphs refers to the spatial frequency where the MRT asymptotically approaches infinity when MRT is plotted against ΔT . MRT deals with an observer's ability to perceive low contrast targets embedded in the image noise. MRT measurements are used to predict the range at which a target can be detected, recognized, and identified. The Johnson criteria link the MRT to range performance for theoretical measurements. The MRT is then used as an input for the ACQUIRE model in calculating range predictions. Different systems may have different MRTs, as is demonstrated in the above four graphs. The general shape

represented in each of the four graphs is mirrored when two of the three variables are held constant, i.e., detector technology (staring) and wavelength (MWIR). The MRT curve shifts as a function of the size of the FOV and how it affects resolution. Those systems with lower MRT at lower spatial frequencies, have a better thermal sensitivity.

It appears that the systems utilizing the FOV configuration of $2.0^\circ \times 1.5^\circ$ have better thermal sensitivity. It also appears that the MWIR bandwidth provides for a greater number of cycles per milliradian regardless of which technology is utilized. This implies that with no further test measurements, an observer would be able to better perceive low contrast targets with the smaller FOV ($2.0^\circ \times 1.5^\circ$) configuration utilizing the MWIR bandwidth. The remaining test measurements may or may not substantiate this claim. It is important to point out the fact that MRT is not dependant on atmospheric conditions or altitudes.

4.3.3 ACQUIRE results

Based on Customer X's requirements for detection and recognition based on the Johnson criteria, the eight MRTs (from each of the detector configurations, Table 4-3) and transmittance values (grouped by environmental condition, Table 4-2) were input into ACQUIRE for both longwave and midwave cases. The Johnson criterion is generally stated as a definition of spatial resolution by using line pairs. For example, a line pair is equal to a bar and a space, or one cycle across a target, i.e., the 50% probability of detection at one cycle. The ACQUIRE program runs in an iterative loop, calculating ranges based on individual sets of MRT values and environmental combinations that have transmittance values entered. (An ACQUIRE input file, using the longwave transmittance values, can be found in Appendix B.)

Detection and recognition ranges for each case are represented in Figures 4-6 through 4-29. Wavelength, technology, atmosphere, and a comparison of each of the two vertical FOV configurations group the information contained within each graph. More range data points needed to be obtained on some of the graphs in order to make the 50% probability point in accordance with the Johnson criteria and Customer X's requirements. Any range point beyond the 50% probability point is additional data.

In each of the following graphs, ranges are represented as a function of a 50% or better probability of being able to "see" a target at a particular range. It goes with reason that being able to detect and/or recognize a target at a greater distance is desirable for this customer's particular application. The closed symbology represents the 2.0° x 1.5° FOV detector configurations, and the open symbology represents the 2.66° x 2.0° FOV detector configurations. The color similarity represents the same altitude for the two different FOVs. It is worth mentioning that the detection/recognition *footprint* generally expands to obtain greater ranging performance the greater the altitude. (An analogy for this would be that if one was holding a flash light and standing only a few inches from a wall in a dark room, the illuminated wall area would be quite small. As one steps back from the wall, the illuminated wall area would grow, with until enough distance and candlepower, until the entire wall is illuminated.)

Results for each grouping (atmospheric condition, technology, and spectral region: two for detection and two for recognition) are stated explicitly following the *Recognition range* graphs. A more concise listing of the results is located in Table 4-4 of section 4.4 entitled *Results Summary*.

4.3.3.1 Detection and Recognition Ranges for Scanning technology in Tropical atmosphere

Detection Ranges:

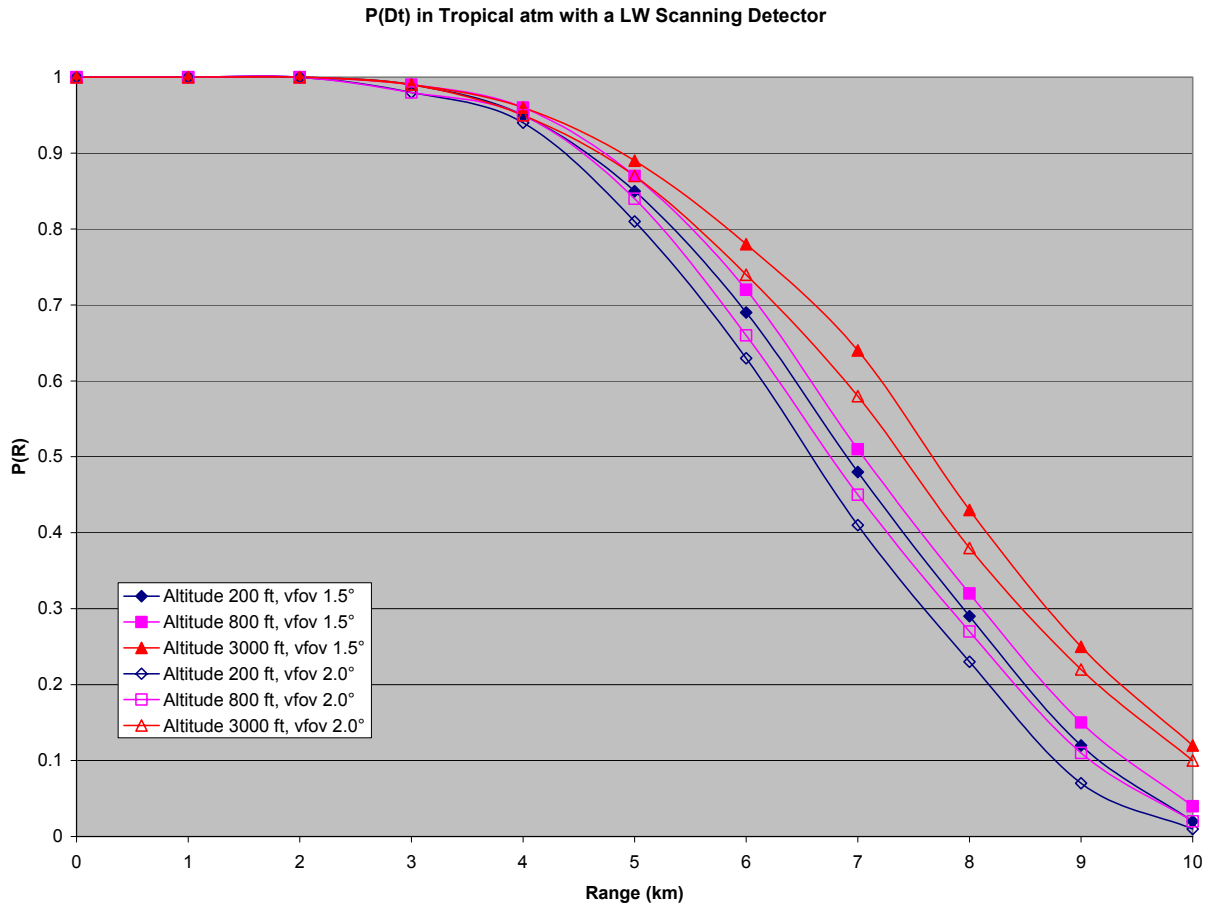


Figure 4-6 Probability of Detection Ranges in Tropical Atmosphere Utilizing Scanning LWIR Detector for the Two FOVs of Interest

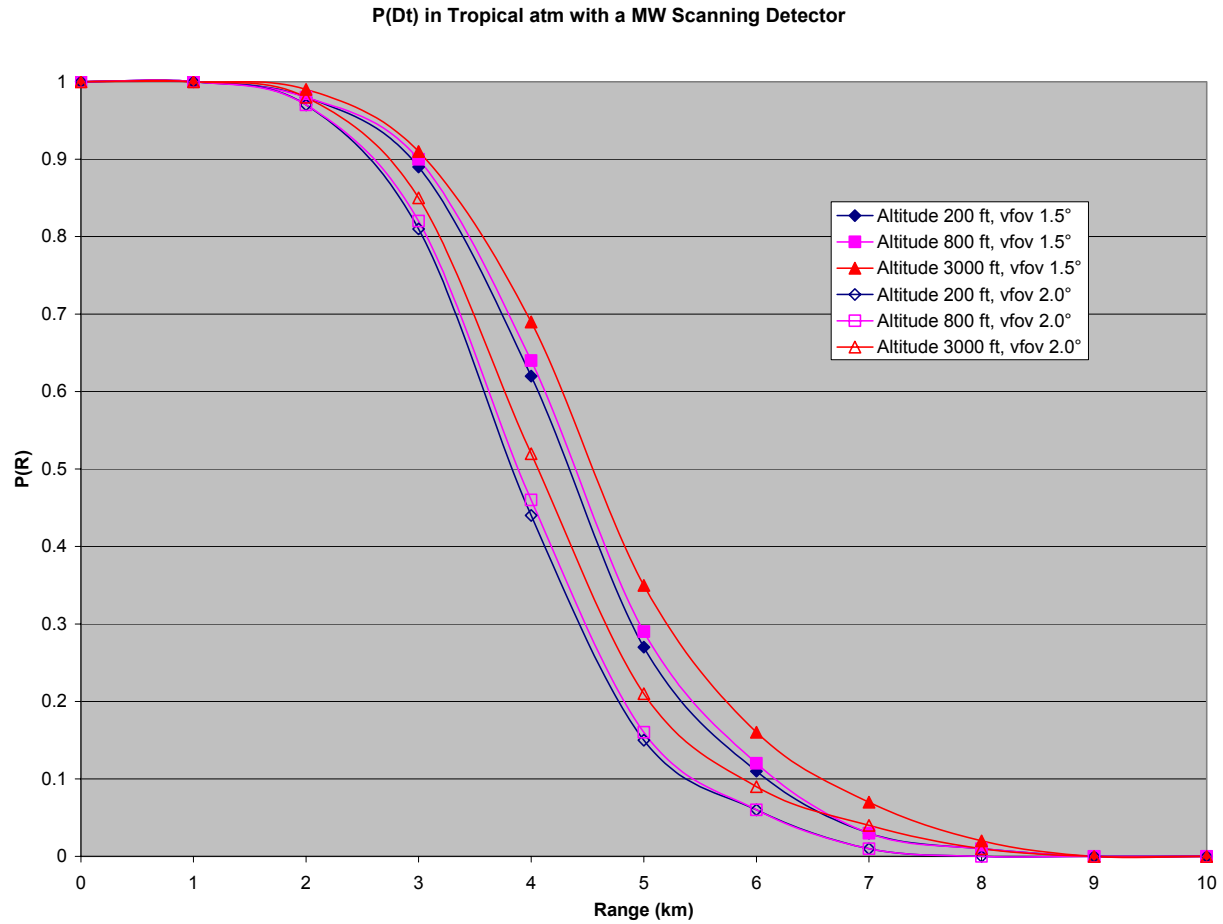


Figure 4-7 Probability of Detection Ranges in Tropical Atmosphere Utilizing Scanning MWIR Detector for the Two FOVs of Interest

Recognition Ranges:

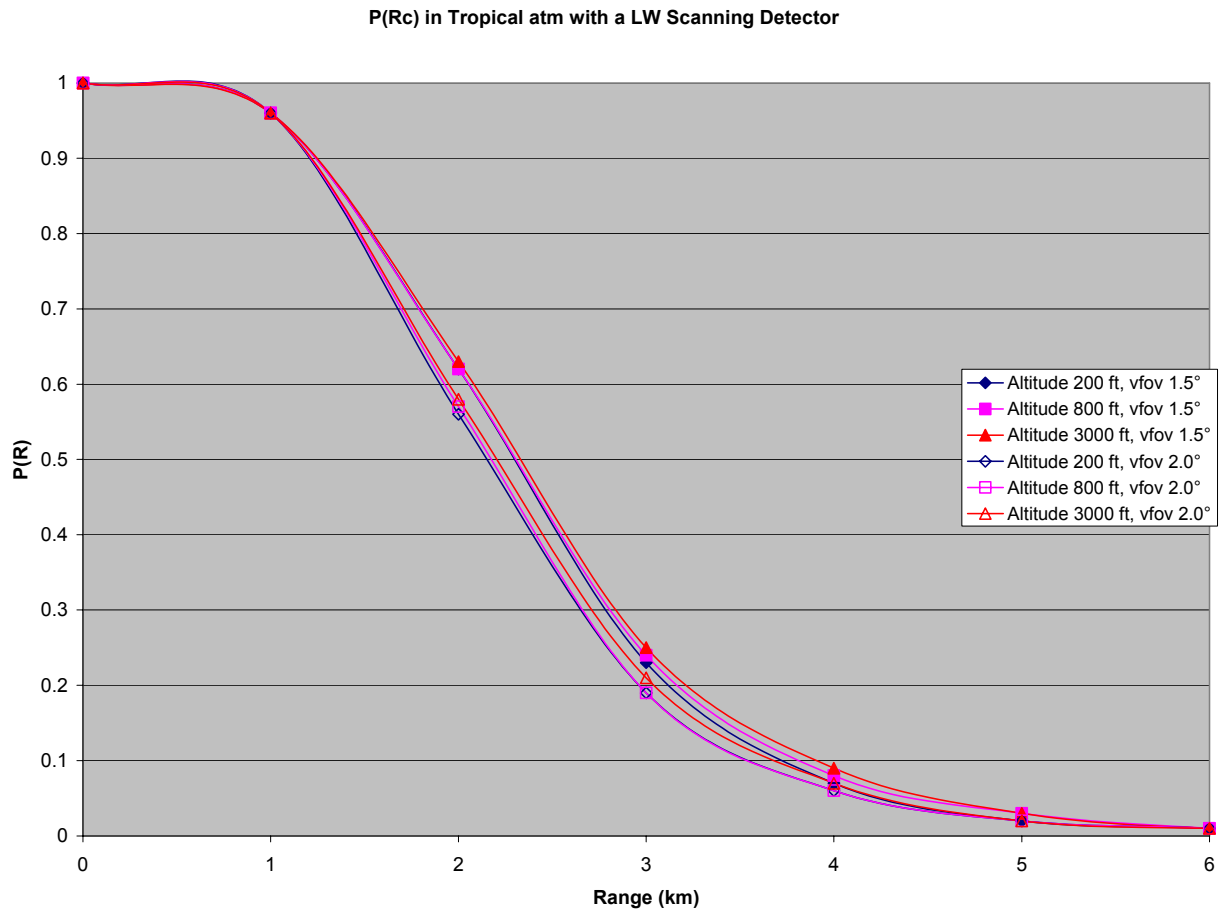


Figure 4-8 Probability of Recognition Ranges in Tropical Atmosphere Utilizing Scanning LWIR Detector for the Two FOVs of Interest

P(Rc) in Tropical atm with a MW Scanning Detector

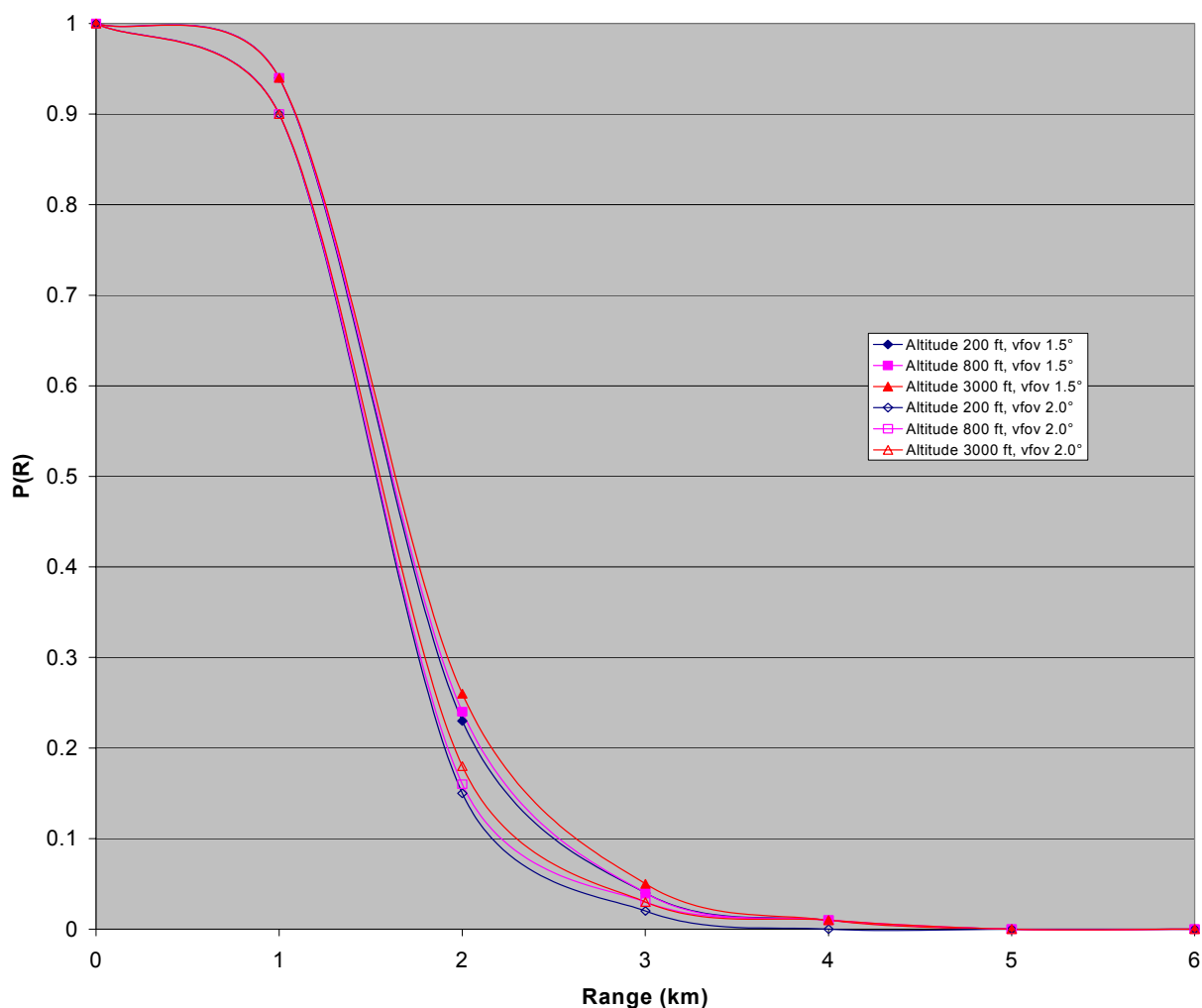


Figure 4-9 Probability of Recognition Ranges in Tropical Atmosphere Utilizing Scanning MWIR Detector for the Two FOVs of Interest

For this particular atmosphere (Tropical) and technology (scanning), a comparison of the two *Detection range* graphs results in two distinct conclusions:

- 1) 1.5° VFOV configuration out-performing the 2.0° VFOV configuration on a consistent basis, all things being equal
- 2) LWIR detector yields longer ranges than does the MWIR detector.

When comparing the 3000 ft (0.9144 km) altitude series for the four configurations, the result is that the 1.5° VFOV configuration produces a 7.75 km range for the LWIR detector,

while the MWIR detector produces a range of 4.75 km. Even at the lowest altitude (200 ft), the LWIR detector has a longer ranging capability than that of the MWIR at an altitude of 3000 ft for both FOV configurations, i.e., LWIR detector with VFOV 1.5° at 200 ft ranges at 7.25 km and LWIR detector with VFOV 2.0° at 200 ft (0.06096 km) altitude ranges at 6.8 km while MWIR detector with VFOV 1.5° at 3000 ft ranges at 4.75 km.

The *Recognition range* graphs yield the same two conclusions, although not with as great a margin. The LWIR detector yields approximately 2.5 km for all altitudes with the VFOV 1.5° configuration, while the MWIR detector yields approximately 1.75 km for all altitudes at the same VFOV 1.5° configuration. For the VFOV 2.0° configuration, the results are again similar, i.e., LWIR detector yields approximately 2.2 km for all altitudes while the MWIR detector yields approximately 1.5 km for all altitudes. These conclusions may not be the same as more data is analyzed.

4.3.3.2 Detection and Recognition Ranges for Scanning technology in Mid-latitude Summer atmosphere

Detection Ranges:

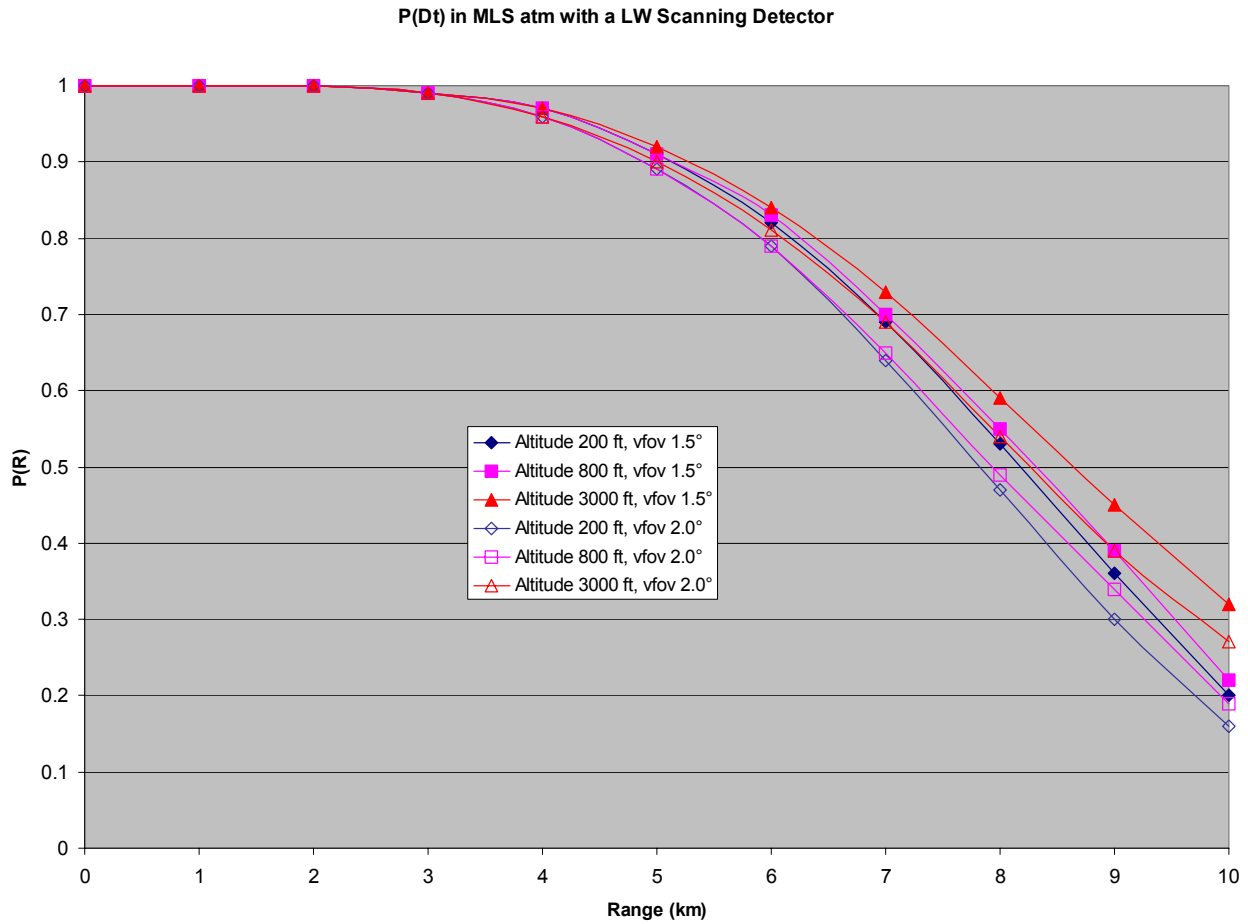


Figure 4-10 Probability of Detection Ranges in Mid-Latitude Summer Atmosphere Utilizing Scanning LWIR Detector for the Two FOVs of Interest

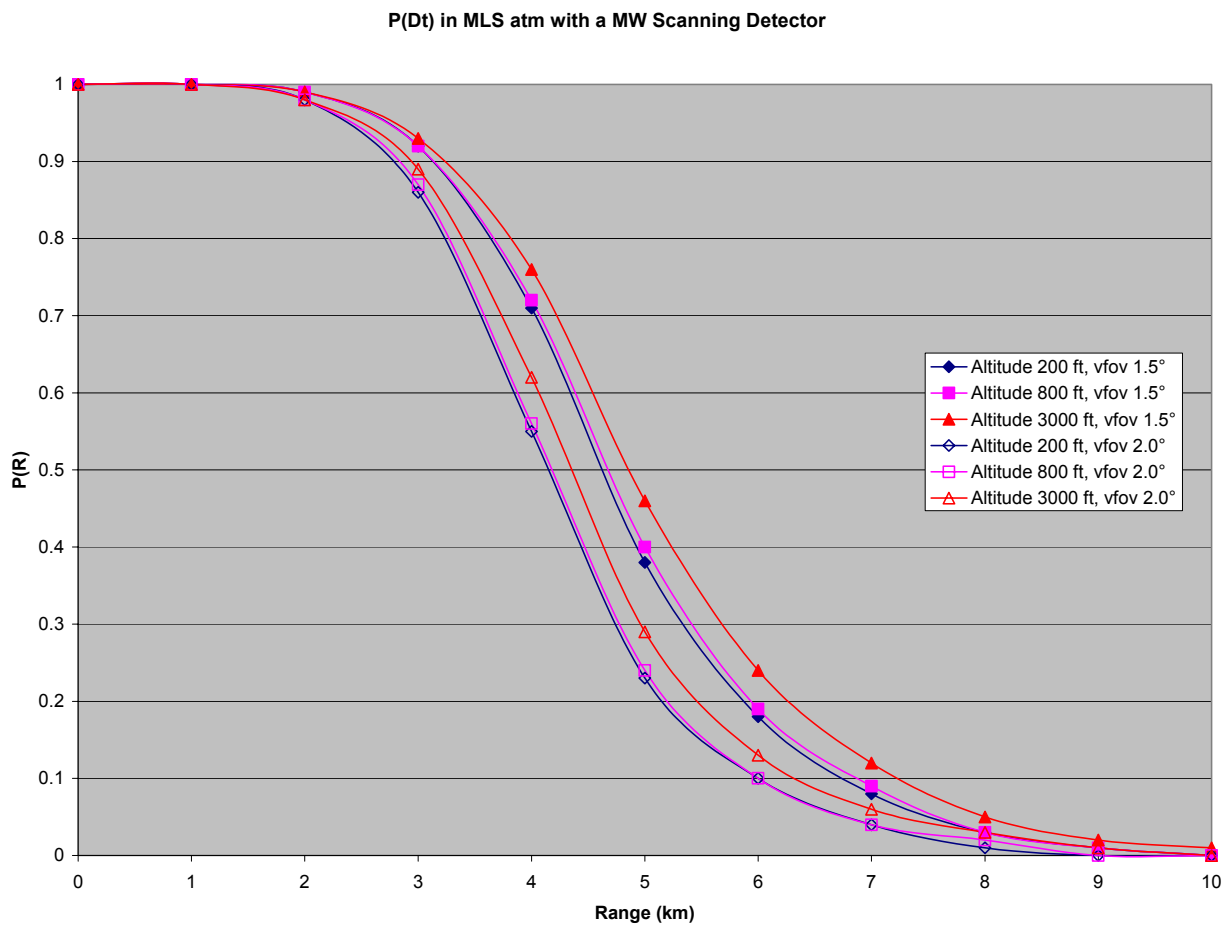


Figure 4-11 Probability of Detection Ranges in Mid-Latitude Summer Atmosphere Utilizing Scanning MWIR Detector for the Two FOVs of Interest

Recognition Ranges:

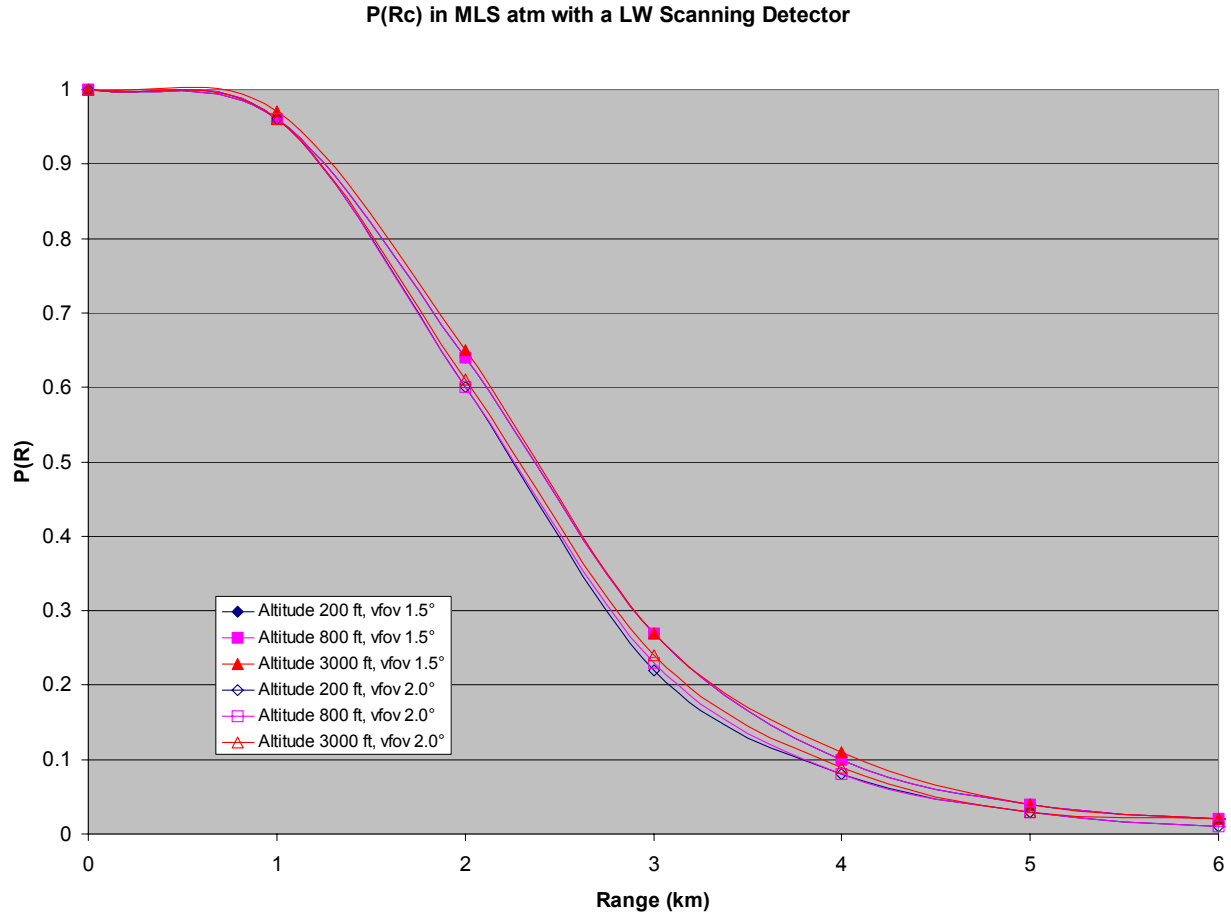


Figure 4-12 Probability of Recognition Ranges in Mid-Latitude Summer Atmosphere Utilizing Scanning LWIR Detector for the Two FOVs of Interest

P(Rc) in MLS atm with a MW Scanning Detector

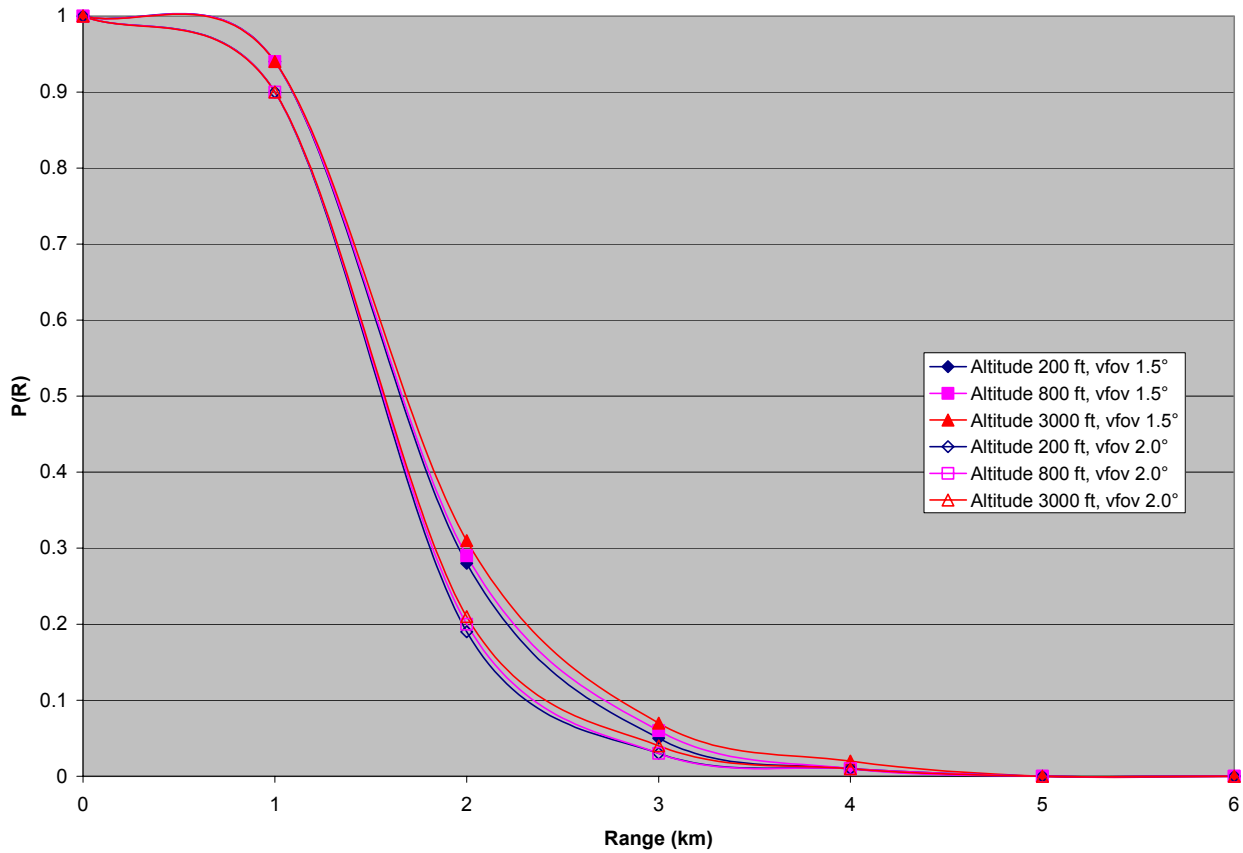


Figure 4-13 Probability of Recognition Ranges in Mid-Latitude Summer Atmosphere Utilizing Scanning MWIR Detector for the Two FOVs of Interest

For this particular atmosphere (Mid-latitude Summer) and technology (scanning), a comparison of the two *Detection range* graphs results in two distinct conclusions:

- 1) 1.5° VFOV configuration out-performing the 2.0° VFOV configuration on a consistent basis, all things being equal
- 2) LWIR detector yields longer ranges than does the MWIR detector.

When comparing the 3000 ft (0.9144 km) altitude series for the four configurations, the result is that the 1.5° VFOV configuration produces an 8.5 km range for the LWIR detector, while the MWIR detector produces a range of 5.0 km. Even at the lowest altitude (200 ft), the LWIR

detector has a longer ranging capability than that of the MWIR at an altitude of 3000 ft for both FOV configurations, i.e., LWIR detector with VFOV 1.5° at 200 ft ranges at 8.1 km and LWIR detector with VFOV 2.0° at 200 ft (0.06096 km) altitude ranges at 7.75 km while MWIR detector with VFOV 1.5° at 3000 ft ranges at 5.0 km. It is interesting to note that for the LWIR detectors, the performance of the VFOV 1.5° configuration at an altitude of 800 ft is almost as good as the VFOV 2.0° configuration at an altitude of 3000 ft. This may be due to the better resolution and greater sensitivity this system has with this FOV configuration (2.0° x 1.5°).

The *Recognition range* graphs yield the same conclusions, although not with as great a margin. The LWIR detector yields approximately 2.5 km for all altitudes with the VFOV 1.5° configuration versus approximately 1.75 km for all altitudes for the MWIR detector with the same VFOV 1.5° configuration. For the VFOV 2.0° configuration, the results are again similar, i.e., LWIR detector yields approximately 2.25 km for all altitudes while the MWIR detector yields approximately 1.5 km for all altitudes. These conclusions may not be the same as more data is analyzed.

4.3.3.3 Detection and Recognition Ranges for Scanning technology in Mid-latitude Winter atmosphere

Detection Ranges:

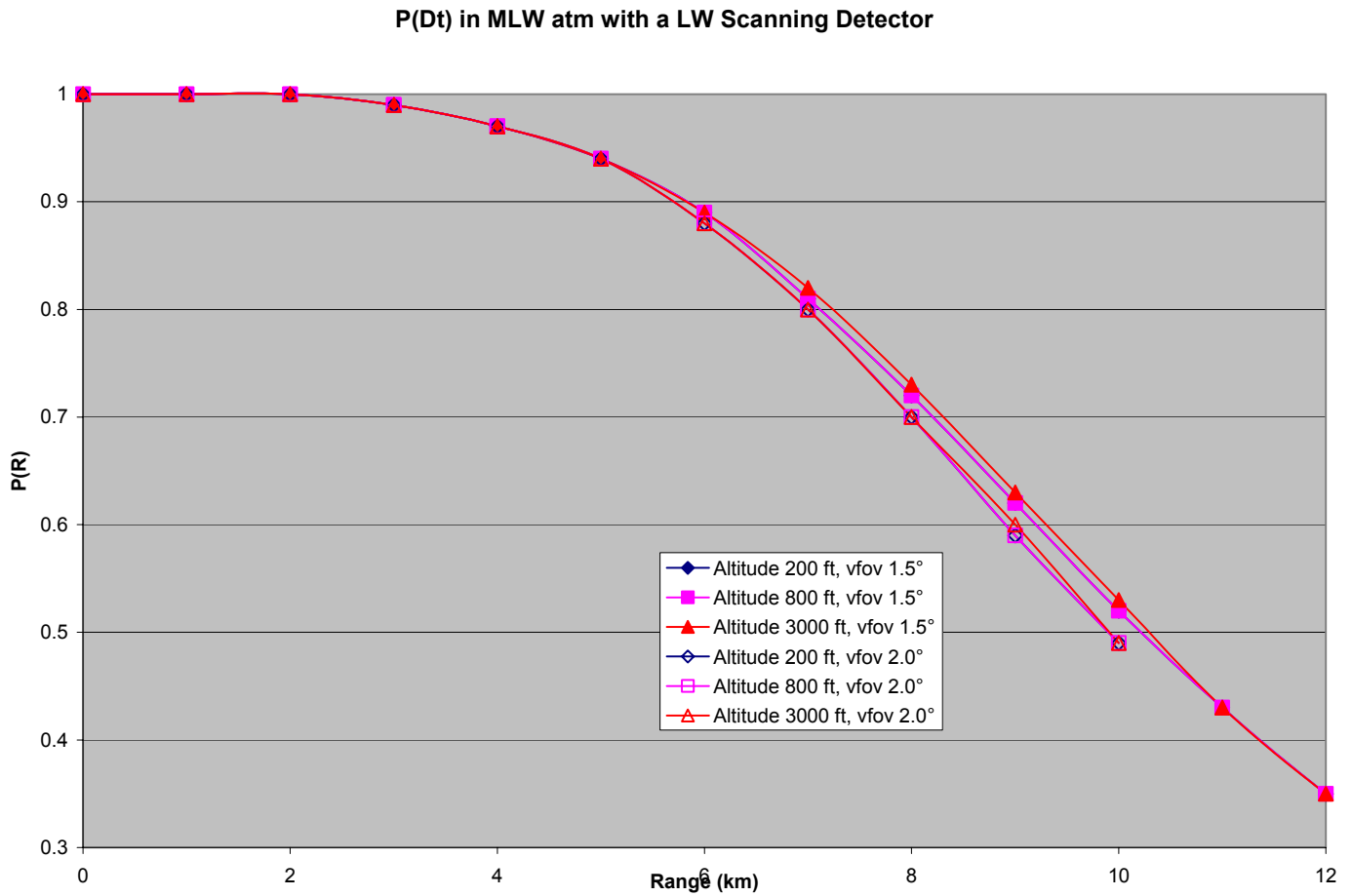


Figure 4-14 Probability of Detection Ranges in Mid-Latitude Winter Atmosphere Utilizing Scanning LWIR Detector for the Two FOVs of Interest

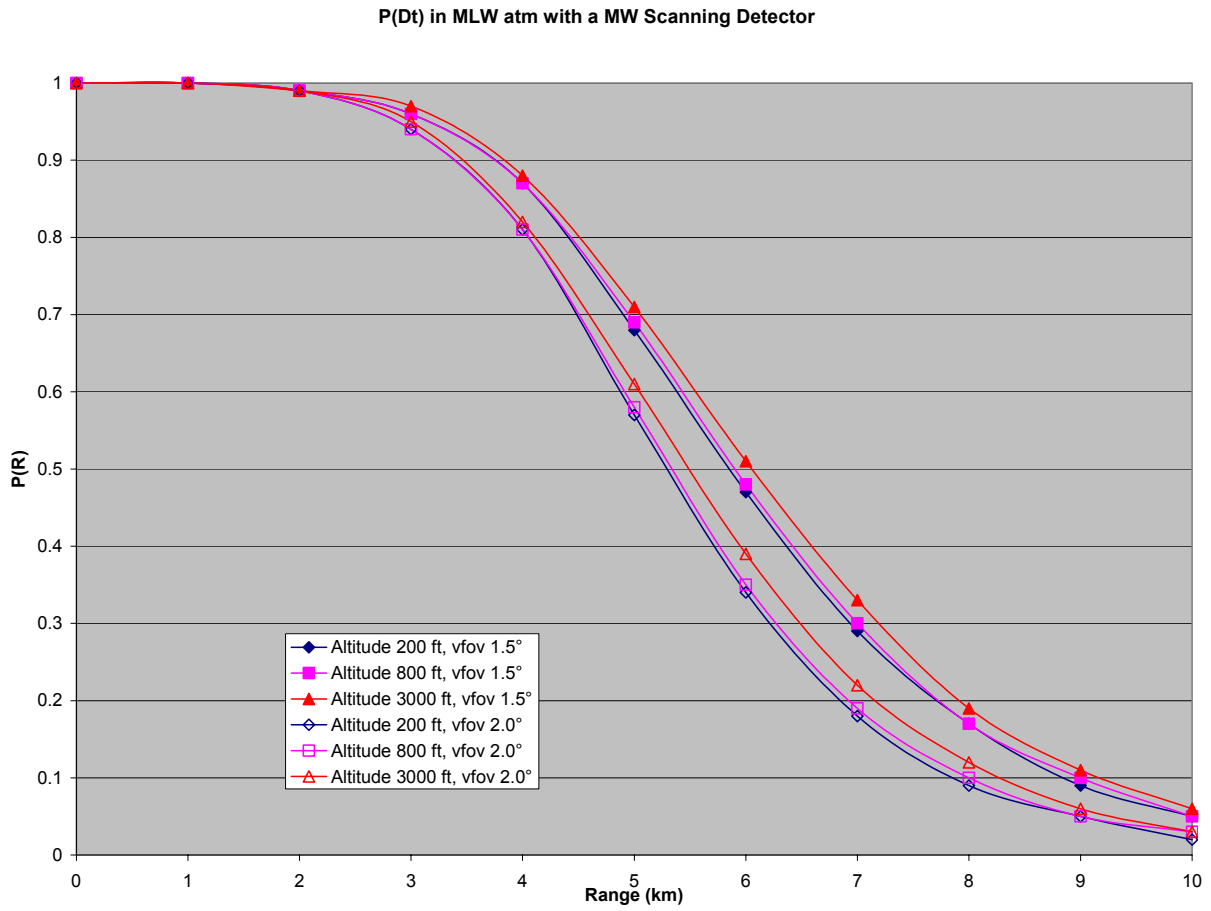


Figure 4-15 Probability of Detection Ranges in Mid-Latitude Winter Atmosphere Utilizing Scanning MWIR Detector for the Two FOVs of Interest

Recognition Ranges:

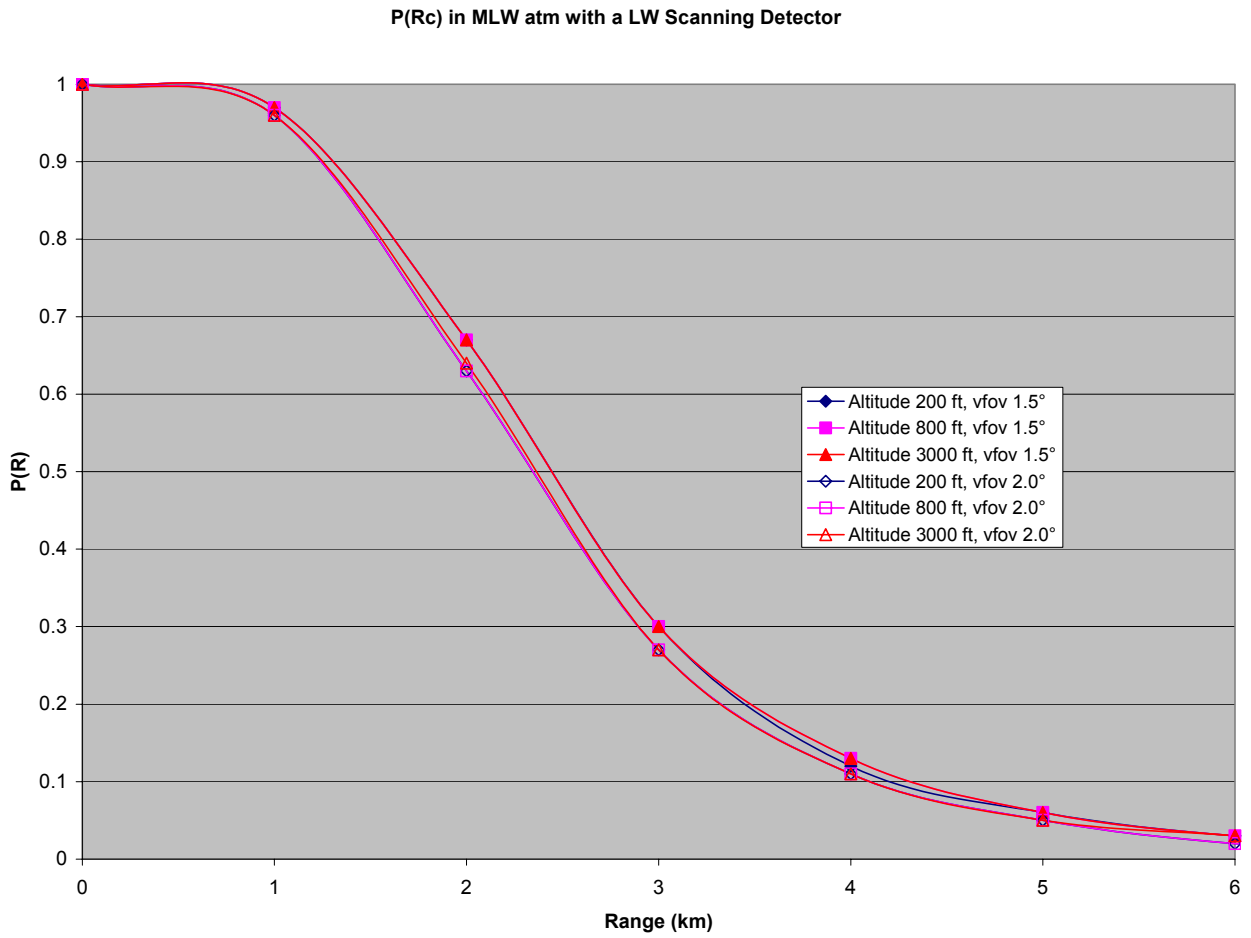


Figure 4-16 Probability of Recognition Ranges in Mid-Latitude Winter Atmosphere Utilizing Scanning LWIR Detector for the Two FOVs of Interest

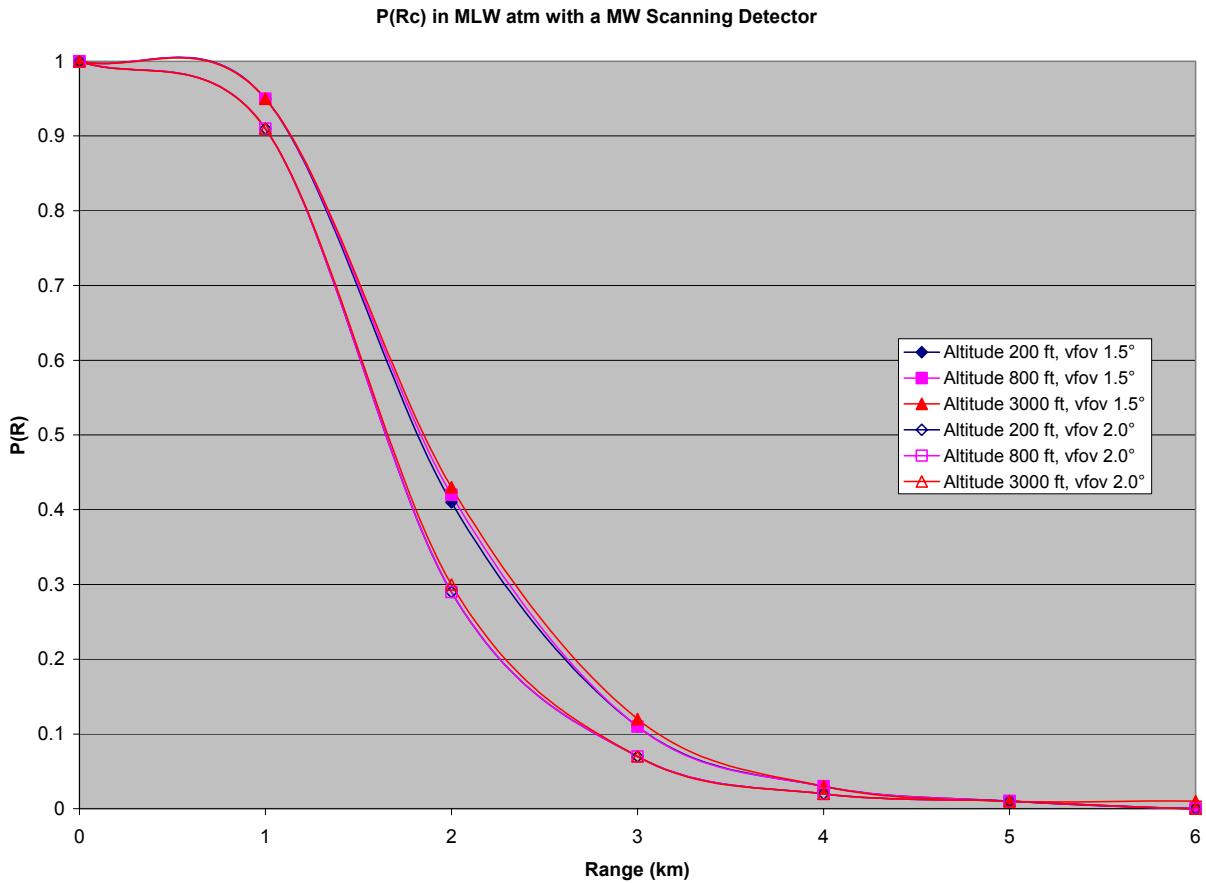


Figure 4-17 Probability of Recognition Ranges in Mid-Latitude Winter Atmosphere Utilizing Scanning MWIR Detector for the Two FOVs of Interest

For this particular atmosphere (Mid-latitude Winter) and technology (scanning), a comparison of the two *Detection range* graphs results in two distinct conclusions:

- 1) 1.5° VFOV configuration out-performing the 2.0° VFOV configuration on a consistent basis, all things being equal.
- 2) LWIR detector yields longer ranges than does the MWIR detector.

When comparing the 3000 ft (0.9144 km) altitude series for the four configurations, the result is that the 1.5° VFOV configuration produces an 10.5 km range for the LWIR detector, while the

MWIR detector produces a range of 6.25 km. Even at the lowest altitude (200 ft), the LWIR detector has a longer ranging capability than that of the MWIR at an altitude of 3000 ft for both FOV configurations, i.e., LWIR detector with VFOV 1.5° at 200 ft ranges at approximately 10.5 km and LWIR detector with VFOV 2.0° at 200 ft (0.06096 km) altitude ranges at 9.75 km while MWIR detector with VFOV 1.5° at 3000 ft ranges at 6.25 km.

The *Recognition range* graphs yield the same conclusions, although not with as great a margin. The LWIR detector yields approximately 2.5 km for all altitudes with the VFOV 1.5° configuration versus approximately 2.0 km for all altitudes for the MWIR detector with the same VFOV 1.5° configuration. For the VFOV 2.0° configuration, the results are again similar, i.e., LWIR detector yields approximately 2.3 km for all altitudes while the MWIR detector yields approximately 1.75 km for all altitudes. These conclusions may not be the same as more data is analyzed.

4.3.3.4 Detection and Recognition Ranges for Staring technology in Tropical atmosphere

Detection:

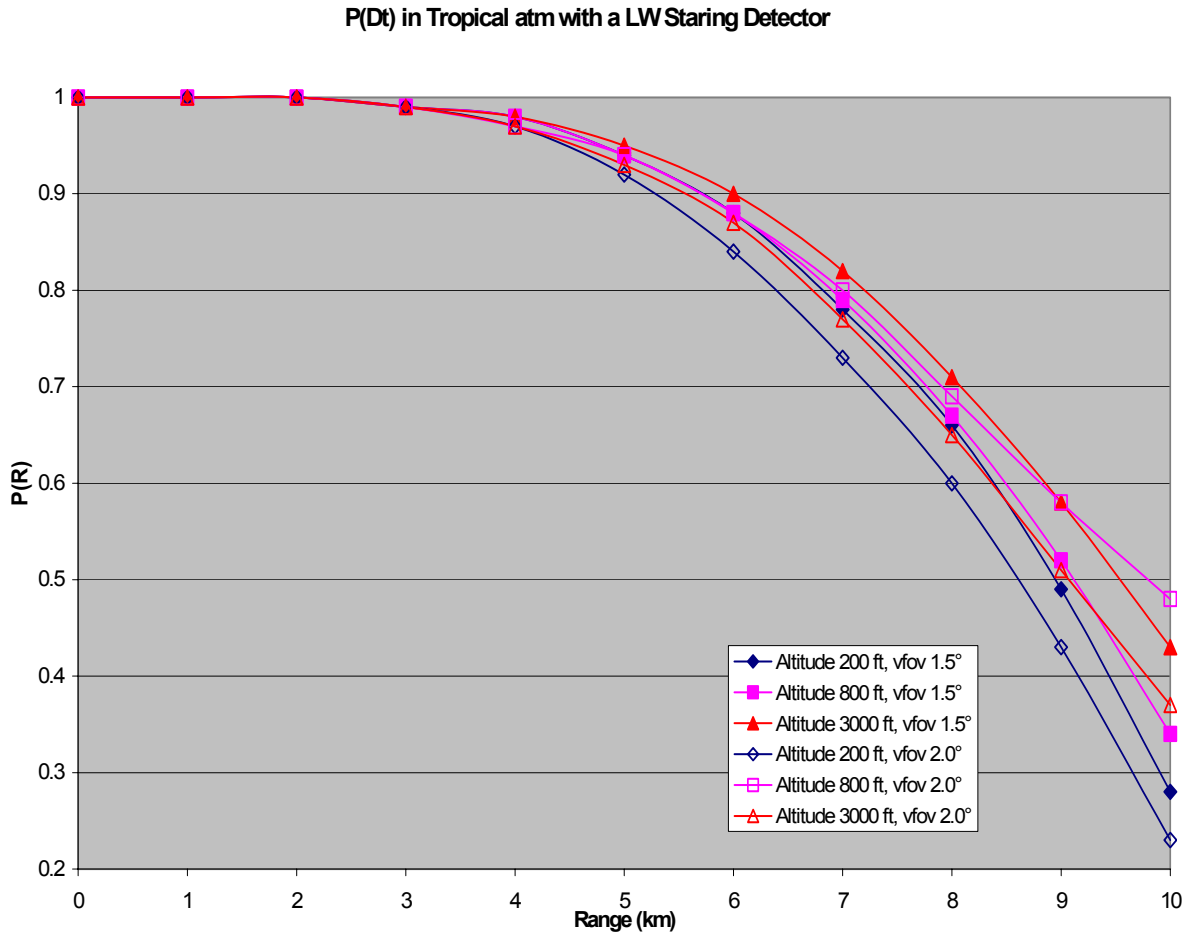


Figure 4-18 Probability of Detection Ranges in Tropical Atmosphere Utilizing Staring LWIR Detector for the Two FOVs of Interest

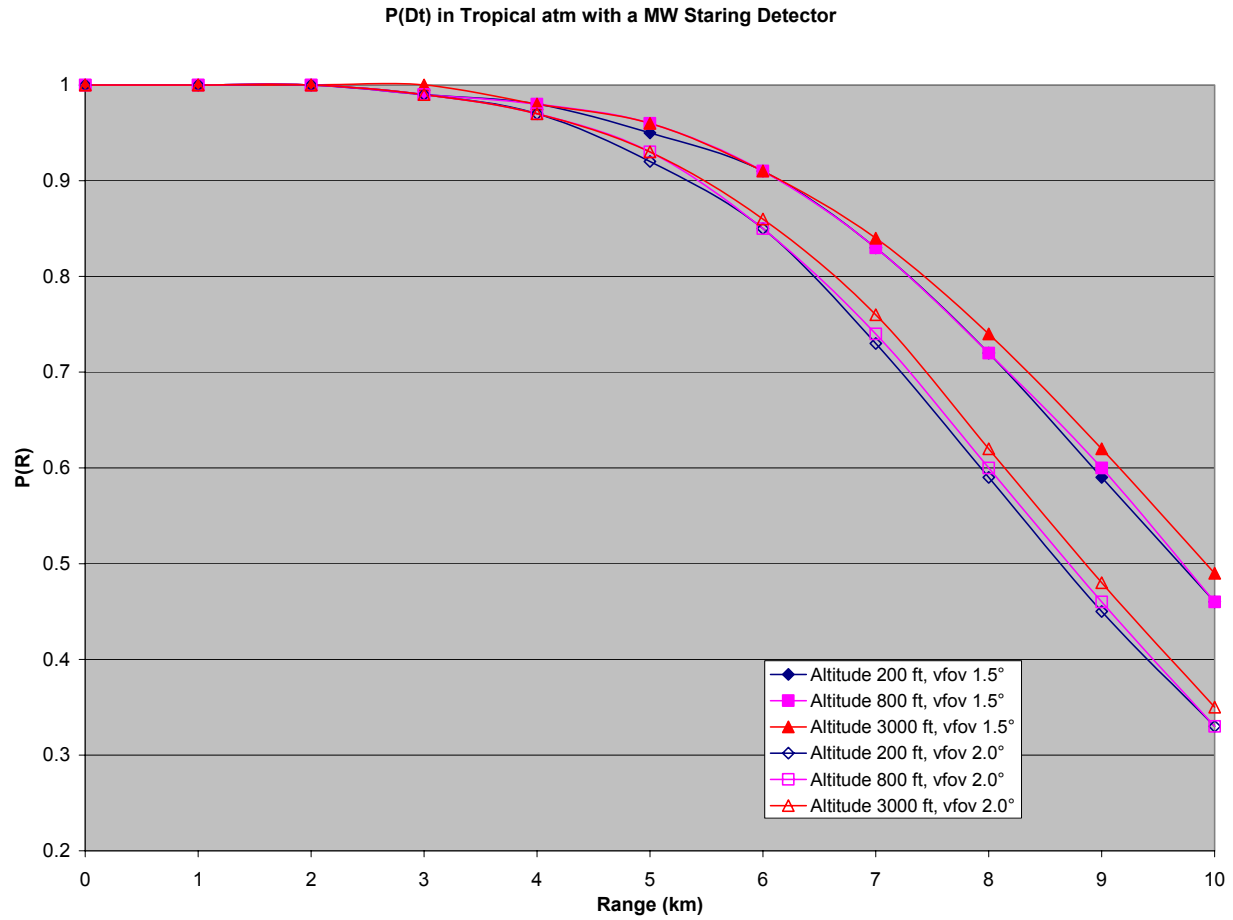


Figure 4-19 Probability of Detection Ranges in Tropical Atmosphere Utilizing Staring MWIR Detector for the Two FOVs of Interest

Recognition:

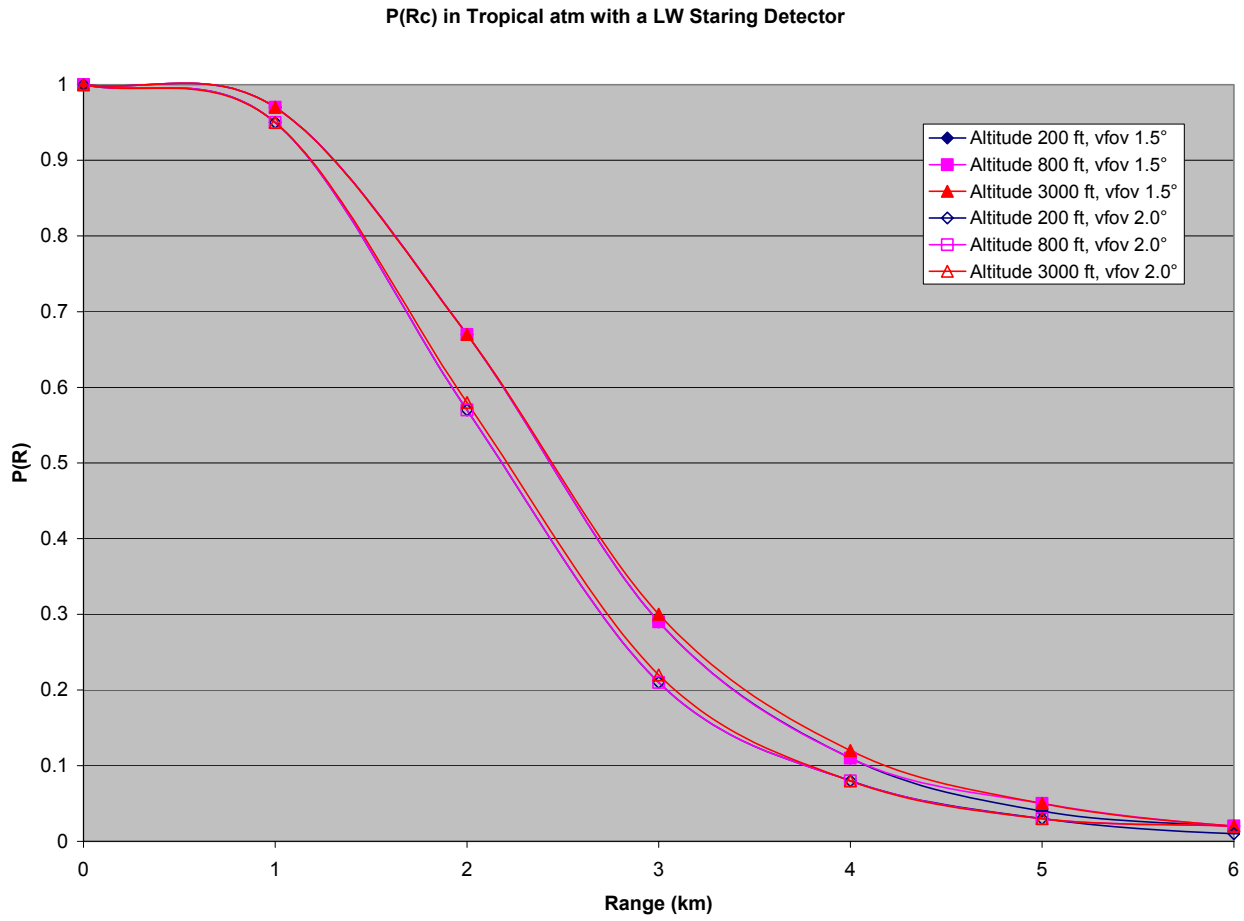


Figure 4-20 Probability of Recognition Ranges in Tropical Atmosphere Utilizing Staring LWIR Detector for the Two FOVs of Interest

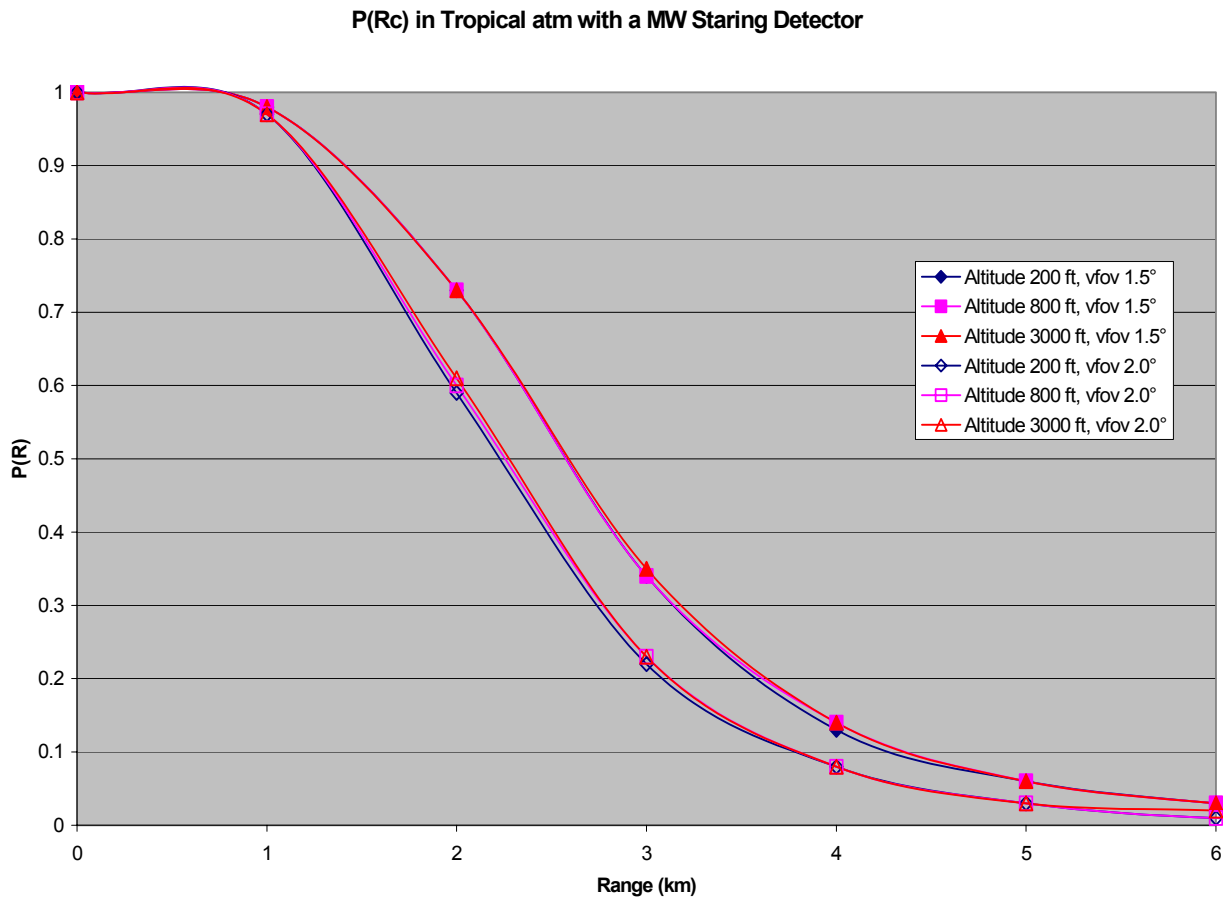


Figure 4-21 Probability of Recognition Ranges in Tropical Atmosphere Utilizing Staring MWIR Detector for the Two FOVs of Interest

For this particular atmosphere (Tropical) and technology (staring), a comparison of the two *Detection range* graphs results in two distinct conclusions:

- 1) 1.5° VFOV configuration out-performing the 2.0° VFOV configuration on a consistent basis, all things being equal
- 2) MWIR detector yields longer ranges than does the LWIR detector.

When comparing the 3000 ft (0.9144 km) altitude series for the four configurations, the result is that the 1.5° VFOV configuration produces an 10.75 km range for the MWIR detector, while

the LWIR detector produces a range of 10.5 km. At the lowest altitude (200 ft), the MWIR detector has a longer ranging capability than that of the LWIR detector at an altitude of 3000 ft. In other words, the MWIR detector with VFOV 1.5° at 200 ft ranges at approximately 9.6 km while LWIR detector with VFOV 1.5° at 3000 ft ranges at 9.5 km.

Looking at the VFOV 2.0° configuration in Figure 4-18 leads one to question why the altitude of 800 ft out performs the 3000 ft altitude of the same configuration. There was a transmittance data input error in the ACQUIRE file. At the very best we would expect the 800 ft altitude to yield ranges equal to those at the 3000 ft altitude.

The *Recognition range* graphs yield the same conclusions, although not with as great a margin. The MWIR detector yields approximately 2.75 km for all altitudes with the VFOV 1.5° configuration, while the LWIR detector yields approximately 2.5 km for all altitudes with the same VFOV 1.5° configuration. For the VFOV 2.0° configuration, the results are virtually the same, i.e., MWIR detector yields approximately 2.25 km for all altitudes, as does the LWIR detector for all altitudes. These conclusions may not be the same as more data is analyzed.

4.3.3.5 Detection and Recognition Ranges for Staring technology in Mid-latitude atmosphere

Detection:

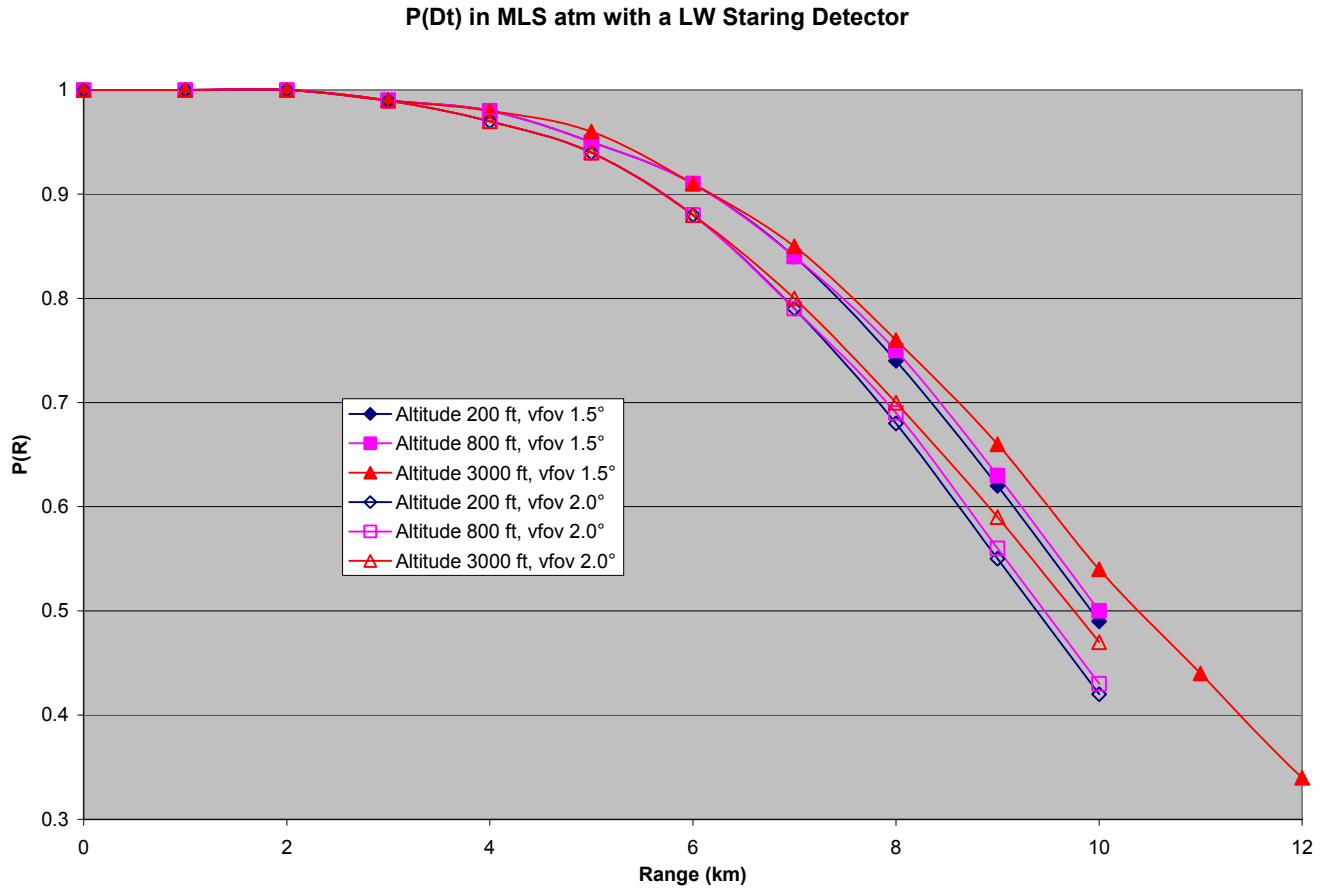


Figure 4-22 Probability of Detection Ranges in Mid-latitude Summer Atmosphere Utilizing Staring LWIR Detector for the Two FOVs of Interest

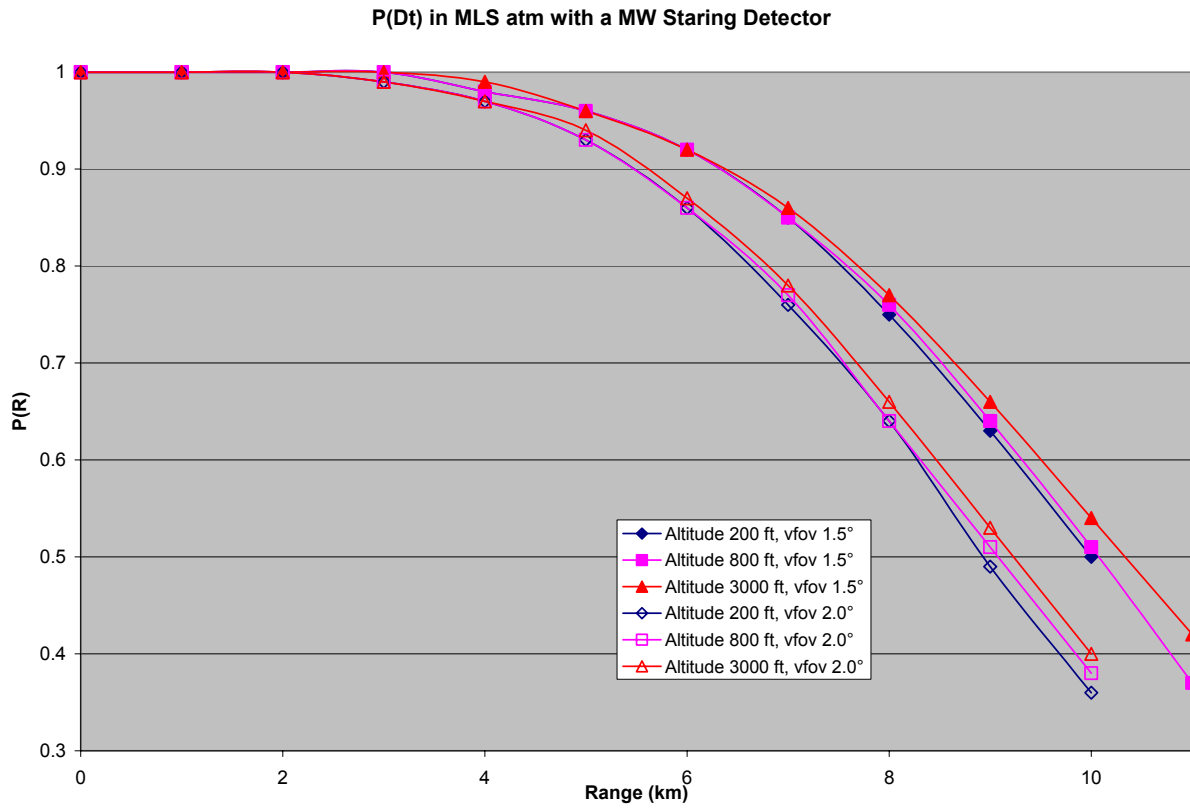


Figure 4-23 Probability of Detection Ranges in Mid-latitude Summer Atmosphere Utilizing Staring MWIR Detector for the Two FOVs of Interest

Recognition:

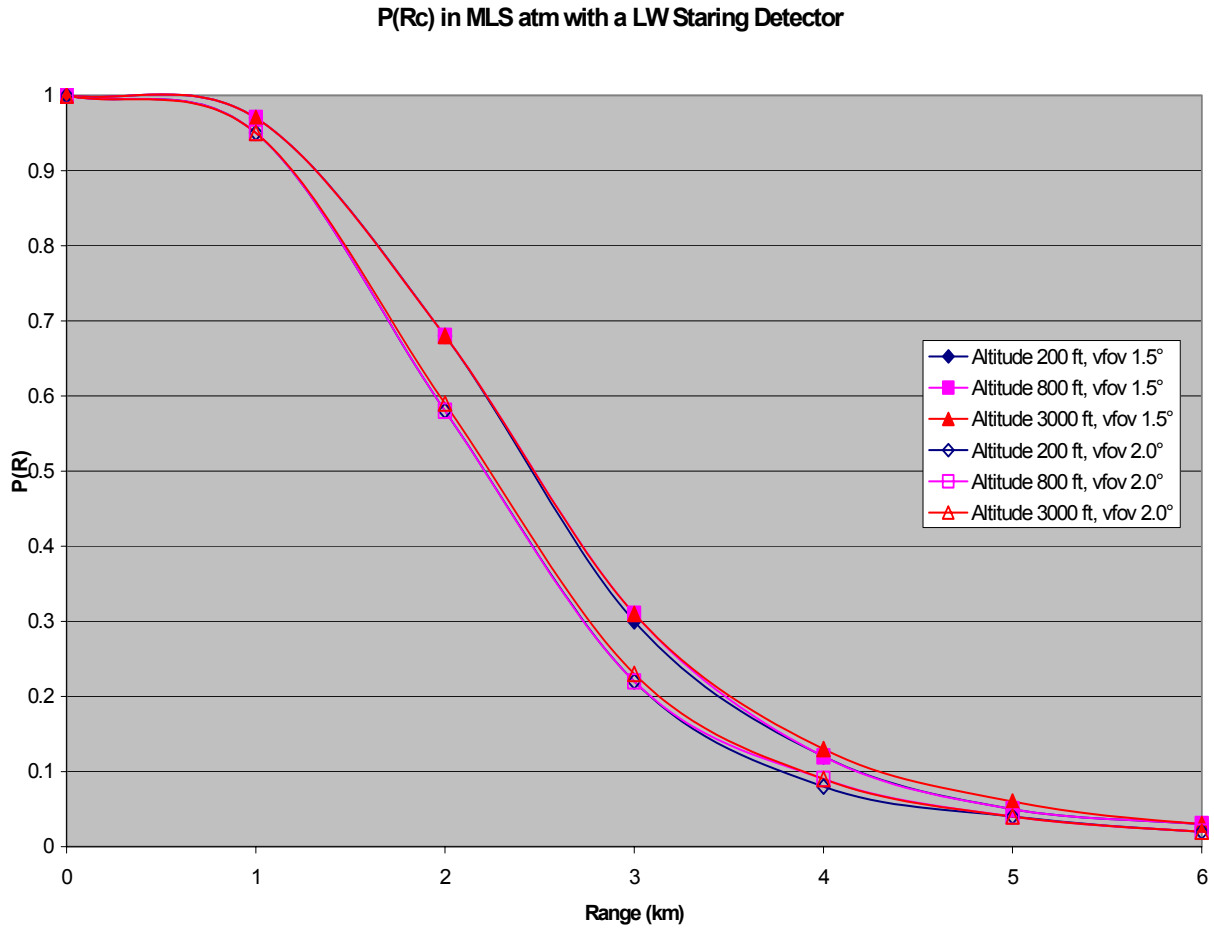


Figure 4-24 Probability of Recognition Ranges in Mid-latitude Summer Atmosphere Utilizing Staring LWIR Detector for the Two FOVs of Interest

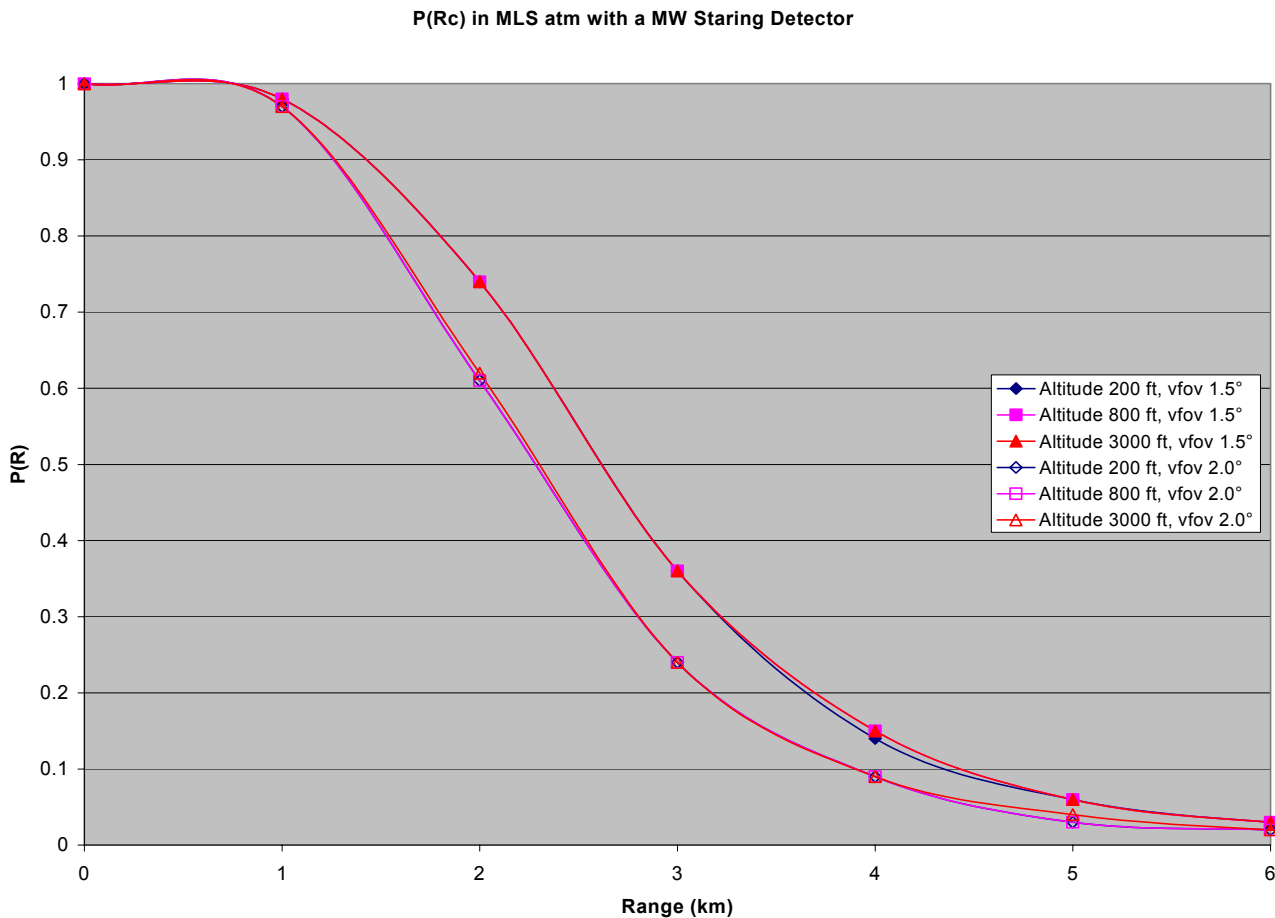


Figure 4-25 Probability of Recognition Ranges in Mid-latitude Summer Atmosphere Utilizing Staring MWIR Detector for the Two FOVs of Interest

For this particular atmosphere (Mid-latitude Summer) and technology (staring), a comparison of the two *Detection range* graphs results in the conclusion of the 1.5° VFOV configuration out-performing the 2.0° VFOV configuration on a consistent basis, all things being equal.

When comparing the 3000 ft (0.9144 km) altitude series for the four configurations, the result is that the 1.5° VFOV configuration produces an 10.5 km range for the MWIR detector,

while the LWIR detector produces a range of 10.25 km. At the lowest altitude (200 ft), the MWIR detector and the LWIR detector have virtually the same ranging capability with the VFOV 1.5° configuration, i.e., both detectors range at approximately 10.0 km.

The *Recognition range* graphs yield the same conclusions. The MWIR detector and the LWIR detector have virtually the same ranging capability for both VFOV configurations, i.e., 2.75 km for both detectors with a VFOV 1.5° configuration for all altitudes. Again for the VFOV 2.0° configuration, the results are virtually the same, i.e., MWIR detector yields approximately 2.25 km for all altitudes, as does the LWIR detector for all altitudes. These conclusions may not be the same as more data is analyzed.

4.3.3.6 Detection and Recognition Ranges for Staring technology in Mid-latitude Winter atmosphere

Detection:

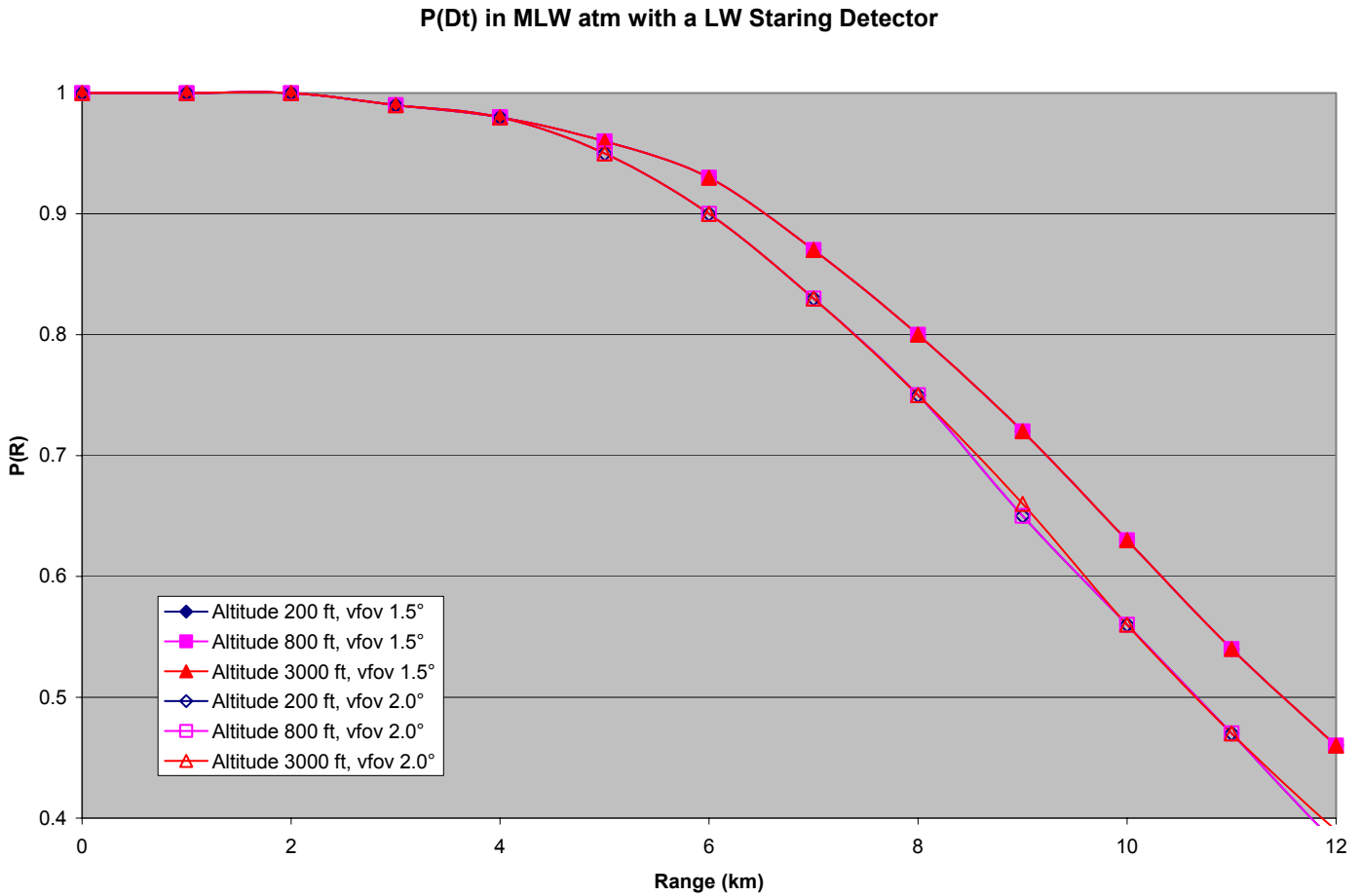


Figure 4-26 Probability of Detection Ranges in Mid-latitude Winter Atmosphere Utilizing Staring LWIR Detector for the Two FOVs of Interest

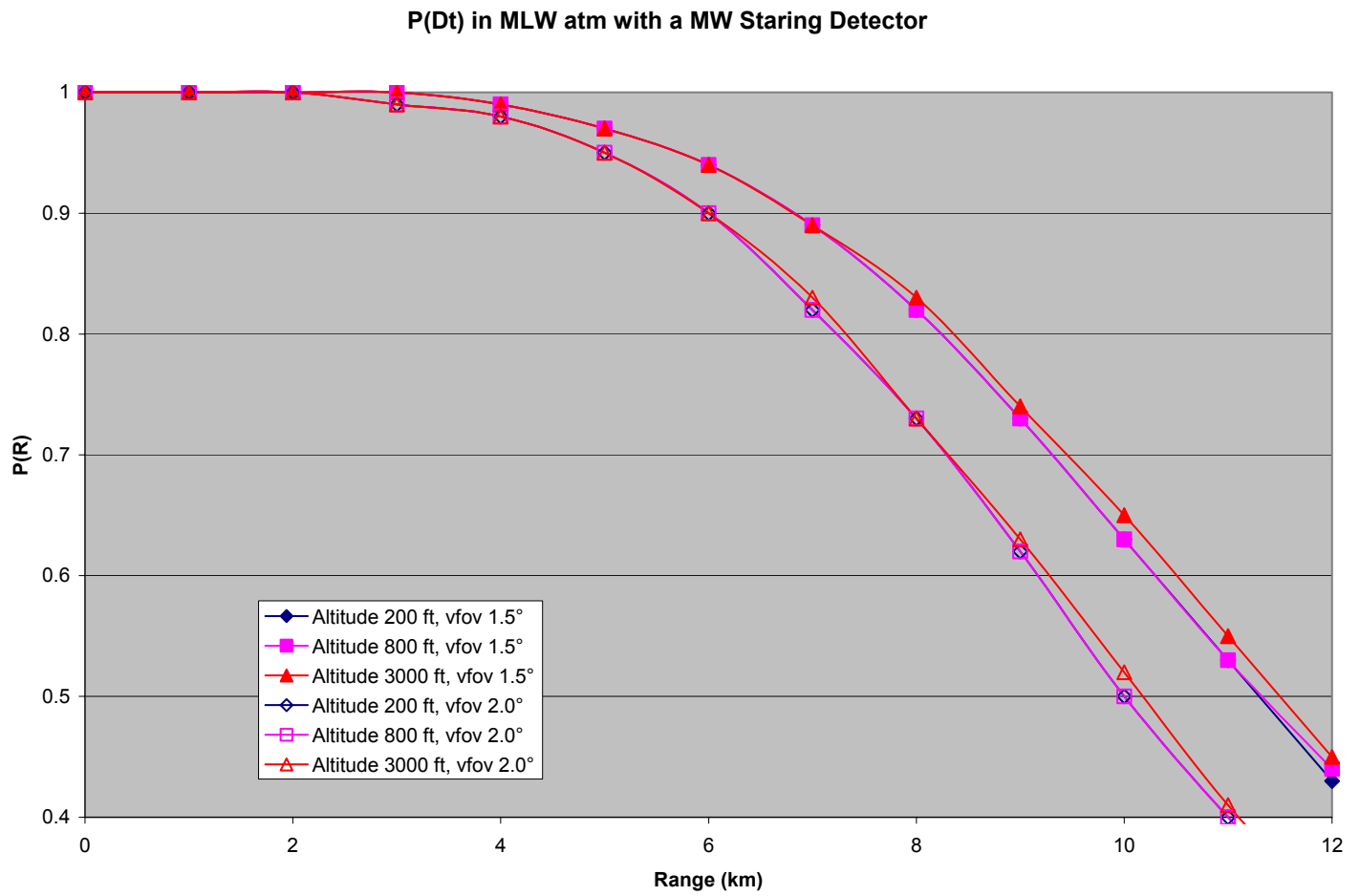


Figure 4-27 Probability of Detection Ranges in Mid-latitude Winter Atmosphere Utilizing Staring MWIR Detector for the Two FOVs of Interest

Recognition:

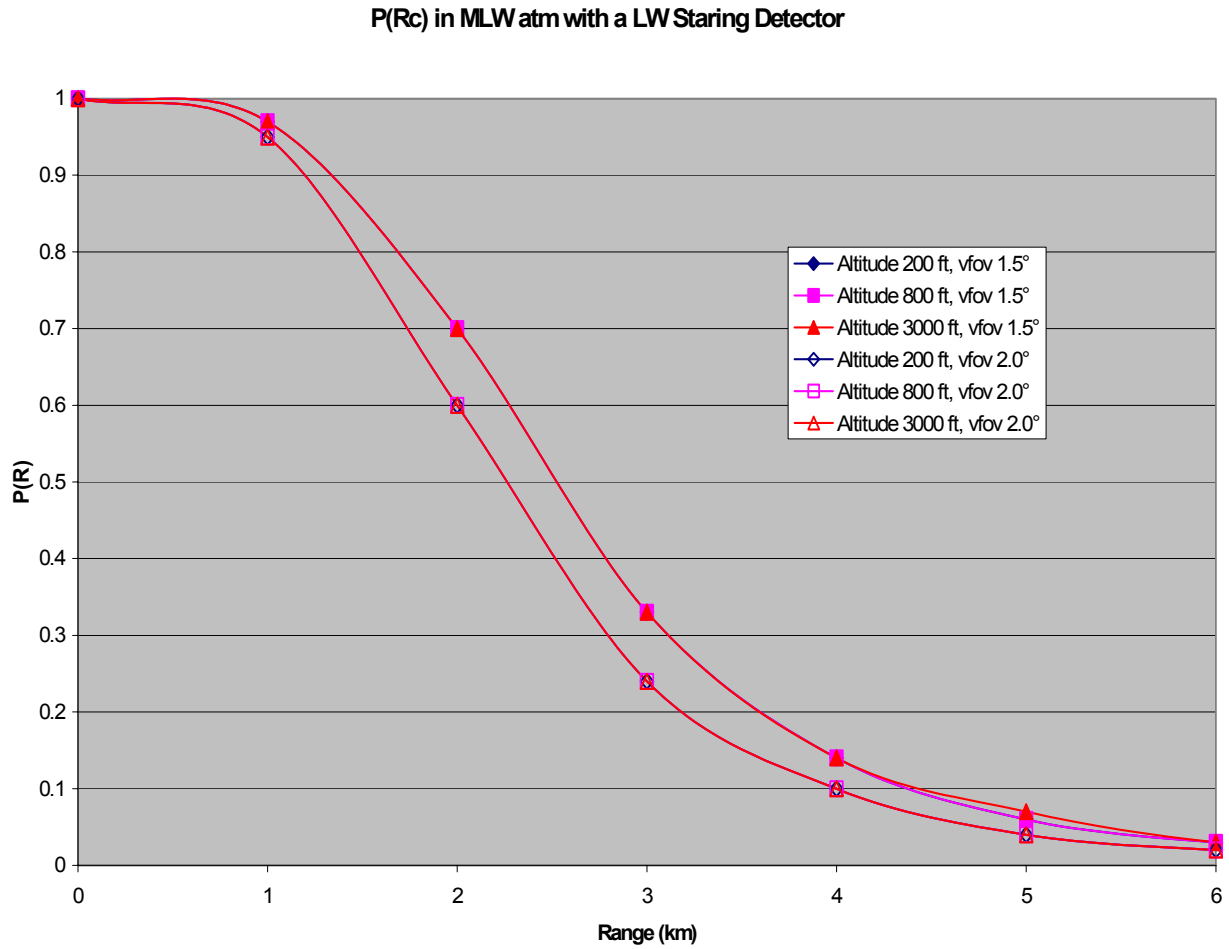


Figure 4-28 Probability of Recognition Ranges in Mid-latitude Winter Atmosphere Utilizing Staring LWIR Detector for the Two FOVs of Interest

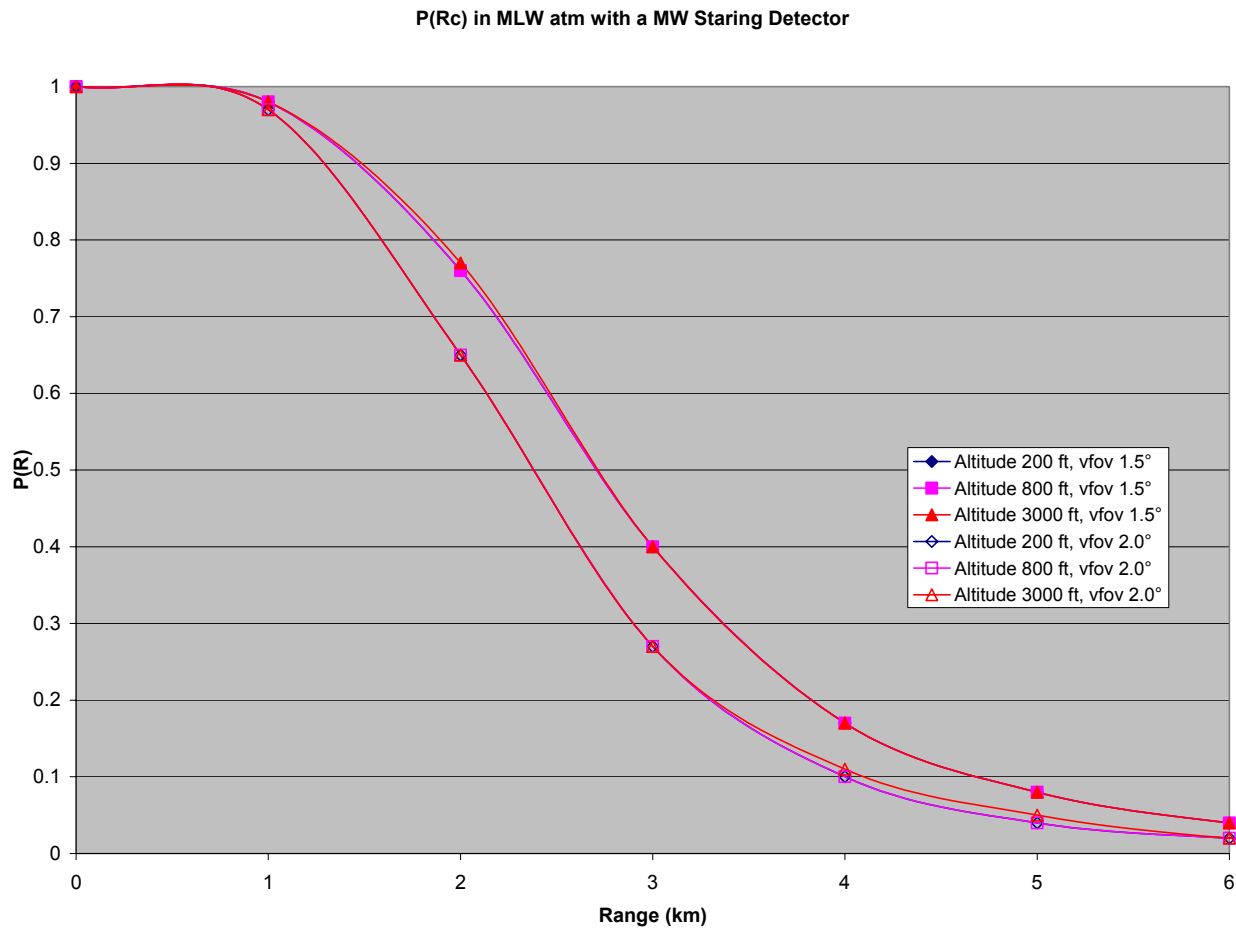


Figure 4-29 Probability of Recognition Ranges in Mid-latitude Winter Atmosphere Utilizing Staring MWIR Detector for the Two FOVs of Interest

For this particular atmosphere (Mid-latitude Winter) and technology (staring), a comparison of the two *Detection range* graphs results in the conclusion of the 1.5° VFOV configuration out-performing the 2.0° VFOV configuration on a consistent basis, all things being equal.

When comparing the series for the four configurations, the result is that the 1.5° VFOV configuration approximately produces an 11.75 km range for the MWIR detector at all altitudes,

while the LWIR detector approximately produces a range of 11.5 km at all altitudes. For the VFOV 2.0° configuration, the MWIR detector yields an approximate range of 10.25 km at all altitudes, and the LWIR detector yields an approximate range of 10.5 km at all altitudes.

The *Recognition range* graphs yield the same marginal conclusions. The MWIR detector yields a slightly longer range for all altitudes with the VFOV 1.5° configuration (approximately 2.8 km). The LWIR detector yields a range of approximately 2.75 km for all altitudes with the same VFOV configuration. Again for the VFOV 2.0° configuration, the results are very similar, i.e., MWIR detector yields approximately 2.5 km for all altitudes, and the LWIR detector yields approximately 2.25 km for all altitudes.

4.4 Results Summary

A brief summary of the results shows that-

For MRT:

- values are better (greater number of cycles per milliradian) for the MWIR detectors in general, regardless of technology
- values resulting from the FOV configuration of 2.0° x 1.5° are better (lower), implying that these detectors have a better thermal sensitivity and have greater resolution, regardless of wavelength.

For ranging:

- LWIR out performed MWIR using scanning technology
- MWIR outperformed LWIR using staring technology
- MWIR staring detector out performed the LWIR scanning detectors overall.

Table 4-4 shows the ranging results in a more concise, consolidated manner.

Table 4-4 Ranging Results Summary

Wavelength: **LWIR (2.0° x 1.5°) MWIR (2.0° x 1.5°)**

Tropical w/ scanning tech:		
detection range	7.75 km	4.75 km
Recognition range	2.5 km	1.75 km
Mid-latitude Summer w/ scanning tech:		
detection range	8.5 km	5.0 m
Recognition range	2.5 km	1.75 km
Mid-latitude Winter w/ scanning tech:		
detection range	10.5 km	6.25 km
Recognition range	2.5 km	2.0 km
Tropical w/ staring tech:		
detection range	10.5 km	10.75 km
Recognition range	2.5 km	2.75 km
Mid-latitude Summer w/ staring tech:		
detection range	10.25 km	10.5 km
Recognition range	2.75 km	2.75 km
Mid-latitude Winter w/ staring tech:		
detection range	11.5 km	11.75 km
Recognition range	2.75 km	3.0 km

- **The staring MWIR detectors utilizing the 2.0° x 1.5° configuration have the better performance for all atmospheric environments used by Customer X.**

CHAPTER V
SELECTION CRITERIA

5.1 Cost/Schedule Risk

This section will focus on determining the most affordable support plan for Customer X. Given the objective for this section, a low cost approach to meet the requirements of Customer X will be defined for both cost and schedule. This support strategy will be based on a series of successful support strategies related to detector configuration decisions. Figure 5-1 is a representation of both cost and schedule containment demonstrating the *critical path* for each task based on time (in months) and personnel loading for manufacture and integration of specific detector configurations. Based on the results of Section 4.3, three detector configurations were chosen for comparison, namely 1) LWIR scanning, 2) MWIR staring, and 3) LWIR staring. Values for the ideal network are listed in Table 5-1. As can be seen, the critical path for the ideal network is C-D-G-K.

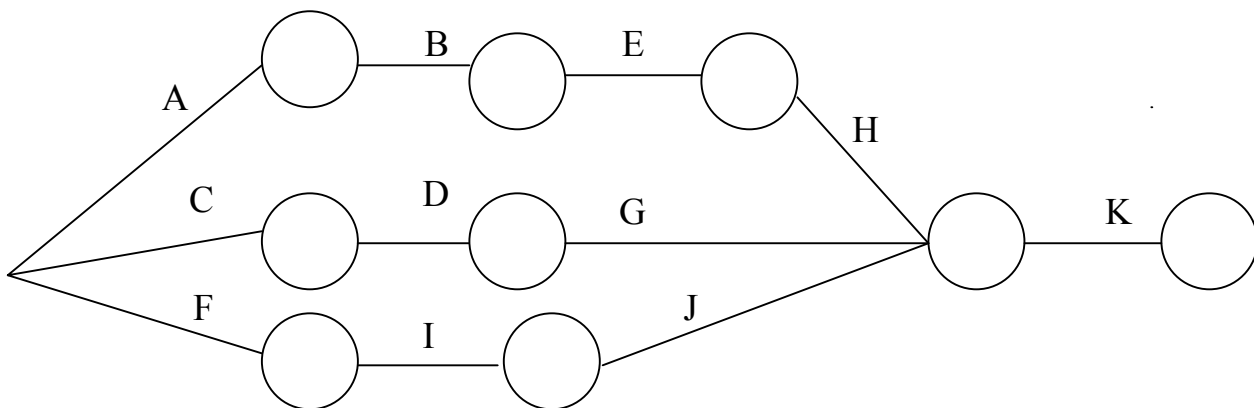


Figure 5-1 Cost/Schedule Containment Analysis Network Flow

Table 5-1 Values for Cost/Schedule Containment Analysis Network Flow

ITEM	A	B	C	D	E	F	G	H	I	J	K
TIME (MONTHS)	3	3	5.8	5.5	5	5	7	4.5	4	4	4
PERSONNEL LOADING	4	2	6	2	3.5	6	3	3	4	5	3
CRITICAL PATH	A+B+E+H+K			C+D+G+K			F+I+J+K				
	19.5			22.25			17				

Based on the risk inherent in each of the three different design choices, a risk level was assigned to each design as follows:

- 1) high risk for task C, associated with LWIR scanning detector
- 2) moderate risk for task E, associated with LWIR staring detector
- 3) low risk for task F, associated with MWIR staring detector.

The ranges for these risk levels are based on the REVIC (Revised Version Intermediate COCOMO) version of COCOMO (Constructive Cost Model) Developed by Dr. Barry Boehm. This concept of risk management is explained in a paper by Dr. Joe Dean [34]. The schedule ranges break down and are represented by the triangular probability distributions (Figures 5-2 through 5-4) as follows:

- 1) High-risk efforts complete within 90-100% of their nominal time 50% of the time and between 100-140% of their nominal time 50% of the time.
- 2) Medium risk efforts complete within 90-100% of their nominal time 50% of the time and between 100-120% of their nominal time 50% of the time.
- 3) Low risk efforts complete within 90-100% of their nominal time 50% of the time and between 100-140% of their nominal time 50% of the time.

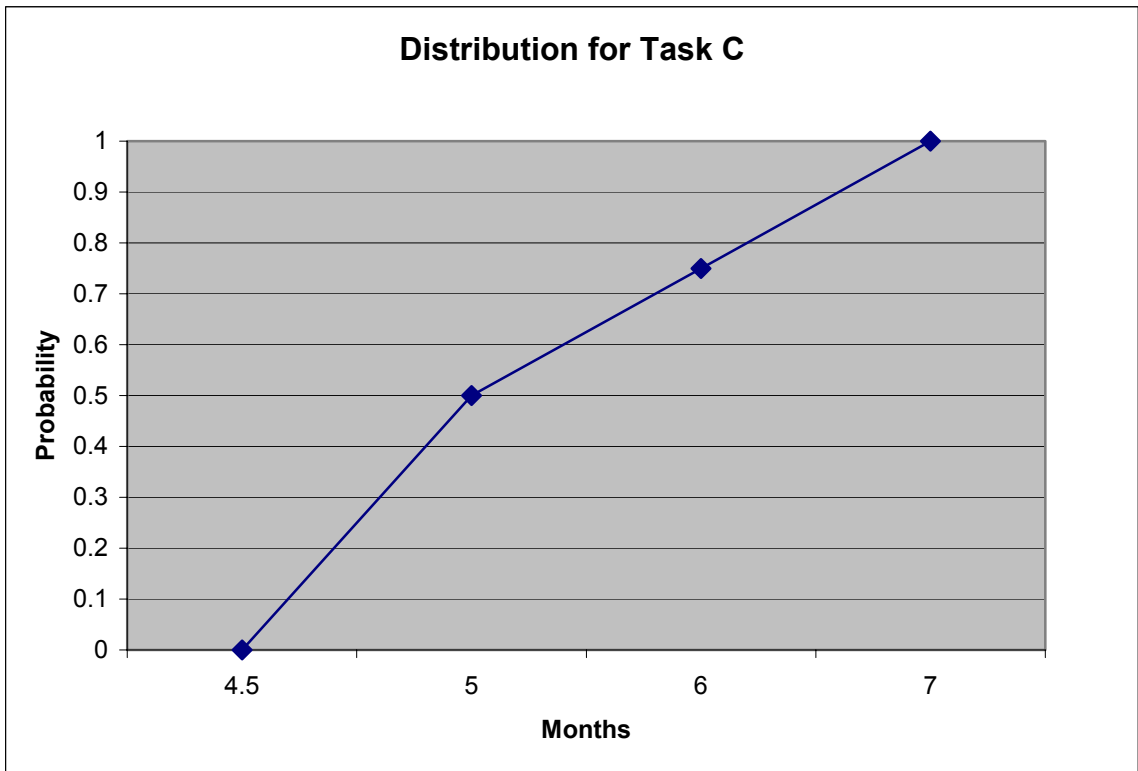


Figure 5-2 Distribution for High Risk Task (LWIR scanning detector)

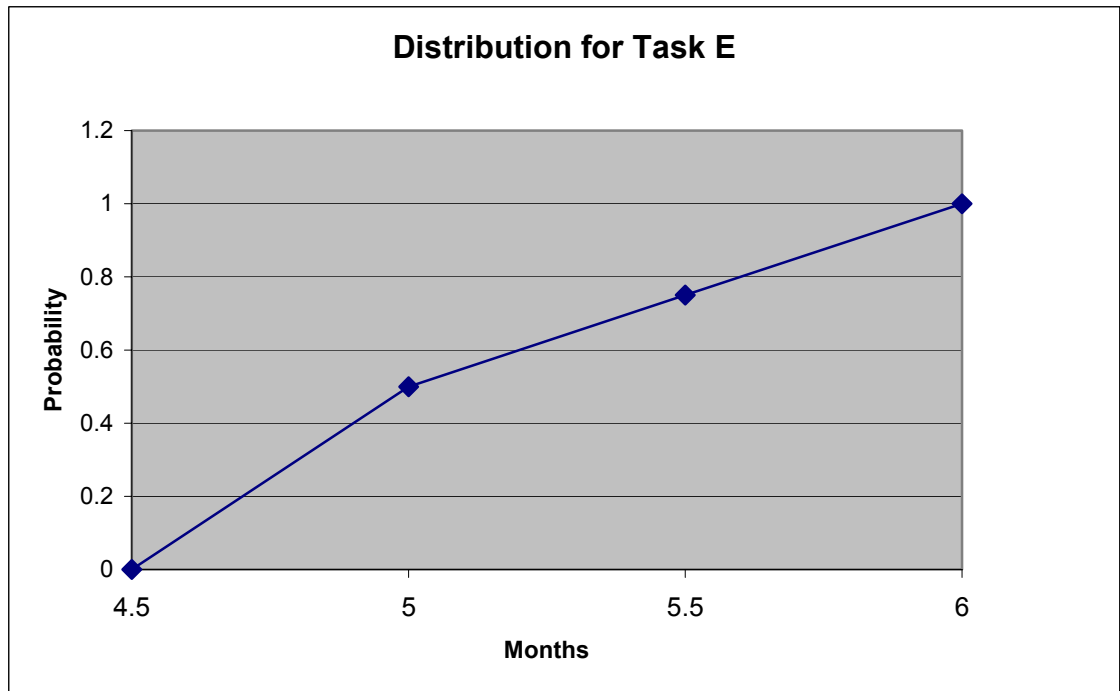


Figure 5-3 Distribution for Moderate Risk Task (LWIR staring detector)

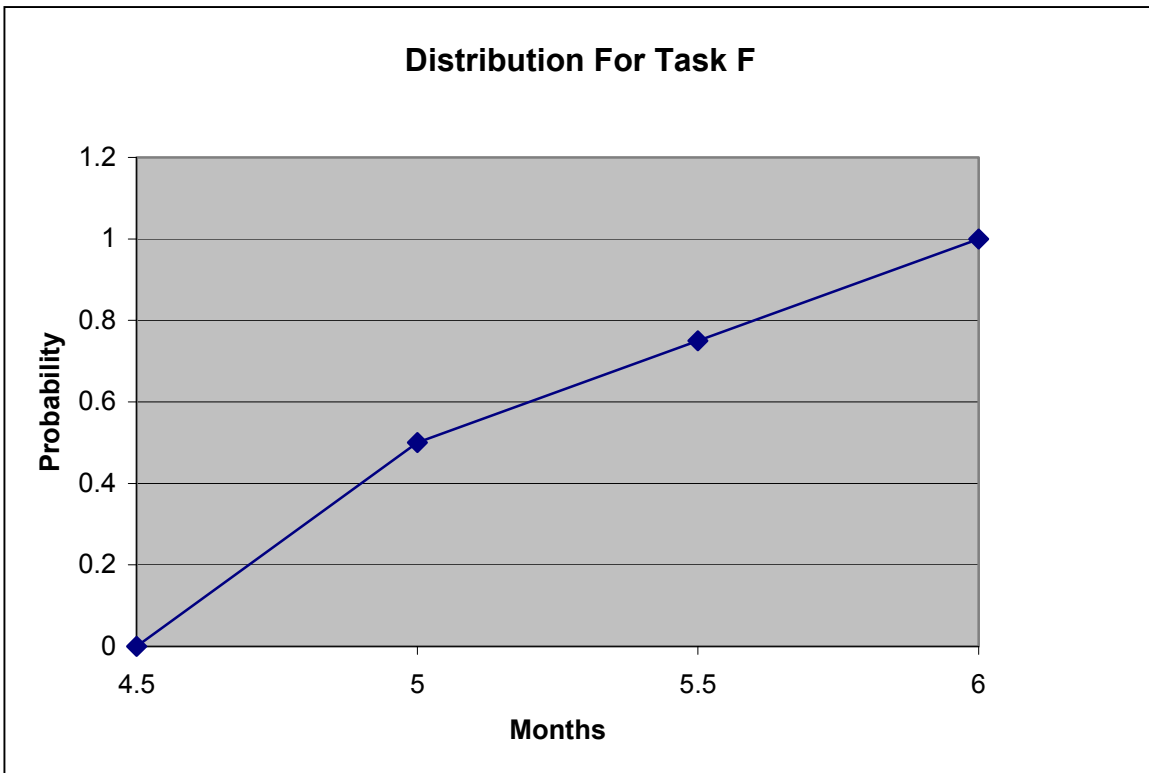


Figure 5-4 Distribution for Low Risk Task (MWIR staring detector)

A Monte Carlo Analysis of approximately 2000 random scenarios was run for each critical path. As an example, a random number generator was used to select a probability for critical task C. This probability was then compared to the triangular distribution, the expected completion time determined and the critical path recalculated. The new costs due to the additional/fewer person months required were also recalculated. This information is plotted on the point scatter chart representation of the cost/schedule containment curve in Figure 5-5 and the next run completed. This information would then be completed for the other two options and the three scatter charts compared to determine the merits of each program. Not all data is represented in these graphs, nor is it represented in its entirety on the spreadsheet capture calculations chart, Figure 5-6.

Cost-Schedule Containment

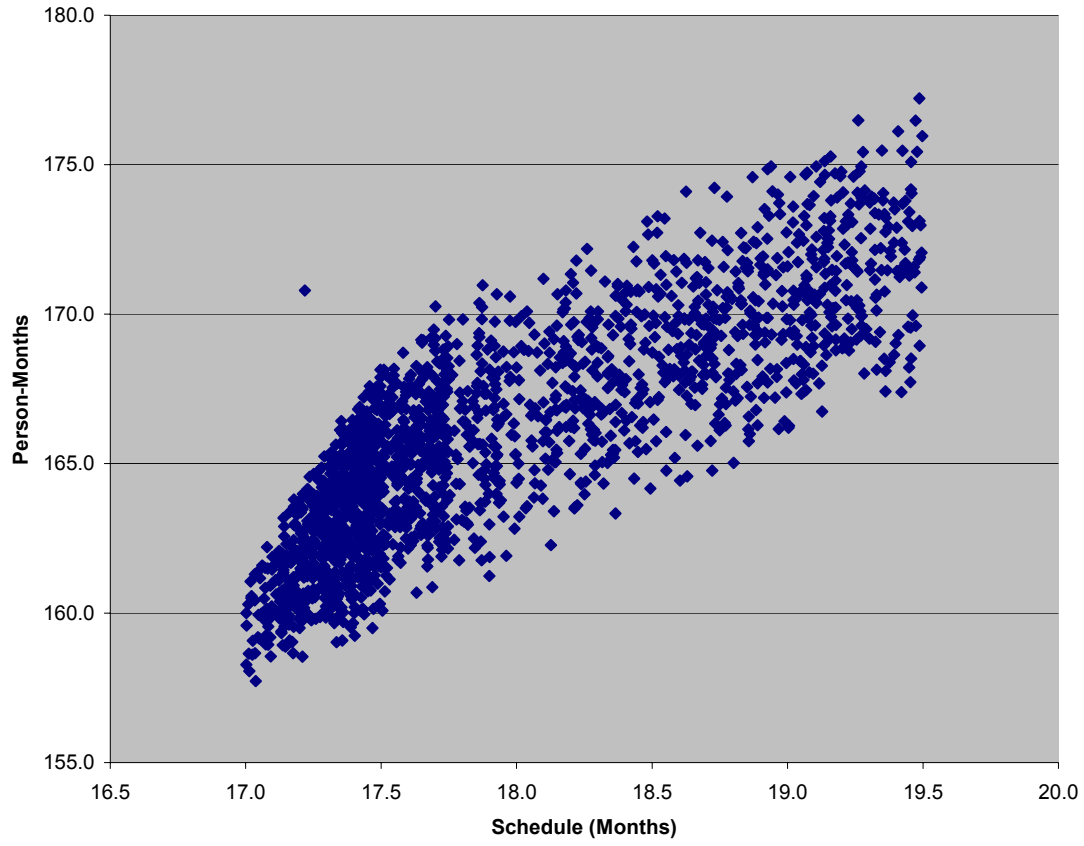


Figure 5-5 Cost/Schedule Containment Curve

Trial	Random A	A	B	C	D	E	F	G	H	I	J	K	A+B+E+H+K	C+D+G+K	F+I+J+K	A	B	C	D	E	F	G	H	I	J	K	Total Manhours (Cost)
1	0.9338	3	2.75	4.62	3.5	4.87	4.60	5	2.5	4	4	4	17.12	17.12	16.60	12	5.5	33.41	7	18.10	28.63	15	7.5	16	20	12	175.14
2	0.6738	3	2.75	4.80	3.5	4.88	4.79	5	2.5	4	4	4	17.13	17.30	16.79	12	5.5	18.46	4	22.16	28.69	15	7.5	16	20	12	161.30
3	0.5151	3	2.75	4.51	3.5	5.25	4.57	5	2.5	4	4	4	17.50	17.01	16.57	12	5.5	21.31	4	21.40	30.68	15	7.5	16	20	12	165.39
4	0.9369	3	2.75	6.61	3.5	4.96	4.59	5	2.5	4	4	4	17.21	19.11	16.59	12	5.5	27.77	4	23.12	29.82	15	7.5	16	20	12	172.72
5	0.1683	3	2.75	5.52	3.5	4.70	5.12	5	2.5	4	4	4	16.95	18.02	17.12	12	5.5	18.08	4	24.28	30.89	15	7.5	16	20	12	165.25
6	0.0326	3	2.75	4.51	3.5	5.38	5.38	5	2.5	4	4	4	17.63	17.01	17.38	12	5.5	22.34	4	23.76	28.23	15	7.5	16	20	12	166.33
7	0.0410	3	2.75	5.37	3.5	4.81	4.51	5	2.5	4	4	4	17.06	17.87	16.51	12	5.5	19.34	4	24.43	29.66	15	7.5	16	20	12	165.43
8	0.6483	3	2.75	6.21	3.5	4.61	5.46	5	2.5	4	4	4	16.86	18.71	17.46	12	5.5	18.85	4	22.74	32.90	15	7.5	16	20	12	166.49
9	0.0353	3	2.75	6.22	3.5	4.76	4.73	5	2.5	4	4	4	17.01	18.72	16.73	12	5.5	27.79	4	21.68	32.13	15	7.5	16	20	12	173.60
10	0.4814	3	2.75	5.25	3.5	4.77	5.10	5	2.5	4	4	4	17.02	17.75	17.10	12	5.5	26.29	4	21.07	28.20	15	7.5	16	20	12	167.56
11	0.0451	3	2.75	4.64	3.5	5.15	5.18	5	2.5	4	4	4	17.40	17.14	17.18	12	5.5	19.52	4	23.15	31.51	15	7.5	16	20	12	166.18
12	0.0779	3	2.75	4.86	3.5	4.70	4.96	5	2.5	4	4	4	16.95	17.36	16.96	12	5.5	19.00	4	20.26	30.20	15	7.5	16	20	12	161.46
13	0.1164	3	2.75	4.57	3.5	4.99	5.36	5	2.5	4	4	4	17.24	17.07	17.36	12	5.5	19.18	4	20.48	27.30	15	7.5	16	20	12	158.96
14	0.1087	3	2.75	4.66	3.5	5.25	5.12	5	2.5	4	4	4	17.50	17.16	17.12	12	5.5	21.08	4	22.38	31.77	15	7.5	16	20	12	167.23
15	0.4164	3	2.75	4.70	3.5	4.53	5.20	5	2.5	4	4	4	16.78	17.20	17.20	12	5.5	19.26	4	23.68	31.70	15	7.5	16	20	12	166.64
16	0.2657	3	2.75	6.68	3.5	4.71	4.64	5	2.5	4	4	4	16.96	19.18	16.64	12	5.5	26.35	4	23.40	31.02	15	7.5	16	20	12	172.77
17	0.0067	3	2.75	6.21	3.5	5.33	5.41	5	2.5	4	4	4	17.58	18.71	17.41	12	5.5	19.38	4	24.40	30.67	15	7.5	16	20	12	166.45
18	0.0899	3	2.75	4.84	3.5	5.31	4.53	5	2.5	4	4	4	17.56	17.34	16.53	12	5.5	18.99	4	22.86	28.40	15	7.5	16	20	12	162.25
19	0.0799	3	2.75	6.85	3.5	5.06	5.44	5	2.5	4	4	4	17.31	19.35	17.44	12	5.5	23.83	4	24.04	32.08	15	7.5	16	20	12	171.96
20	0.9567	3	2.75	5.41	3.5	4.99	4.96	5	2.5	4	4	4	17.24	17.91	16.96	12	5.5	19.92	4	24.39	31.06	15	7.5	16	20	12	167.38
21	0.9977	3	2.75	4.50	3.5	5.33	5.13	5	2.5	4	4	4	17.58	17.00	17.13	12	5.5	19.12	4	23.47	31.72	15	7.5	16	20	12	166.30
22	0.3597	3	2.75	6.16	3.5	4.54	5.20	5	2.5	4	4	4	16.79	18.66	17.20	12	5.5	25.29	4	23.22	30.31	15	7.5	16	20	12	170.82
23	0.9626	3	2.75	4.91	3.5	4.52	4.90	5	2.5	4	4	4	16.77	17.41	16.90	12	5.5	26.38	4	22.02	32.97	15	7.5	16	20	12	173.37
24	0.6708	3	2.75	4.63	3.5	4.67	4.69	5	2.5	4	4	4	16.92	17.13	16.69	12	5.5	19.61	4	22.10	27.76	15	7.5	16	20	12	161.47
25	0.2359	3	2.75	5.76	3.5	5.19	4.62	5	2.5	4	4	4	17.44	18.26	16.62	12	5.5	27.95	4	22.72	29.02	15	7.5	16	20	12	171.69
26	0.5375	3	2.75	6.16	3.5	5.10	4.94	5	2.5	4	4	4	17.35	18.66	16.94	12	5.5	20.38	4	22.72	29.89	15	7.5	16	20	12	164.99
27	0.5369	3	2.75	6.55	3.5	5.42	5.09	5	2.5	4	4	4	17.67	19.05	17.09	12	5.5	19.44	4	22.25	27.93	15	7.5	16	20	12	161.62
28	0.3596	3	2.75	4.80	3.5	5.00	4.73	5	2.5	4	4	4	17.25	17.30	16.73	12	5.5	19.33	4	22.92	32.97	15	7.5	16	20	12	167.23
29	0.0229	3	2.75	4.69	3.5	4.80	5.35	5	2.5	4	4	4	17.05	17.19	17.35	12	5.5	18.57	4	23.25	31.52	15	7.5	16	20	12	165.34
30	0.5461	3	2.75	4.81	3.5	5.32	5.43	5	2.5	4	4	4	17.57	17.31	17.43	12	5.5	19.15	4	22.17	30.58	15	7.5	16	20	12	163.90
31	0.5473	3	2.75	4.63	3.5	4.88	4.59	5	2.5	4	4	4	17.13	17.13	16.59	12	5.5	18.16	4	24.47	30.54	15	7.5	16	20	12	165.17
32	0.0617	3	2.75	6.10	3.5	5.02	4.76	5	2.5	4	4	4	17.27	18.60	16.76	12	5.5	23.97	4	21.90	31.25	15	7.5	16	20	12	169.12
33	0.1141	3	2.75	4.75	3.5	4.99	4.77	5	2.5	4	4	4	17.24	17.25	16.77	12	5.5	27.27	4	23.51	27.63	15	7.5	16	20	12	170.42
34	0.4668	3	2.75	5.04	3.5	4.52	5.44	5	2.5	4	4	4	16.77	17.54	17.44	12	5.5	23.03	4	24.05	32.51	15	7.5	16	20	12	171.59
35	0.7327	3	2.75	4.51	3.5	4.73	5.21	5	2.5	4	4	4	16.98	17.01	17.21	12	5.5	18.32	4	24.56	28.32	15	7.5	16	20	12	163.19
36	0.5064	3	2.75	6.26	3.5	4.99	4.63	5	2.5	4	4	4	17.24	18.76	16.63	12	5.5	19.55	4	23.24	27.35	15	7.5	16	20	12	162.14
37	0.9176	3	2.75	5.14	3.5	4.96	5.32	5	2.5	4	4	4	17.21	17.64	17.32	12	5.5	19.78	4	21.03	29.64	15	7.5	16	20	12	162.45
38	0.2887	3	2.75	4.51	3.5	5.30	4.51	5	2.5	4	4	4	17.55	17.01	16.51	12	5.5	23.36	4	23.56	28.82	15	7.5	16	20	12	167.74
39	0.8137	3	2.75	4.52	3.5	5.49	4.91	5	2.5	4	4	4	17.74	17.02	16.91	12	5.5	22.16	4	23.58	32.45	15	7.5	16	20	12	170.18

Figure 5-6 Cost/Schedule Containment Analysis Calculations- Representation of Data

5.1.1 Supportability of LWIR Scanning Detector

Partial justification for the LWIR scanning detector listed as a high risk task is due to the number of parts contained within this detector and, therefore, the probability of failure. Parts obsolescence is another reason for this detector being classified as a high risk task. The process used was as follows: look at each obsolete component and determine when its stock would be depleted to zero using a consumption rate that was the average of that experienced over the last

three years by other programs using this LWIR scanning detector configuration. If the stock was calculated to deplete prior to the end of FY2010, then the program procured additional parts from available stock, if possible, to extend the depletion date to beyond the year 2009. When adequate parts were not available (or could not be procured) to extend the stock depletion date beyond the year 2010, the quantity of shop replaceable unit (SRU) spares using that part and the SRU scrap rates were looked at. This was to determine whether or not SRU spare stocks were adequate to extend the date beyond the year 2011. This evaluation considered the additional SRU spares that would be made available after the year 2009 when line replaceable unit (LRU) cannibalization is expected to begin. An SRU is an item that has to be sent back to a “manufacturing” (shop) area for repair or replacement, a component on a circuit board for example. A LRU is an item that can be replaced “on the line” or in the field, a complete mother board for example.

5.1.1.1 LWIR Scanning Detector Components

The components evaluated in this study were those on the example program’s Bill of Material (BOM). The BOM evaluated consisted of 1060 electrical component part numbers and 16,641 actual components. A total of 28 percent, 301 part numbers or 3636 components, were active electrical components. The rest were passive components such as resistors, capacitors, transformers and inductors, relays or switches. Evaluation of the parts, concentrating on the electrical parts (active and passive circuit card components) was performed. Mechanical parts within the example program were also evaluated, but due to the longer life cycles of these parts, they were not evaluated to the same detail.

5.1.2 Supportability of MWIR Staring Detector

Evaluation of the MWIR staring detector, low risk task, resulted in the following:

- Maintains existing architecture, interface, and wiring configurations for both of Customer X's platforms (land vehicle or UAV)
- Eliminates complex scanning assemblies (scanner and interlacer), historically high failure rate items
- Reduces video chain components from 23 SRUs to 6 SRUs
- Incorporates available (in large scale production) MWIR staring FPA assemblies
- Better detection and ranging performance per Customer X's requirements
- Same initial cost, when compared to LWIR scanning detector
- Lower maintenance and support costs due to reduction in parts used and stored.

5.1.3 Supportability of LWIR Staring Detector

The LWIR staring detector, moderate risk task, was also evaluated. It is considered a moderate risk task for the following:

- Currently not in large scale production
- More expensive to obtain at this time
- Technology not being pursued/focus shifting to dual band sensors, which may present another option for Customer X.

CHAPTER VI

SUMMARY AND CONCLUSION

6.1 Summary

A MWIR staring detector was chosen as the assembly to meet Customer X's requirements. The decision was based on the ability to meet the systems engineering criteria laid out at the beginning of this document. Having met the selection criteria and demonstrated ability to detect and recognize potential targets at a longer range, the MWIR staring detector assembly had better overall performance. It is also the most reliable system, having a large-scale production in place [5, 35], and overall used fewer components [36] leading to a more reliable system by reducing the probability of failure. The MWIR detector assembly meets schedule restraints and poses less risk. In short the MWIR detector is the lowest risk, lowest cost, and has the most efficient schedule. It is notable that LWIR scanning systems compete well with staring systems for equivalent frame rates, but improvements in multiplexer technology, giving higher storage capacity and/or faster read-out rates, will increasingly favor staring systems for all wave bands.

6.2 Conclusion

There are numerous applications for IR imagers, and looking toward the future, IR industry believes that customers are looking for detector assemblies that are smaller, use less power, operational capability over larger portions of the electromagnetic spectrum concurrently (dual or greater bandwidths), and cost less. This being said, customers will still require the

superior image quality and temperature discrimination attributes the larger detector assemblies have been creating and providing over the past years. Designers and engineers must allow for these incorporations into their designs. Several technologists are currently working in these areas and making progress toward simultaneously employing operation in two or more spectral bands.

REFERENCES

1. R. D. Hudson, Jr., *Infrared System Engineering*, New York: John Wiley & Sons, Inc., 1969.
2. W. L. Wolfe and G. J. Zissis, *The Infrared Handbook*, The IR Information and Analysis Center, Environmental Research Institute of Michigan for the Office of Naval Research, Department of the Navy, Washington, DC, 1978.
3. Frost & Sullivan webpage,
<http://www.frost.com/prod/servlet/fcom?/ActionName=DisplayReport&ID=7984-01-00-00-00&ed=1&fcmseq=1032199227447>
4. M. J. Kelly, "The Bell Telephone Laboratories- An Example of an Institute of Creative Technology," *Proceedings of the Royal Society London*, 203A, 287, 1950.
5. Leonard P. Chen, "Advanced FPAs for Multiple Applications," *Aerosense, International Conference on Infrared Technology and Applications: SPIE, vol. 4721, Infrared Detectors and Focal Plane Arrays VII*, Proceeding of SPIE, Orlando, FL, 2002.
6. Horn, S. B., J. Campbell, R.G. Driggers, T. J. Soyka, P. R. Norton, P. Perconti, U.S Army Night Vision and Electronic Sensors Directorate; T.E. Ostromek, J.P. Estrera, A.V. Bacarella, T. R. Beystum, Litton EO Systems (USA); D. A. Scribner, P. R. Warren, Naval Research Laboratory (USA), "Fused reflected/emitted light sensors," *Aerosense, International Conference on Infrared Technology and Applications: SPIE, vol. 4369, Infrared Technology and Applications XXVII*, Proceeding of SPIE, Orlando, FL, 2002.
7. D. M. T. Cochrane, P. A. Manning, Defence Evaluation and Research Agency Malvern (UK); T. A. Wyllie, Defence Evaluation and Research Agency Farnborough (UK), "Uncooled thermal imaging sensor for UAV applications," *Aerosense, International Conference on Infrared Technology and Applications: SPIE, vol. 4369, Infrared Technology and Applications XXVII*, Proceeding of SPIE, Orlando, FL, 2002.
8. S. B. Horn, D. Lohrmann, J. Campbell, P. Perconti, U.S. Army Night Vision & Electronic Sensors Directorate; R. S. Balcerak, Defense Advanced Research Projects Agency (USA), "Uncooled IR technology and applications," *Aerosense, International Conference on Infrared Technology and Applications: SPIE, vol. 4369, Infrared Technology and Applications XXVII*, Proceeding of SPIE, Orlando, FL, 2002.
9. M. E. Couture, OPTICS 1, Inc. (USA), "Challenges in IR Optics," *Aerosense, International Conference on Infrared Technology and Applications: SPIE, vol. 4369, Infrared Technology and Applications XXVII*, Proceeding of SPIE, Orlando, FL, 2002.
10. R. Etienne-Cummings, D. I. Gruev, M. Clapp, Johns Hopkins University (USA), "High-resolution focal plane image processing," *Aerosense, International Conference on Infrared Technology and Applications: SPIE, vol. 4369, Infrared Technology and Applications XXVII*, Proceeding of SPIE, Orlando, FL, 2002.
11. J. Ziegler, M. Bruder, W. A. Cabanski, H. Figgemeier, M. Finck, P. Menger, Th. Simon, R. Wollrab, AIM AEG Infrarot-Module BmbH (Germany), "Improved HgCdTe technology for high-performance infrared detectors," *Aerosense, International Conference on Infrared Technology and Applications: SPIE, vol. 4721, Infrared Detectors and Focal Plane Arrays VII*, Proceeding of SPIE, Orlando, FL, 2002.
12. Z. Celik-Butler, D. P. Butler, A. Yildiz, Southern Methodist University (USA), "Room-temperature YBaCuO infrared detectors on a flexible substrate," *Aerosense, International*

- Conference on Infrared Technology and Applications: SPIE, vol. 4721, Infrared Detectors and Focal Plane Arrays VII*, Proceeding of SPIE, Orlando, FL, 2002.
13. H. Shen, K. Aliberti, M. R. Stead, W. C. Ruff, B. L. Stann, Army Research Lab (USA), "Rectification in metal-semiconductor-metal detectors used as optoelectronic mixers," *Aerosense, International Conference on Infrared Technology and Applications: SPIE, vol. 4721, Infrared Detectors and Focal Plane Arrays VII*, Proceeding of SPIE, Orlando, FL, 2002.
 14. J. T. Montroy, J. D. Garnett, S. A. Cabelli, M. Loose, A. B. Joshi, G. W. Hughes, L. J. Kozlowski, A. K. Haas, S. S. Wong, M. Zandian, A. C. Chen, J. G. Pasko, M/ C Farris, C. A. Cabelli, D. E. Cooper, J. M. Arias, J. Bajaj, K. Vural, Rockwell Scientific Co., LLC (USA), "Advanced imaging sensors at Rockwell Scientific Company," *Aerosense, International Conference on Infrared Technology and Applications: SPIE, vol. 4721, Infrared Detectors and Focal Plane Arrays VII*, Proceeding of SPIE, Orlando, FL, 2002.
 15. W. A. Cabanski, R. Breiter, K. H. Mauk, W. Rode, J. Ziegler, AIM AEG Infrarot-Module GmbH (Germany), "Broadband and dual-color high-speed MCT MWIR modules," *Aerosense, International Conference on Infrared Technology and Applications: SPIE, vol. 4721, Infrared Detectors and Focal Plane Arrays VII*, Proceeding of SPIE, Orlando, FL, 2002.
 16. M. G. Stapelbroek, E. W. Atkins, DRS Sensors and Targeting Systems, Inc. (USA), "Two-color blocked-impurity-band detector arrays," *Aerosense, International Conference on Infrared Technology and Applications: SPIE, vol. 4721, Infrared Detectors and Focal Plane Arrays VII*, Proceeding of SPIE, Orlando, FL, 2002.
 17. G. T. Petrovsky, S. I. Filachev, State Unitary Enterprise Research, Development, and Production Ctr. Orion (Russia), "Fundamental problems of IR optics and optical industry," *Aerosense, International Conference on Infrared Technology and Applications: SPIE, vol. 4369, Infrared Technology and Applications XXVII*, Proceeding of SPIE, Orlando, FL, 2002.
 18. D. Vickler, R. LeBlanc, Lockheed Martin Missiles and Fire Control (USA), "Midwave infrared imager with plastic laminated diffractive/aspheric surfaces," *Aerosense, International Conference on Infrared Technology and Applications: SPIE, vol. 4369, Infrared Technology and Applications XXVII*, Proceeding of SPIE, Orlando, FL, 2002.
 19. U. Hingst, S. Korber, Badenseewerk Geratetechnik GmbH (Germany), "IR window design for hypersonic missile seekers: thermal shock and cooling systems," *Aerosense, International Conference on Infrared Technology and Applications: SPIE, vol. 4369, Infrared Technology and Applications XXVII*, Proceeding of SPIE, Orlando, FL, 2002.
 20. H. S. Kim, W. K. Yu, Y. C. Park, E. S. Yoon, C. W. Kim, I. S. Song, S. M. Hong, Agency for Defense Development (Korea), "Compact MWIR camera with X20 zoom optics," *Aerosense, International Conference on Infrared Technology and Applications: SPIE, vol. 4369, Infrared Technology and Applications XXVII*, Proceeding of SPIE, Orlando, FL, 2002.
 21. D. Scribner, J. Schuler, P. Warren, G. Howard, R. Klein, Naval Research Laboratory, "Melding images for information," *OE Magazine, vol. 2, number 9*, Published monthly by SPIE, 1000 20th St, Bellingham, WA 98225, 2002.
 22. W. A. Cabanski, R. Breiter, R. Koch, K. H. Mauk, W. Rode, J. Ziegler, AEG Infrarot-Module GmbH (Germany); H. Schneider, M. Walther, Fraunhofer-Institut für Angewandte Festkörperphysik (Germany); R. Oelmaier, Amtel Wireless and

- Microcontrollers (Germany), "Third-generation focal plane array IR detection modules at AIM," *Aerosense, International Conference on Infrared Technology and Applications: SPIE, vol. 4369, Infrared Technology and Applications XXVII*, Proceeding of SPIE, Orlando, FL, 2002.
23. J. S. Anderson, D. Bradley, C. W. Chen, R. Chin, K. Jurgelewicz, Raytheon Co. (USA); W. A. Radford, A. Kennedy, D. F. Murphy, M. Ray, R. Wyles, Raytheon Infrared Operations (USA); J. C. Brown, G. W. Newsome, U. S. Army Night Vision & Electronic Sensors Dictorate, "Low-cost microsensors program," *Aerosense, International Conference on Infrared Technology and Applications: SPIE, vol. 4369, Infrared Technology and Applications XXVII*, Proceeding of SPIE, Orlando, FL, 2002.
 24. M. A. Kinch, DRS Infrared Technologies (USA), "HDVIP FPA technology at DRS Infrared Technologies," *Aerosense, International Conference on Infrared Technology and Applications: SPIE, vol. 4369, Infrared Technology and Applications XXVII*, Proceeding of SPIE, Orlando, FL, 2002.
 25. R. Brieter, W. A. Cabanski, K. H. Mauk, W. Rode, J. Ziegler, AEG Infrarot-Module GmbH (Germany), "Portable sequential multicolor thermal imager based on a MCT 384 x 288 focal plane array," *Aerosense, International Conference on Infrared Technology and Applications: SPIE, vol. 4369, Infrared Technology and Applications XXVII*, Proceeding of SPIE, Orlando, FL, 2002.
 26. LOWTRAN, MODTRAN, and HITRAN are discussed in many texts. See, for example, M. E. Thomas and L. D. Duncan, "Atmospheric Transmission," in *Atmospheric Propagation of Radiation*, F. G. Smith, ed. This is volume 2 of *The Infrared and Electro-Optical Systems Handbook*, J. S. Accetta and D. L. Shumaker, eds., copublished by Environmental Research Institute of Michigan, Ann Arbor, MI and SPIE Press, Bellingham, WA, 1993.
 27. G. C. Holst, *Common Sense Approach to Thermal Imaging*, co-published by JCD Publishing, Winter Park, FL and SPIE- The International Society for Optical Engineering, Bellingham, WA, 2000.
 28. J. M. Lloyd, *Thermal Imaging Systems*, New York: Plenum Press, 1975.
 29. D. Brown, B. Daniel, T. Horikiri, P. King, D. Nelson, and M. Small, "Advances in High-performance Sensors for the Military and Commercial Market," *Aerosense, International Conference on Infrared Technology and Applications: SPIE, XXVII Cooled Focal Plane Arrays and Their Applications*, Proceeding of SPIE, Vol. 4369, Orlando, FL, 2001.
 30. W. J. Smith, *Modern Optical Engineering*, New York: McGraw-Hill, 1990.
 31. F. X. Kneizys, E. P. Shuttle, L. W. Abreau, J. H. Chetwynd, Jr., G. P. Anderson, W. O. Gallery, J. E. Selby, and S. A. Clough, "Users Guide to LOWTRAN 7/MODTRAN 2," Air Force Geophysical Laboratory Report AFGL-TR-88-0177, Hanscom AFB, MA 01731, 1988.
 32. U. S. Army Night Vision and Electronic Sensors Dictorate, Science and Technology Division, Visionics Modeling and Simulation Branch, "ACQUIRE Range Performance Model for Target Acquisition Systems, User's Guide," U. S. Army CECOM RDEC, Night Vision and Electronic Sensors Dictorate, Ft. Belvoir, VA, 1995.
 33. U. S. Army Night Vision and Electronic Sensors Dictorate, Modeling and Simulation Division, "Night Vision Thermal Imaging Systems Performance Model, User's Manual and Reference Guide," U. S. Army Night Vision and Electronic Sensors Dictorate, Ft. Belvoir, VA, 2002.

34. Dr. J. Dean, Engineering Chief Risk & System Analysis LFWC and D. Benson, Jr., Engineering Specialist, Avionic Software Engineering LFWC, "Schedule Risk Analysis of Software Development," SMU Systems Engineering Class Notes, 2002.
35. D. Murphy, M. Ray, R. Wyles, J. Asbrock, N. Lum, C. Hewitt, A. Kennedy, and D. Van Lue, Raytheon Infrared Operations (USA); J. Anderson, D. Bradley, R. Chin, T. Kostrzewa, Raytheon Electronic Systems (USA); "High Sensitivity 25 μm Microbolometer FPAs," *Aerosense, International Conference on Infrared Technology and Applications: SPIE, vol. 4721, Infrared Detectors and Focal Plane Arrays VII*, Proceeding of SPIE, Orlando, FL, 2002.
36. B. Backer, Dr. N. Butler, Dr. M. Kohin, Dr. M. Gurnee, J. Whitman, and T. Breen, BAE Systems (USA); "Recent Improvements and Developments in Uncooled Systems at BAE North America," *Aerosense, International Conference on Infrared Technology and Applications: SPIE, vol. 4721, Infrared Detectors and Focal Plane Arrays VII*, Proceeding of SPIE, Orlando, FL, 2002.

APPENDIX A

List of Acronyms

BOM:	bill of material
CRT:	cathode ray tube
D*:	detectivity
EFL:	effective focal length
EO:	electro-optical
FLIR:	forward looking infrared
FOV:	field of view
FPA:	focal plane array
IR:	infrared
LRU:	line replaceable unit
LWIR:	longwave infrared
MRC:	minimum resolvable contrast
MRT:	minimum resolvable temperature
MTF:	modulation transfer function
MWIR:	midwave infrared
NETD:	noise equivalent temperature difference
NUC:	non-uniformity correction
R _D :	responsivity
SRU:	shop replaceable unit
SWIR:	short-wave infrared
TDI:	time delay and integration
UAV:	unmanned aerial vehicle
VFOV:	vertical field of view
VLWIR:	very longwave infrared

APPENDIX B

Model Inputs

NVTherm inputs

1. This is an example of a scanning LWIR input file. It has an FOV of $2.0^\circ \times 1.5^\circ$, $f/\#$ of 3.75 and a peak D^* of $6E11 \text{ cm-sqr(Hz)/Watt}$.

Sensor Name = scl153

4:01:27 PM 7/30/02

*****SENSOR INPUT DATA*****

Type Of Imager = Scanning Continuous

Single Frame = No

Cut On Wavelength = 8.2

Cut Off Wavelength = 12

Magnification In = 0.00

Horizontal FOV In = 2.00

VerticalFOV In = 1.50

Frame Rate = 30.00

Vertical Interlace = 2.00

Vertical Interlace = No

Diffraction Wavelength = 10.00

Average Optics Transmission = 0.60

Focal Length In = 18.00

FNumber In = 3.75

Aperture Diameter In = 4.80

Optics Blur = 0.00

Optics Blur Units = Milliradians in Object Space

Optics Blur Type = RMS or Standard Deviation

Vib Blur X = 0.02

Vib Blur Y = 0.02

Vib Blur Type = RMS or Standard Deviation

Detector Horr Dimension = 12.00

Detector Vertical Dimension = 20.00

PeakDstar In = $6.00E+11$

Integration Time In = 1,000.00

Number of TDI = 1

Samples Per HIFOV = 0.00

Scan Efficiency = 0.90

Number of Horr Detectors = 1

Number of Vert Detectors = 140.00

Noise Factor X = 0.00

Noise Factor Y = 0.00

Sigmavh = 0.00

Sigmav = 0.00

FPN = None

PtSi = No

Emission Coefficient = 0.00

Barrier Height = 0.00

Uncooled = No

NETD = 0.00

Measured Frame Rate (for Uncooled) = 0.00

Measured Fnumber (for Uncooled) = 0.00

Measured Optic Transmission (for Uncooled) = 0.00
Dither = No
LowPass 3dB Cutoff = 22,000.00
LowPass Filter Order = 1
Noise Gain = 0
Frame Integration = 1
Horr Interpolation = None
Vert Interpolation = None
Horr Interp Type = Pixel Replication
Vert Interp Type = Pixel Replication
EZoom = None
EZoom Type = Pixel Replication
Horr Boost = No
Vert Boost = No
Display Type = CRT
EoMUX = No
Horizontal LED Size = 0.00
Vertical LED Size = 0.00
CRT Type = Shrinking Raster
Bar Chart Type = MRT
LED Height = 0.00
LED Width = 0.00
Display Spot Height = 0.02
Display Spot Width = 0.02
Average Display Luminance = 10
Minimum Display Luminance = 0
Scene Contrast Temp = 1
Display Height = 15.24
Display Viewing Distance = 38.30
Number of Eyes = 2

2. This is an example of a scanning MWIR input file. It has an FOV of $2.0^\circ \times 1.5^\circ$, $f/\#$ of 3.75 and a peak D^* of $6E11 \text{ cm-sqr(Hz)/Watt}$.

Sensor Name = scm153
5:20:34 PM 7/30/02
*****SENSOR INPUT DATA*****

Type Of Imager = Scanning Continuous
Single Frame = No
Cut On Wavelength = 3.7
Cut Off Wavelength = 5.05
Magnification In = 0.00
Horizontal FOV In = 2.00
VerticalFOV In = 1.50
Frame Rate = 30.00
Vertical Interlace = 2.00
Vertical Interlace = No
Diffraction Wavelength = 4.38
Average Optics Transmission = 0.60
Focal Length In = 18.00
FNumber In = 3.75
Aperture Diameter In = 4.80
Optics Blur = 0.00

Optics Blur Units = Milliradians in Object Space
Optics Blur Type = RMS or Standard Deviation
Vib Blur X = 0.02
Vib Blur Y = 0.02
Vib Blur Type = RMS or Standard Deviation
Detector Horr Dimension = 12.00
Detector Vertical Dimension = 20.00
PeakDstar In = 6.00E+11
Integration Time In = 1,000.00
Number of TDI = 1
Samples Per HIFOV = 0.00
Scan Efficiency = 0.90
Number of Horr Detectors = 1
Number of Vert Detectors = 140.00
Noise Factor X = 0.00
Noise Factor Y = 0.00
Sigmavh = 0.00
Sigmav = 0.00
FPN = None
PtSi = No
Emission Coefficient = 0.00
Barrier Height = 0.00
Uncooled = No
NETD = 0.00
Measured Frame Rate (for Uncooled) = 0.00
Measured Fnumber (for Uncooled) = 0.00
Measured Optic Transmission (for Uncooled) = 0.00
Dither = No
LowPass 3dB Cutoff = 22,000.00
LowPass Filter Order = 1
Noise Gain = 0
Frame Integration = 1
Horr Interpolation = None
Vert Interpolation = None
Horr Interp Type = Pixel Replication
Vert Interp Type = Pixel Replication
EZoom = None
EZoom Type = Pixel Replication
Horr Boost = No
Vert Boost = No
Display Type = CRT
EoMUX = No
Horizontal LED Size = 0.00
Vertical LED Size = 0.00
CRT Type = Shrinking Raster
Bar Chart Type = MRT
LED Height = 0.00
LED Width = 0.00
Display Spot Height = 0.02
Display Spot Width = 0.02
Average Display Luminance = 10
Minimum Display Luminance = 0
Scene Contrast Temp = 1
Display Height = 15.24
Display Viewing Distance = 38.30
Number of Eyes = 2

ACQUIRE inputs

1. This is an example of a scanning LWIR input ACQUIRE file. It has an FOV of $2.0^\circ \times 1.5^\circ$, $f/\#$ of 3.75 and a peak D^* of $6E11$ cm-sqr(Hz)/Watt.
2. The data file name calls the MRT look-up file which lists the MRT of each sensor individually.
3. The sensor ID calls out whether the sensor is scanning (sc) or staring (str).

NVESD acquire: LW scan (EFL7.09") (c:\ACQ96\scanning\lw\ for cases scl153 to scl23)

```
>sensor
  optics_cut_on           8.2   micrometers
  optics_cutoff          12.0  micrometers
  horizontal_FOV         2.00  degrees
  WFOV_to_NFOV_ratio     4.0   ---
>sensor_lookup
  data_file_name         lwsc.prn   ---
  sensor_id              sc           ---
  performance_mode       MRT          MRT_MDT_MRC_or_MDC
>target
  characteristic_dimension 2.0    meters
  target_signature         1.0    degrees_C_or_contrast
>cycle_criteria
  detection_n50           .75    wfov
  detection_n50           .75    nfov
  classification_n50     1.5    nfov
  recognition_n50        3.0    nfov
  identification_n50     6.0    nfov
```

Next 3 band-averaged atm are MODTRAN Tropical enviro w/ no aerosol attenuation with altitude and slant path specified for each run. Simulates warm-humid climate.

```
>band-averaged_atmosphere
  #_points: 3    km....transmittance...200ft...lw
           2    .4755
           5    .1843
           10   .0434
```

```
>repeat
>band-averaged_atmosphere
  #_points: 3    km....transmittance...800ft...lw
           2    .4950
           5    .2023
           10   .0514
```

```
>repeat
>band-averaged_atmosphere
  #_points: 3    km...transmittance...3Kft...lw
           2    .5596
           5    .2683
           10   .0867
```

Next 3 band-averaged atm are MODTRAN Mid-latitude Summer enviro w/ no aerosol attenuation with altitude and slant path specified for each run. Simulates warm-dry climate.

```
>band-averaged_atmosphere
  #_points: 3    km....transmittance...200ft...lw
           2    .6189
           5    .3380
```

```

10 .1336
>repeat
>band-averaged_atmosphere
  #_points: 3 km...transmittance...800ft...lw
            2 .6336
            5 .3568
            10 .1475

```

```

>repeat
>band-averaged_atmosphere
  #_points: 3 km...transmittance...3Kft...lw
            2 .6807
            5 .4211
            10 .2008

```

>repeat
 Next 25 band-averaged atm are MODTRAN Mid-latitude Winter enviro w/ no aerosol attenuation with altitude and slant path specified for each run. Simulates cold-dry climate.

```

>band-averaged_atmosphere
  #_points: 7 km...transmittance...200ft...lw
            2 .9091
            5 .8121
            10 .6862
            15 .5864
            20 .5039
            25 .4354
            30 .3774

```

```

>repeat
>band-averaged_atmosphere
  #_points: 9 km...transmittance...800ft...lw
            2 .9122
            5 .8183
            10 .6957
            15 .5981
            20 .5172
            25 .4492
            30 .3917
            35 .3421
            50 .2301

```

```

>repeat
>band-averaged_atmosphere
  #_points: 9 km...transmittance...3kft...lw
            2 .9221
            5 .8382
            10 .7268
            15 .6372
            20 .5611
            25 .4963
            30 .4407
            35 .3919
            50 .2780

```

```
>end
```

□

APPENDIX C

Model outputs

NVTherm output

1. This is an example of a scanning LWIR output file. It has an FOV of 2.0° x 1.5°, f/# of 3.75 and a peak D* of 6E11 cm-sqr(Hz)/Watt. It is the output of file number one listed in Appendix B.

Sensor Name = scl153
4:01:27 PM 7/30/02

*****BASIC SYSTEM CALCULATIONS*****

Vertical FOV = 1.50 Degrees
Horizontal FOV = 2.00 Degrees
Magnification Calculated - No E-Zoom
Magnification = 15.00 Unitless

*****SPACE CALCULATIONS*****

Vertical Detector Angular Subtense (or IFOV) = 0.11 Milliradians
Horizontal Detector Angular Subtense (or IFOV) = 0.07 Milliradians
Airy Disc Diameter (distance between zeroes) = 0.51 Milliradians
Vertical Angular Sample Spacing = 0.09 Milliradians
Horizontal Angular Sample Spacing = 0.00 Milliradians

*****FREQUENCY CALCULATIONS*****

Vertical Detector Cutoff Frequency = 9.00 Cycles per milliradian
Horizontal Detector Cutoff Frequency = 15.00 Cycles per milliradian
Diffraction Cutoff Frequency = 4.80 Cycles per milliradian
Vertical Sampling Frequency = 10.70 Cycles per milliradian
Vertical Half-Sample Frequency = 5.35 Cycles per milliradian

*****TEMPORAL CALCULATIONS*****

Efficiency Factor = 0.001 unitless
Dwell Time = 28.65 microseconds
Scan Velocity = 2,327.10 milliradians per second
Eye Integration Time = 0.062 seconds

***** NOISE CALCULATIONS *****

System Bandwidth = 32,255.90
System Random Spatio-Temporal Noise (sigma tvh) = 105.84 milliKelvin

***** SAMPLING CALCULATIONS *****

Horizontal Spurious Response = 0.00
Horizontal Out-of-Band SR = 0.00
Vertical Spurious Response = 0.29
Vertical Out-of-Band SR = 0.29

*****HORIZONTAL PRESAMPLE MTF*****

Freq	Diff	Blur	MsOp	Vibr	DetSp	SandH	Cust
0.00	1.00	1.00	1.00	1.00	1.00	1.00	1.00
0.75	0.80	1.00	1.00	1.00	1.00	1.00	1.00
1.50	0.61	1.00	1.00	0.99	0.98	1.00	1.00
2.25	0.43	1.00	1.00	0.98	0.96	1.00	1.00
3.00	0.26	1.00	1.00	0.96	0.94	1.00	1.00
3.75	0.12	1.00	1.00	0.94	0.90	1.00	1.00
4.50	0.02	1.00	1.00	0.91	0.86	1.00	1.00
5.25	0.00	1.00	1.00	0.88	0.81	1.00	1.00
6.00	0.00	0.99	1.00	0.85	0.76	1.00	1.00
6.75	0.00	0.99	1.00	0.82	0.70	1.00	1.00
7.50	0.00	0.99	1.00	0.78	0.64	1.00	1.00
8.25	0.00	0.99	1.00	0.74	0.57	1.00	1.00
9.00	0.00	0.99	1.00	0.70	0.50	1.00	1.00
9.75	0.00	0.98	1.00	0.66	0.44	1.00	1.00
10.50	0.00	0.98	1.00	0.61	0.37	1.00	1.00
11.25	0.00	0.98	1.00	0.57	0.30	1.00	1.00
12.00	0.00	0.97	1.00	0.53	0.23	1.00	1.00
12.75	0.00	0.97	1.00	0.49	0.17	1.00	1.00
13.50	0.00	0.97	1.00	0.45	0.11	1.00	1.00
14.25	0.00	0.96	1.00	0.41	0.05	1.00	1.00

*****VERTICAL PRESAMPLE MTF*****

Freq	Diff	Blur	MsOp	Vibr	DetSp	Cust
0.00	1.00	1.00	1.00	1.00	1.00	1.00
0.75	0.80	1.00	1.00	1.00	0.99	1.00
1.50	0.61	1.00	1.00	0.99	0.95	1.00
2.25	0.43	1.00	1.00	0.98	0.90	1.00
3.00	0.26	1.00	1.00	0.96	0.83	1.00
3.75	0.12	1.00	1.00	0.94	0.74	1.00
4.50	0.02	1.00	1.00	0.91	0.64	1.00
5.25	0.00	1.00	1.00	0.88	0.53	1.00
6.00	0.00	0.99	1.00	0.85	0.41	1.00
6.75	0.00	0.99	1.00	0.82	0.30	1.00
7.50	0.00	0.99	1.00	0.78	0.19	1.00
8.25	0.00	0.99	1.00	0.74	0.09	1.00
9.00	0.00	0.99	1.00	0.70	0.00	1.00
9.75	0.00	0.98	1.00	0.66	-0.08	1.00
10.50	0.00	0.98	1.00	0.61	-0.14	1.00
11.25	0.00	0.98	1.00	0.57	-0.18	1.00
12.00	0.00	0.97	1.00	0.53	-0.21	1.00
12.75	0.00	0.97	1.00	0.49	-0.22	1.00
13.50	0.00	0.97	1.00	0.45	-0.21	1.00
14.25	0.00	0.96	1.00	0.41	-0.19	1.00

*****HORIZONTAL POSTSAMPLE MTF*****

Freq	LPass	Boost	Itrp	Ezoom	EOMux	Disp	Eye	Cust
0.00	1.00	1.00	1.00	1.00	1.00	1.00	1.00	1.00
0.75	1.00	1.00	1.00	1.00	1.00	1.00	0.87	1.00

1.50	0.99	1.00	1.00	1.00	1.00	0.98	0.78	1.00
2.25	0.97	1.00	1.00	1.00	1.00	0.97	0.70	1.00
3.00	0.95	1.00	1.00	1.00	1.00	0.94	0.63	1.00
3.75	0.93	1.00	1.00	1.00	1.00	0.91	0.58	1.00
4.50	0.90	1.00	1.00	1.00	1.00	0.87	0.52	1.00
5.25	0.87	1.00	1.00	1.00	1.00	0.83	0.47	1.00
6.00	0.84	1.00	1.00	1.00	1.00	0.78	0.43	1.00
6.75	0.81	1.00	1.00	1.00	1.00	0.73	0.39	1.00
7.50	0.78	1.00	1.00	1.00	1.00	0.68	0.35	1.00
8.25	0.75	1.00	1.00	1.00	1.00	0.63	0.32	1.00
9.00	0.72	1.00	1.00	1.00	1.00	0.58	0.29	1.00
9.75	0.70	1.00	1.00	1.00	1.00	0.52	0.26	1.00
10.50	0.67	1.00	1.00	1.00	1.00	0.47	0.23	1.00
11.25	0.64	1.00	1.00	1.00	1.00	0.42	0.21	1.00
12.00	0.62	1.00	1.00	1.00	1.00	0.38	0.19	1.00
12.75	0.60	1.00	1.00	1.00	1.00	0.33	0.17	1.00
13.50	0.57	1.00	1.00	1.00	1.00	0.29	0.15	1.00
14.25	0.55	1.00	1.00	1.00	1.00	0.25	0.13	1.00

*****VERTICAL POSTSAMPLE MTFS*****

Freq	Boost	Itrp	Ezoom	EOMux	Disp	Eye	Cust
0.00	1.00	1.00	1.00	1.00	1.00	1.00	1.00
0.75	1.00	1.00	1.00	1.00	1.00	0.87	1.00
1.50	1.00	1.00	1.00	1.00	0.98	0.78	1.00
2.25	1.00	1.00	1.00	1.00	0.97	0.70	1.00
3.00	1.00	1.00	1.00	1.00	0.94	0.63	1.00
3.75	1.00	1.00	1.00	1.00	0.91	0.58	1.00
4.50	1.00	1.00	1.00	1.00	0.87	0.52	1.00
5.25	1.00	1.00	1.00	1.00	0.83	0.47	1.00
6.00	1.00	1.00	1.00	1.00	0.78	0.43	1.00
6.75	1.00	1.00	1.00	1.00	0.73	0.39	1.00
7.50	1.00	1.00	1.00	1.00	0.68	0.35	1.00
8.25	1.00	1.00	1.00	1.00	0.63	0.32	1.00
9.00	1.00	1.00	1.00	1.00	0.58	0.29	1.00
9.75	1.00	1.00	1.00	1.00	0.52	0.26	1.00
10.50	1.00	1.00	1.00	1.00	0.47	0.23	1.00
11.25	1.00	1.00	1.00	1.00	0.42	0.21	1.00
12.00	1.00	1.00	1.00	1.00	0.38	0.19	1.00
12.75	1.00	1.00	1.00	1.00	0.33	0.17	1.00
13.50	1.00	1.00	1.00	1.00	0.29	0.15	1.00
14.25	1.00	1.00	1.00	1.00	0.25	0.13	1.00

*****HORIZONTAL SYSTEM MTFS*****

Freq	Pre	Post No Eye	Base	SR
0.00	1.00	1.00	1.00	0.00
0.75	0.80	0.99	0.79	0.00
1.50	0.59	0.97	0.58	0.00
2.25	0.40	0.94	0.38	0.00
3.00	0.23	0.90	0.21	0.00
3.75	0.10	0.84	0.08	0.00
4.50	0.01	0.79	0.01	0.00
5.25	0.00	0.72	0.00	0.00

6.00	0.00	0.66	0.00	0.00
6.75	0.00	0.60	0.00	0.00
7.50	0.00	0.53	0.00	0.00
8.25	0.00	0.47	0.00	0.00
9.00	0.00	0.42	0.00	0.00
9.75	0.00	0.36	0.00	0.00
10.50	0.00	0.32	0.00	0.00
11.25	0.00	0.27	0.00	0.00
12.00	0.00	0.23	0.00	0.00
12.75	0.00	0.20	0.00	0.00
13.50	0.00	0.17	0.00	0.00
14.25	0.00	0.14	0.00	0.00
15.00	0.00	0.12	0.00	0.00
15.75	0.00	0.10	0.00	0.00
16.50	0.00	0.08	0.00	0.00
17.25	0.00	0.06	0.00	0.00
18.00	0.00	0.05	0.00	0.00
18.75	0.00	0.04	0.00	0.00
19.50	0.00	0.03	0.00	0.00
20.25	0.00	0.03	0.00	0.00
21.00	0.00	0.02	0.00	0.00
21.75	0.00	0.02	0.00	0.00
22.50	0.00	0.01	0.00	0.00
23.25	0.00	0.01	0.00	0.00
24.00	0.00	0.01	0.00	0.00
24.75	0.00	0.01	0.00	0.00
25.50	0.00	0.00	0.00	0.00
26.25	0.00	0.00	0.00	0.00
27.00	0.00	0.00	0.00	0.00
27.75	0.00	0.00	0.00	0.00
28.50	0.00	0.00	0.00	0.00
29.25	0.00	0.00	0.00	0.00

*****VERTICAL SYSTEM MTF*****

Freq	Pre	Post No Eye	Base	SR
0.00	1.00	1.00	1.00	0.00
0.75	0.79	1.00	0.79	0.00
1.50	0.58	0.98	0.57	0.00
2.25	0.37	0.97	0.36	0.00
3.00	0.21	0.94	0.19	0.00
3.75	0.08	0.91	0.07	0.00
4.50	0.01	0.87	0.01	0.00
5.25	0.00	0.83	0.00	0.00
6.00	0.00	0.78	0.00	0.00
6.75	0.00	0.73	0.00	0.02
7.50	0.00	0.68	0.00	0.04
8.25	0.00	0.63	0.00	0.07
9.00	0.00	0.58	0.00	0.09
9.75	0.00	0.52	0.00	0.10
10.50	0.00	0.47	0.00	0.10
11.25	0.00	0.42	0.00	0.08
12.00	0.00	0.38	0.00	0.04
12.75	0.00	0.33	0.00	0.02
13.50	0.00	0.29	0.00	0.01

14.25	0.00	0.25	0.00	0.00
15.00	0.00	0.22	0.00	0.00
15.75	0.00	0.19	0.00	0.00
16.50	0.00	0.16	0.00	0.00
17.25	0.00	0.13	0.00	0.00
18.00	0.00	0.11	0.00	0.00
18.75	0.00	0.09	0.00	0.00
19.50	0.00	0.08	0.00	0.00
20.25	0.00	0.06	0.00	0.00
21.00	0.00	0.05	0.00	0.00
21.75	0.00	0.04	0.00	0.00
22.50	0.00	0.03	0.00	0.00
23.25	0.00	0.03	0.00	0.00
24.00	0.00	0.02	0.00	0.00
24.75	0.00	0.02	0.00	0.00
25.50	0.00	0.01	0.00	0.00
26.25	0.00	0.01	0.00	0.00
27.00	0.00	0.01	0.00	0.00
27.75	0.00	0.01	0.00	0.00
28.50	0.00	0.00	0.00	0.00
29.25	0.00	0.00	0.00	0.00

*****HORR and VERT MRTS*****

Freq	Horr	Vert
0.75	0.027	0.027
1.50	0.047	0.048
2.25	0.086	0.090
3.00	0.170	0.185
3.75	0.479	0.549
4.50	4.123	5.087
5.25	10.000	10.000
6.00	10.000	10.000
6.75	10.000	10.000
7.50	10.000	10.000
8.25	10.000	10.000
9.00	10.000	10.000
9.75	10.000	10.000
10.50	10.000	10.000
11.25	10.000	10.000
12.00	10.000	10.000
12.75	10.000	10.000
13.50	10.000	10.000
14.25	10.000	10.000

*****RECOGN/IDENTIF HORR and VERT MRTS*****

FrqID	Horr	Vert
0.68	0.025	0.025
1.37	0.043	0.044
2.05	0.079	0.082
2.73	0.156	0.169
3.42	0.441	0.501
4.10	3.812	4.641
4.79	10.000	10.000

5.47	10.000	10.000
6.15	10.000	10.000
6.84	10.000	10.000
7.52	10.000	10.000
8.20	10.000	10.000
8.89	10.000	10.000
9.57	10.000	10.000
10.26	10.000	10.000
10.94	10.000	10.000
11.62	10.000	10.000
12.31	10.000	10.000
12.99	10.000	10.000

*****TWO DIM MRT WITH NO SAMPLING MRTS*****

Frq2D	MRT2D
0.13	0.027
0.19	0.027
0.25	0.027
0.31	0.027
0.38	0.027
0.44	0.027
0.50	0.027
0.56	0.027
0.63	0.027
0.69	0.027
0.89	0.030
1.27	0.040
1.55	0.050
1.78	0.060
1.97	0.070
2.14	0.080
2.28	0.090
2.39	0.100
3.09	0.200
3.37	0.300
3.58	0.400
3.73	0.500
3.80	0.600
3.86	0.700
3.90	0.800
3.94	0.900
3.98	1.000
4.22	2.000
4.36	3.000
4.45	4.000
4.58	5.000
4.75	6.000
4.90	7.000
5.03	8.000
5.15	9.000

2. This is an example of a scanning MWIR output file. It has an FOV of 2.0° x 1.5°, f/# of 3.75 and a peak D* of 6E11 cm-sqr(Hz)/Watt. It is the output of file number two listed in Appendix B.

Sensor Name = scm153
5:20:34 PM 7/30/02

*****BASIC SYSTEM CALCULATIONS*****

Vertical FOV = 1.50 Degrees
Horizontal FOV = 2.00 Degrees
Magnification Calculated - No E-Zoom
Magnification = 15.00 Unitless

*****SPACE CALCULATIONS*****

Vertical Detector Angular Subtense (or IFOV) = 0.11 Milliradians
Horizontal Detector Angular Subtense (or IFOV) = 0.07 Milliradians
Airy Disc Diameter (distance between zeroes) = 0.22 Milliradians
Vertical Angular Sample Spacing = 0.09 Milliradians
Horizontal Angular Sample Spacing = 0.00 Milliradians

*****FREQUENCY CALCULATIONS*****

Vertical Detector Cutoff Frequency = 9.00 Cycles per milliradian
Horizontal Detector Cutoff Frequency = 15.00 Cycles per milliradian
Diffraction Cutoff Frequency = 10.96 Cycles per milliradian
Vertical Sampling Frequency = 10.70 Cycles per milliradian
Vertical Half-Sample Frequency = 5.35 Cycles per milliradian

*****TEMPORAL CALCULATIONS*****

Efficiency Factor = 0.001 unitless
Dwell Time = 28.65 microseconds
Scan Velocity = 2,327.10 milliradians per second
Eye Integration Time = 0.062 seconds

***** NOISE CALCULATIONS *****

System Bandwidth = 32,255.90
System Random Spatio-Temporal Noise (sigma tvh) = 911.48 milliKelvin

***** SAMPLING CALCULATIONS *****

Horizontal Spurious Response = 0.00
Horizontal Out-of-Band SR = 0.00
Vertical Spurious Response = 0.40
Vertical Out-of-Band SR = 0.36

*****HORIZONTAL PRESAMPLE MTF*****

Freq	Diff	Blur	MsOp	Vibr	DetSp	SandH	Cust
0.00	1.00	1.00	1.00	1.00	1.00	1.00	1.00

0.75	0.91	1.00	1.00	1.00	1.00	1.00	1.00
1.50	0.83	1.00	1.00	0.99	0.98	1.00	1.00
2.25	0.74	1.00	1.00	0.98	0.96	1.00	1.00
3.00	0.66	1.00	1.00	0.96	0.94	1.00	1.00
3.75	0.57	1.00	1.00	0.94	0.90	1.00	1.00
4.50	0.49	1.00	1.00	0.91	0.86	1.00	1.00
5.25	0.41	1.00	1.00	0.88	0.81	1.00	1.00
6.00	0.34	0.99	1.00	0.85	0.76	1.00	1.00
6.75	0.27	0.99	1.00	0.82	0.70	1.00	1.00
7.50	0.20	0.99	1.00	0.78	0.64	1.00	1.00
8.25	0.14	0.99	1.00	0.74	0.57	1.00	1.00
9.00	0.09	0.99	1.00	0.70	0.50	1.00	1.00
9.75	0.04	0.98	1.00	0.66	0.44	1.00	1.00
10.50	0.01	0.98	1.00	0.61	0.37	1.00	1.00
11.25	0.00	0.98	1.00	0.57	0.30	1.00	1.00
12.00	0.00	0.97	1.00	0.53	0.23	1.00	1.00
12.75	0.00	0.97	1.00	0.49	0.17	1.00	1.00
13.50	0.00	0.97	1.00	0.45	0.11	1.00	1.00
14.25	0.00	0.96	1.00	0.41	0.05	1.00	1.00

*****VERTICAL PRESAMPLE MTF*****

Freq	Diff	Blur	MsOp	Vibr	DetSp	Cust
0.00	1.00	1.00	1.00	1.00	1.00	1.00
0.75	0.91	1.00	1.00	1.00	0.99	1.00
1.50	0.83	1.00	1.00	0.99	0.95	1.00
2.25	0.74	1.00	1.00	0.98	0.90	1.00
3.00	0.66	1.00	1.00	0.96	0.83	1.00
3.75	0.57	1.00	1.00	0.94	0.74	1.00
4.50	0.49	1.00	1.00	0.91	0.64	1.00
5.25	0.41	1.00	1.00	0.88	0.53	1.00
6.00	0.34	0.99	1.00	0.85	0.41	1.00
6.75	0.27	0.99	1.00	0.82	0.30	1.00
7.50	0.20	0.99	1.00	0.78	0.19	1.00
8.25	0.14	0.99	1.00	0.74	0.09	1.00
9.00	0.09	0.99	1.00	0.70	0.00	1.00
9.75	0.04	0.98	1.00	0.66	-0.08	1.00
10.50	0.01	0.98	1.00	0.61	-0.14	1.00
11.25	0.00	0.98	1.00	0.57	-0.18	1.00
12.00	0.00	0.97	1.00	0.53	-0.21	1.00
12.75	0.00	0.97	1.00	0.49	-0.22	1.00
13.50	0.00	0.97	1.00	0.45	-0.21	1.00
14.25	0.00	0.96	1.00	0.41	-0.19	1.00

*****HORIZONTAL POSTSAMPLE MTF*****

Freq	LPass	Boost	Itrp	Ezoom	EOMux	Disp	Eye	Cust
0.00	1.00	1.00	1.00	1.00	1.00	1.00	1.00	1.00
0.75	1.00	1.00	1.00	1.00	1.00	1.00	0.87	1.00
1.50	0.99	1.00	1.00	1.00	1.00	0.98	0.78	1.00
2.25	0.97	1.00	1.00	1.00	1.00	0.97	0.70	1.00
3.00	0.95	1.00	1.00	1.00	1.00	0.94	0.63	1.00
3.75	0.93	1.00	1.00	1.00	1.00	0.91	0.58	1.00
4.50	0.90	1.00	1.00	1.00	1.00	0.87	0.52	1.00
5.25	0.87	1.00	1.00	1.00	1.00	0.83	0.47	1.00

6.00	0.84	1.00	1.00	1.00	1.00	0.78	0.43	1.00
6.75	0.81	1.00	1.00	1.00	1.00	0.73	0.39	1.00
7.50	0.78	1.00	1.00	1.00	1.00	0.68	0.35	1.00
8.25	0.75	1.00	1.00	1.00	1.00	0.63	0.32	1.00
9.00	0.72	1.00	1.00	1.00	1.00	0.58	0.29	1.00
9.75	0.70	1.00	1.00	1.00	1.00	0.52	0.26	1.00
10.50	0.67	1.00	1.00	1.00	1.00	0.47	0.23	1.00
11.25	0.64	1.00	1.00	1.00	1.00	0.42	0.21	1.00
12.00	0.62	1.00	1.00	1.00	1.00	0.38	0.19	1.00
12.75	0.60	1.00	1.00	1.00	1.00	0.33	0.17	1.00
13.50	0.57	1.00	1.00	1.00	1.00	0.29	0.15	1.00
14.25	0.55	1.00	1.00	1.00	1.00	0.25	0.13	1.00

*****VERTICAL POSTSAMPLE MTF*****

Freq	Boost	Itrp	Ezoom	EOMux	Disp	Eye	Cust
0.00	1.00	1.00	1.00	1.00	1.00	1.00	1.00
0.75	1.00	1.00	1.00	1.00	1.00	0.87	1.00
1.50	1.00	1.00	1.00	1.00	0.98	0.78	1.00
2.25	1.00	1.00	1.00	1.00	0.97	0.70	1.00
3.00	1.00	1.00	1.00	1.00	0.94	0.63	1.00
3.75	1.00	1.00	1.00	1.00	0.91	0.58	1.00
4.50	1.00	1.00	1.00	1.00	0.87	0.52	1.00
5.25	1.00	1.00	1.00	1.00	0.83	0.47	1.00
6.00	1.00	1.00	1.00	1.00	0.78	0.43	1.00
6.75	1.00	1.00	1.00	1.00	0.73	0.39	1.00
7.50	1.00	1.00	1.00	1.00	0.68	0.35	1.00
8.25	1.00	1.00	1.00	1.00	0.63	0.32	1.00
9.00	1.00	1.00	1.00	1.00	0.58	0.29	1.00
9.75	1.00	1.00	1.00	1.00	0.52	0.26	1.00
10.50	1.00	1.00	1.00	1.00	0.47	0.23	1.00
11.25	1.00	1.00	1.00	1.00	0.42	0.21	1.00
12.00	1.00	1.00	1.00	1.00	0.38	0.19	1.00
12.75	1.00	1.00	1.00	1.00	0.33	0.17	1.00
13.50	1.00	1.00	1.00	1.00	0.29	0.15	1.00
14.25	1.00	1.00	1.00	1.00	0.25	0.13	1.00

*****HORIZONTAL SYSTEM MTF*****

Freq	Pre	Post No Eye	Base	SR
0.00	1.00	1.00	1.00	0.00
0.75	0.91	0.99	0.90	0.00
1.50	0.80	0.97	0.78	0.00
2.25	0.70	0.94	0.65	0.00
3.00	0.59	0.90	0.53	0.00
3.75	0.48	0.84	0.41	0.00
4.50	0.38	0.79	0.30	0.00
5.25	0.30	0.72	0.21	0.00
6.00	0.22	0.66	0.14	0.00
6.75	0.15	0.60	0.09	0.00
7.50	0.10	0.53	0.05	0.00
8.25	0.06	0.47	0.03	0.00
9.00	0.03	0.42	0.01	0.00
9.75	0.01	0.36	0.00	0.00

10.50	0.00	0.32	0.00	0.00
11.25	0.00	0.27	0.00	0.00
12.00	0.00	0.23	0.00	0.00
12.75	0.00	0.20	0.00	0.00
13.50	0.00	0.17	0.00	0.00
14.25	0.00	0.14	0.00	0.00
15.00	0.00	0.12	0.00	0.00
15.75	0.00	0.10	0.00	0.00
16.50	0.00	0.08	0.00	0.00
17.25	0.00	0.06	0.00	0.00
18.00	0.00	0.05	0.00	0.00
18.75	0.00	0.04	0.00	0.00
19.50	0.00	0.03	0.00	0.00
20.25	0.00	0.03	0.00	0.00
21.00	0.00	0.02	0.00	0.00
21.75	0.00	0.02	0.00	0.00
22.50	0.00	0.01	0.00	0.00
23.25	0.00	0.01	0.00	0.00
24.00	0.00	0.01	0.00	0.00
24.75	0.00	0.01	0.00	0.00
25.50	0.00	0.00	0.00	0.00
26.25	0.00	0.00	0.00	0.00
27.00	0.00	0.00	0.00	0.00
27.75	0.00	0.00	0.00	0.00
28.50	0.00	0.00	0.00	0.00
29.25	0.00	0.00	0.00	0.00

*****VERTICAL SYSTEM MTF*****

Freq	Pre	Post No Eye	Base	SR
0.00	1.00	1.00	1.00	0.00
0.75	0.90	1.00	0.90	0.00
1.50	0.78	0.98	0.77	0.00
2.25	0.65	0.97	0.63	0.00
3.00	0.52	0.94	0.49	0.01
3.75	0.40	0.91	0.36	0.03
4.50	0.29	0.87	0.25	0.05
5.25	0.19	0.83	0.16	0.07
6.00	0.12	0.78	0.09	0.09
6.75	0.07	0.73	0.05	0.10
7.50	0.03	0.68	0.02	0.12
8.25	0.01	0.63	0.01	0.12
9.00	0.00	0.58	0.00	0.12
9.75	0.00	0.52	0.00	0.12
10.50	0.00	0.47	0.00	0.11
11.25	0.00	0.42	0.00	0.08
12.00	0.00	0.38	0.00	0.06
12.75	0.00	0.33	0.00	0.04
13.50	0.00	0.29	0.00	0.02
14.25	0.00	0.25	0.00	0.01
15.00	0.00	0.22	0.00	0.01
15.75	0.00	0.19	0.00	0.01
16.50	0.00	0.16	0.00	0.00
17.25	0.00	0.13	0.00	0.00
18.00	0.00	0.11	0.00	0.00

18.75	0.00	0.09	0.00	0.00
19.50	0.00	0.08	0.00	0.00
20.25	0.00	0.06	0.00	0.00
21.00	0.00	0.05	0.00	0.00
21.75	0.00	0.04	0.00	0.00
22.50	0.00	0.03	0.00	0.00
23.25	0.00	0.03	0.00	0.00
24.00	0.00	0.02	0.00	0.00
24.75	0.00	0.02	0.00	0.00
25.50	0.00	0.01	0.00	0.00
26.25	0.00	0.01	0.00	0.00
27.00	0.00	0.01	0.00	0.00
27.75	0.00	0.01	0.00	0.00
28.50	0.00	0.00	0.00	0.00
29.25	0.00	0.00	0.00	0.00

*****HORR and VERT MRTS*****

Freq	Horr	Vert
0.75	0.212	0.213
1.50	0.325	0.331
2.25	0.459	0.479
3.00	0.622	0.675
3.75	0.910	1.042
4.50	1.415	1.746
5.25	2.328	3.182
6.00	4.053	6.388
6.75	7.511	10.000
7.50	10.000	10.000
8.25	10.000	10.000
9.00	10.000	10.000
9.75	10.000	10.000
10.50	10.000	10.000
11.25	10.000	10.000
12.00	10.000	10.000
12.75	10.000	10.000
13.50	10.000	10.000
14.25	10.000	10.000

*****RECOGN/IDENTIF HORR and VERT MRTS*****

FrqID	Horr	Vert
0.67	0.189	0.190
1.33	0.290	0.295
2.00	0.409	0.426
2.67	0.557	0.601
3.34	0.818	0.927
4.00	1.276	1.554
4.67	2.107	2.832
5.34	3.679	5.685
6.01	6.832	10.000
6.67	10.000	10.000
7.34	10.000	10.000
8.01	10.000	10.000
8.68	10.000	10.000

9.34	10.000	10.000
10.01	10.000	10.000
10.68	10.000	10.000
11.35	10.000	10.000
12.01	10.000	10.000
12.68	10.000	10.000

*****TWO DIM MRT WITH NO SAMPLING MRTS*****

Frq2D	MRT2D
0.07	0.213
0.11	0.213
0.14	0.213
0.18	0.213
0.21	0.213
0.25	0.213
0.29	0.213
0.32	0.213
0.36	0.213
0.39	0.213
0.43	0.213
0.46	0.213
0.50	0.213
0.54	0.213
0.57	0.213
0.61	0.213
0.64	0.213
0.68	0.213
0.71	0.213
1.34	0.300
1.92	0.400
2.40	0.500
2.82	0.600
3.15	0.700
3.39	0.800
3.61	0.900
3.79	1.000
4.84	2.000
5.38	3.000
5.73	4.000
5.99	5.000
6.20	6.000
6.40	7.000
6.64	8.000
6.89	9.000